Investigating Cellular and Molecular Mechanisms of Neuronal Layering in Self-Organising Aggregates of Zebrafish Retinal Cells

Megan Kate Eldred

University of Cambridge, St Edmund's College

This dissertation is submitted for the degree of Doctor of Philosophy

September 2017

Declaration

This dissertation is the result of my own work and includes nothing which is the outcome of work done in collaboration except as declared in the Acknowledgements and specified in the main text.

It is not substantially the same as any that I have submitted, or, is being concurrently submitted for a degree or diploma or other qualification at the University of Cambridge or any other University or similar institution except as declared in the Preface and specified in the text. I further state that no substantial part of my dissertation has already been submitted, or, is being concurrently submitted for any such degree, diploma or other qualification at the University of Cambridge or any other University or similar institution except as declared in the Preface and specified in the text

This thesis does not exceed 60,000 words in length.

The majority of this work has been published in the following papers:

Eldred, M.K., Charlton-Perkins, M., Muresan, L. &. Harris, W. (2017). Self-organising aggregates of zebrafish retinal cells for investigating mechanisms of neural lamination. Development, 144(6), pp.1097–1106.

Eldred, M.K., Muresan, L. & Harris, W.A. (2017). Disaggregation and Reaggregation of Zebrafish Retinal Cells for the Analysis of Neuronal Layering. In Methods in molecular biology (Clifton, N.J.).

Megan Kate Eldred
September 2017

Acknowledgements

I would like to take this opportunity to thank the many people who have supported and guided me during the course of this PhD, for it is almost impossible to undertake this task alone...

Firstly, I thank Bill Harris for his continued guidance and expertise, for allowing me the freedom to pursue the questions I was most interested in, and for pushing me to aim big. I also thank him for teaching me how to manage my work and communicate complex scientific issues. These are skills I will take with me into my future and for which I am extremely grateful to have learned from him.

Many thanks also go to Xana Almeida for her guidance and support from day one and throughout my time in the lab. She not only had great scientific advice to give, but also supported me when times were tough. I thank Leila Muresan for her help in writing the Matlab Scripts, without which my data wouldn't have made much sense. Thanks also go to Ryan MacDonald, Mark Charlton-Perkins and Afnan Azizi for all their help with the work and for allowing me to bounce around ideas and problems. Thanks go to all the members of the Harris / Holt lab and the PDN Fish Facility for their support, useful discussions, and generally making this PhD a whole lot of fun.

I couldn't have done all this work without the funding of my PhD Programme. Thank you to the BBSRC DTP for taking a chance on me by funding this opportunity.

But of course, I wouldn't have even been in the position to pursue a PhD if it wasn't for the support and guidance of my family and friends. I especially thank my Dad for providing me with the foundation on which to pursue opportunities, my Mum for making sure I pursued the opportunities that would make me happy, and my Brother for being proud of me no matter what I pursued. I am so grateful for you all…

Summary

The central nervous system is a complex, yet well-organised, often laminated, tissue. This robust organisation is evident in the architecture of the retina: consisting of 5 different neuronal types organised into distinct layers: Retinal Ganglion Cell (RGC), Amacrine Cell (AC), Bipolar Cell (BP), Horizontal Cell (HC) and Photoreceptor cell (PR) layers. This remarkable organisation is evolutionarily conserved in vertebrates, yet little is known about the mechanisms by which these cells form the correct layers. Live imaging has revealed overlapping periods of birth and extensive inter-digitation followed by cells sorting out into their appropriate positions, suggesting cell-cell interactions are important. To investigate possible cellular and molecular mechanisms responsible for the establishment of the tissue architecture I developed an organoid culture system for zebrafish retinal cells.

To identify the cells in culture I used a Spectrum of Fates fish line which is a multiply transgenic line in which each retinal cell type can be identified based on expression of a combination of fluorescently tagged cell fate markers. The development of the protocol by which I cultured the cells and observed their cell-cell interactions involved establishing the best methods to dissociate and culture zebrafish retinal cells in a non-adhesive environment, then imaging the resulting reaggregates to examine the position of the different retinal cell types. By doing this I observed their inherent self-organising properties, in the absence of extrinsic cues or scaffolds. These cells appeared to be arranged in an inside-out layering, although all cell types are layered in the same relative order as they are *in vivo*.

To analyse the organization in these aggregates I developed a Matlab script in collaboration with Leila Muresan which analyses the relative positioning of cells in concentric rings from the periphery to the centre of the aggregates according to the cell fate-tagged fluorescent markers. The script then fits this data as an empirical cumulative distribution function for different groups of cells to determine how spatially distinct populations of cells are. This gave me my measure of organisation.

I then investigated the cell-cell interactions involved in this self-organisation by genetically or pharmacologically removing individual cell types and assaying the resulting organisation of the reaggregated, cell-type deficient, retinal organoids. I revealed that Müller Glia are important for retinal cell self-organisation. I also investigated the role of Retinal Pigment Epithelial (RPE) cells and Retinal Ganglion Cells and found they had no impact on the ability of the remaining cell types to organize. I began to investigate the role of Amacrine Cells but found that retinas void of ACs were susceptible to disaggregating in our dissection setup, preventing me from collecting the material needed for culture. I also investigated the role of candidate molecules in this system and revealed that R-Cognin is critical for retinal cells to reaggregate.

Not only can I remove cells or molecules from the system, but I show how it can also be manipulated to replace molecules of interest such as laminin, by coating beads with the substance of choice and placing it amongst the cells to see if their organizational behaviour is affected. In summary, I have developed a system which provides a simple and easy platform to manipulate in various ways to help us potentially reveal some of the important players in neuronal patterning.

Unnamed, Prof. William A Harris, 2016

Table of Contents

List of Figures

List of Tables

List of Abbreviations

AC	Amacrine Cell
BP	Bipolar Cell
CNS	Central Nervous System
dAC	Displace Amacrine Cell
FP	Fluorophore
GCL	Ganglion Cell Layer
HC	Horizontal Cell
ILM	Inner Limiting Membrane
INL	Inner Nuclear Layer
IPL	Inner Plexiform Layer
MG	Müller Glia
nAC	Normally placed Amacrine Cell
NR	Neural Retina
OLM	Outer Limiting Membrane
PR	Photoreceptor
PTU	N-Phenylthiourea
PSF	Penicillin, Streptomycin and Fungizone
RGC	Retinal Ganglion Cell
RIN	Retinal Inhibitory Neuron
RPE	Retinal Pigment Epithelium

CHAPTER 1

Introduction

1. Introduction

One of the most fundamental questions in developmental biology is how do tissues, comprised of multiple cell types, become organised? During development, the tissues of an organism go through complex programmes of growth, specification, and cellular rearrangements before they reach their final, functional form. These developmental programmes are crucial for correct functioning of the tissues, but we do not yet fully understand them. The brain is one of the most complex tissues in the body, comprised of multiple neuronal cell types arranged in a highly-organised manner, required for its function of receiving, processing and responding to internal and external stimuli. Santiago Ramon y Cajal first studied these complex networks when he described many of the astonishing morphologies of different neuronal cells and the organisation of their networks. Since then the field of developmental neurobiology has sought to understand how a neuroepithelium, comprised of seemingly indifferent neural progenitors, produces the various classes of neurons that organise into discrete layers and establish intricate connections required for the functioning of these neural circuits.

In this thesis, I focus on the mechanisms by which these different cell types find their distinct layers. I use the zebrafish retina as a model to explore the cellular and molecular mechanisms. This is a highly organised neural tissue consisting of 5 main cell types organised into 3 cell layers, separated by 2 synaptic layers. Due to a relatively short developmental time and the embryo being transparent during early retinal development is it easy to access and study the process of retinal lamination. In zebrafish, we can easily label and manipulate cells and molecules of interest to investigate their role in these processes. Furthermore, I take advantage of the simplicity of aggregate cultures to model lamination. I have developed an *in vitro* organoid model of zebrafish retinal development to elucidate the fundamental cellular and molecular mechanisms in the absence of extrinsic scaffolds and cues present during retinal development.

1.1. The laminar architecture of the retina

The retina is the most accessible part of the central nervous system, and like other parts of the brain, it's laminar arrangement of cells is crucial to establish the appropriate connections and indeed for the correct functioning of the neuronal circuitry. Comprised of just 5 main neuronal cell types and one glial cell type, the retina is a strikingly well-organised neural tissue, with each of the major cell types sitting in its own specific layer and synapsing within specific plexiform layers (Holt et al. 1988; Cepko et al. 1996; Harris 1997) (Figure 1.1). Photoreceptors (PRs), the most apically positioned cells, sit in the outer nuclear layer (ONL) receiving light input which they convert to electric current. Bipolar Cells (BPs) sit in the inner nuclear layer (INL) and synapse with PRs in the outer plexiform layer (OPL). Due to their bipolar morphology, they also synapse with Retinal Ganglion Cells (RGCs) in the inner nuclear layer (INL), passing the signal from PRs to Retinal Ganglion Cells (RGCs). RGCs, the sole output neurons in the retina, sit in the most basal layer, the ganglion cell layer (GCL), and project their axons to the optic tectum in the brain via the optic nerve. As signals pass from PRs to BPs to RGCs they are modulated by the inhibitory neurons Horizontal Cells (HCs) and Amacrine Cells (ACs). Horizontal Cells sit in the apical portion of the INL, synapsing with PRs and BPs in the OPL and modulating signals passing between them. Amacrine cells sit mostly in the basal portion of the INL, synapsing with BPs and RGCs on the apical side of the IPL, however some displaced Amacrine cells (dACs) sit on the basal side of the IPL, in the GCL.

All retinal cells are all supported by the sole glial cell type, the Müller Glia which span the width of the retina, extending processes into every layer and are thought to play several roles in the retina. As glial cells, they support neuronal signalling by aiding in retinal cell metabolism and neurotransmitter recycling (Reichenbach & Bringmann 2013), they aid in light transfer through the retina to the PRs (Franze et al. 2007), and with well-established end feet anchored in the outer limiting membrane (OLM) and the inner limiting membranes (ILM) of the retina, they provide tensile strength and support to the developing retina (MacDonald et al. 2015). Finally, the neural retina is surrounded by the retinal pigment epithelium (RPE) a pigmented monolayer of cells

which prevents light scattering in the retina, and supports the function of PRs (Fuhrmann et al. 2014).

The distinct organisation of these cell layers and the two plexiform layers of the retina allow close proximity of cells to allow distinct connections. Sublamination of the plexiform layers permits specialised groups of neurons to connect in highly specialised circuitries for fine tuning of signals. For instance, ON-bipolar cells synapse with ACs and RGCs within the inner lamina of the IPL, whereas OFF-bipolar cells synapse within the outer lamina layer. Indeed, scientists have so far been able to categorise 5 main sublaminar layers in the IPL in mammals (Wässle 2004).

The proportions of different cell types and thickness of different cell and plexiform layers varies between species, according to functional specialisations, however the fundamentals of this architecture and the developmental mechanisms governing its formation are remarkably conserved amongst vertebrates. This laminar architecture may be crucial to allow for these complex circuitries to become established and there are many ways in which we can investigate its development and function, but a fundamental question remains unanswered: how do these cells arrange into the basic laminar layers in the first place?

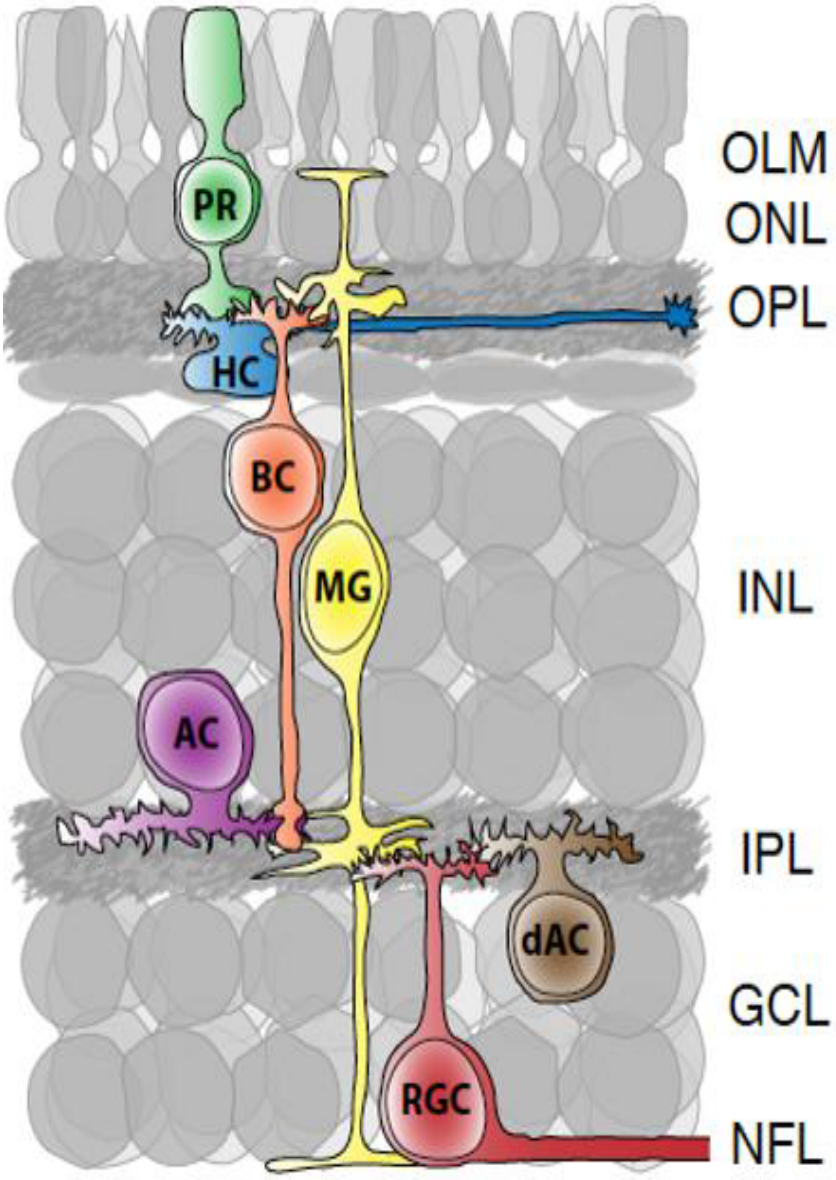

Figure 1-1: Schematic of the mature retina comprised of 7 different cell types organised into distinct layers.

Photoreceptors (PRs) sit in the outer nuclear layer (ONL) and synapse in the outer plexiform layer (OPL). Horizontal Cells (HC) sit in the inner nuclear layer (INL) and synapse in the OPL. Bipolar Cells (BP) sit in the INL and synapse in the OPL and inner plexiform layer (IPL). Amacrine Cells (AC) sit in the INL and synapse in the IPL. Displaced Amacrine Cells (dACs) sit in the ganglion cell layer (GCL) and synapse in the IPL. Retinal Ganglion Cells sit in the GCL and synapse in the IPL. Müller Glia sit in the INL and synapse in bother the OPL and IPL. Figure used with permission from Ryan MacDonald.

1.2. The process of retinal lamination

Following eye field specification, the presumptive retina undergoes a series of exquisite, complex morphogenetic transformations to transform it into a pseudostratified retinal neuroepithelium before lamination can begin.

1.2.1. Early Retinal Development

First, the presumptive eye tissues form as an outgrowth of the neuroepithelium of the ventral forebrain, the diencephalon, which evaginates on both sides to form bilateral optic vesicles (shown in Figure 1.2). At this time, numerous transcription factors begin to be expressed, such as Mitf and Vsx2, that begin to specify the different tissues of the eye. Next, the optic vesicle invaginates, together with the lens ectoderm, to form the bilayered hemispheric optic cup, that will later become the neural retina and the RPE, and lens vesicle that will become the lens. The complex process of optic cup morphogenesis is reviewed in (Fuhrmann 2010). I will not go into detail in this thesis, instead I will focus on the events that follow, necessary for lamination.

Following optic cup formation, the single layered neuroepithelium begins to proliferate and the numbers of RPCs increase, expanding the thickness of the optic cup (He et al. 2012). At this stage, retinal progenitor cells (RPCs) appear to be stratified due to their cell bodies being positioned in many layers, but their apical and basal processes remain attached at both the apical and basal surfaces, the OLM and ILM respectively. The cell bodies of these multipotent RPCs then undergo a series of movements in a process known as interkinetic nuclear migration (IKNM) whereby cells move from the apical to basal surfaces in sync with phases of the cell cycle. Cells divide in M-phase at the apical surface then migrate towards the basal surface during G1, S and G2 phase. Following division, cells either exit the cell-cycle, migrate basally and differentiate, or return to the apical surface to enter M-phase again and continue the cycle of IKNM until cell-cycle exit. It is thought that this series of movements is necessary for correct cell differentiation due to exposure to gradients of Notch signalling across the neuroepithelium (Meyer et al. 2011; Leung et al. 2011). Cell divisions in the retina occur either as symmetric divisions, or asymmetric divisions. During early development,

symmetric divisions produce two daughter RPCs and increase the pool of RPCs. Later, asymmetric divisions produce one RPC and one neuron that goes on to differentiate and symmetric divisions produce two neurons that will go on to differentiate. This is when the pool of RPCs begins to become depleted (He et al. 2012). It is also around this time that the process of lamination begins.

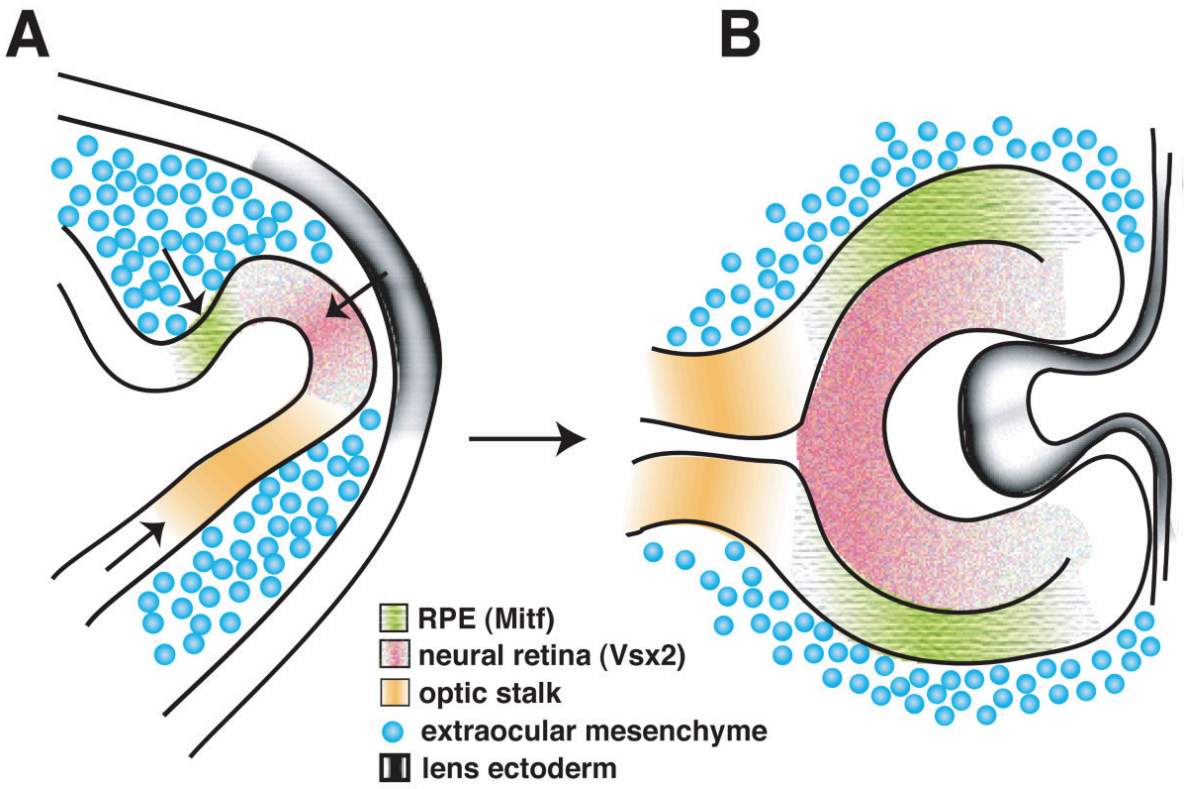

Figure 1-2: Schematic of optic cup morphogenesis.

(A) The optic vesicle forms as an outpocketing of the forebrain when the presumptive RPE, neural retina and lens ectoderm begin to specify. (B) After a series of morphogenetic transformations, the layers of the optic vesicle and lens ectoderm involute to become the bilayered hemispheric optic cup and lens vesicle. Figure taken from (Fuhrmann 2010).

1.2.2. Retinal histogenesis

Studies of retinal histogenesis started as far back as the time of Cajal, when he described the intricate morphologies of retinal cells of many species, including frog, lizard, chicken and cow (Ramón y Cajal 1892). Since then, techniques such as the use of H-Thymidine labelling have been used to begin to understand the process and timing of events in neurogenesis (Angevine & Sidman 1961; Sidman 1961; Nawrocki 1985). But these studies were carried out in fixed tissues, meaning a lot of dynamic processes could not be easily seen. More recent advancements in technology allow us to access the process of neurogenesis using live imaging, to track the movement of cells as they differentiate and laminate (Das et al. 2003; He et al. 2012; Almeida et al. 2014). Work is ongoing to understand how cells differentiate, migrate and laminate in neural tissues, and particularly the retina.

In neural tissues, there is often a clear histogenetic order to cell layering. For instance, in the cortex, first born cells occupy the deeper layers, and the later born cells occupy the upper layers (McConnell 1995). Much like in the cortex, cells of the retina also show a histogenetic arrangement, with early born RGCs residing in the innermost retinal layer and late born PRs in the outermost (Holt et al. 1988; Cepko et al. 1996; Harris 1997). Retinogenesis in the zebrafish retina occurs as a wave of differentiation across the retina, starting in the ventronasal portion and spreading in the peripheral-temporal direction (Schmitt & Dowling 1999; Almeida et al. 2014). At any one position in the retina, cells differentiate in roughly the same order. RGCs begin to specify at around 28hpf and occupy the most basal layer of the retina, the GCL (Zolessi et al. 2006). ACs begin to specify at around 35hpf and occupy the space just apical of the GCL (Jusuf & Harris 2009). Shortly after, BPs begin to specify at around 40hpf and sit in the INL (Vitorino et al. 2009), and PRs also differentiate around 48hpf (Hu & Easter 1999). Finally, MGs begin to appear at around 48hpf (MacDonald et al. 2015). Retinogenesis happens over a relatively short time in zebrafish as compared to other mammals. Within just a 24-hour time window all cell types have begun to differentiate, and by just 72hpf all cell types are present and laminated. Zebrafish are also unique in that there continues to be retinogenesis throughout adulthood at the periphery of the retina, in the ciliary marginal zone (Marcus et al. 1999; Wan et al. 2016).

There is a clear order of cell fate acquisition across the retina, and it is generally thought that RPCs pass through different states of competency in a particular order due to temporally expressed transcription factors (Livesey & Cepko 2001). However, on an individual RPC level, there doesn't seem to be a specific order in which retinal fates are acquired. Clonal analysis carried out in zebrafish has revealed that individual RPCs produce clones of different sizes and compositions. It is thought that fate choice within a single RPC is stochastic and cell autonomous, as two clones differentiating next to each other at the same time can give rise to lineages of different compositions (He et al. 2012). This means that at any one time, different cell types are being born within small regions of the retina indicating there may be interactions between cell populations before finding their appropriate layers. Indeed live imaging has revealed that there is significant interdigitation of cell types before a period of sorting out, and that cells appear to use each other to find their distinct laminar layers (Almeida et al. 2014).

With different cell fates being specified at different times across the retina, the mechanism of lamination cannot simply be a matter of timing – i.e. cells piling up on top of each other according to their birthdate. In fact, it is known that sister cells born at exactly the same time may migrate to different but appropriate layers (He et al. 2012). Timing alone does not account for lamination in other neural tissues either, as is clearly shown in the example of *reeler* mutant mice, where the neocortex shows the opposite "outside-in" order of histogenesis even though the different types of cortical cells are generated and migrate to the cortical plate at the correct times (Rakic 1970; Caviness & Sidman 1973).

1.2.3. Cellular migration

Since retinal cells do not just rely on time or position of birth to find their layers, how do they find their correct position? In the cortex, it is seen that early born cells move by somal translocation, whereas later born cells, like pyramidal cells move by glia-guided migration and even some cells move by tangential migration (Nadarajah et al. 2001; Nadarajah & Parnavelas 2002; Nadarajah et al. 2003). Three modes of migration have also been proposed in the retina (Link & Godinho 2006; Baye & Link 2008). Some

hypothesise that MG could be helping cells to migrate, like radial glia do in the cortex (Nadarajah & Parnavelas 2002). Electron microscopy studies revealed cell-cell contacts and distinct radial patterning of MG in chick retina, leading scientists to propose that MG could be acting like scaffolds along which cells migrate (Meller & Tetzlaff 1976). However it is now known that MG are born much later in the cell fate cycle than other cell types and even some RGCS and ACs are already laminated before MG appear (MacDonald et al. 2015). Others suggest the neuroepithlial cells themselves could act as scaffolds, since they are still attached to the OLM and ILM (Prada, 1987; Malicki 2004), but there is no evidence of this yet.

Somal (also known as nuclear) translocation is the most commonly seen form of migration in the CNS, particularly the retina and in early cerebral cortex development (Nadarajah et al. 2001). In this form of migration, post mitotic cells move their soma to the appropriate laminar position while maintaining attachments to the OLM and ILM. Once in position, they will detach these processes. Somal translocation has been hypothesised as the mode of transport for RGCs and BPs for some time, in studies of fixed tissues (Hinds & Hinds 1974; Prada et al. 1981; Snow & Robson 1994) and confirmed in live imaging studies (Poggi et al. 2005; Zolessi et al. 2006).

For some cells, attachments to the apical and basal surfaces are not necessary and they migrate using a more active, unconstrained mode of migration. For example early studies revealed some cell types were found in various positions in the developing retina, without apical or basal attachments (Hinds & Hinds 1978; Hinds & Hinds 1979; Hinds & Hinds 1983). Recently, live imaging studies of inhibitory retinal neurons have described how HCs, iACs and dACs in the zebrafish retina all initially move to the INL via somal translocation with a bipolar morphology, but then retract one or both processes and enter distinct modes of multipolar, unconstrained migration in both the radial and tangential direction to find their final position (Chow et al. 2015). The modes of migration of the different retinal types has been summarised in Figure 1.3.

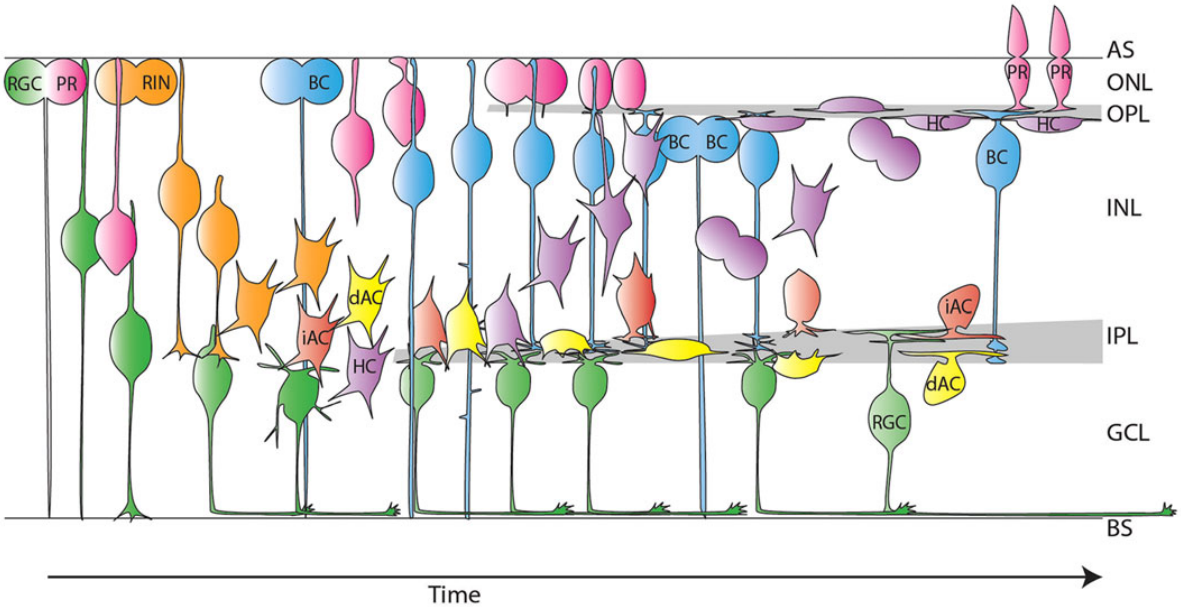

Figure 1-3: Schematic summarising retinal cell migration during lamination

Schematic depicting the various modes of migration of retinal cells over time. RGCs, the first cells to be born, migrate basally with a bipolar morphology then detach their apical process once they reach the GCL. PRs initially migrate basally, extending a short basal process, but then return to the apical surface. Retinal inhibitory neurons (RINs), consisting of iACs, dACs and HCs, all initially migrate to the middle INL where ACs find a basal position within the INL but HCs migrate apically again to the apical side of the INL and find tune their position with tangential migration. BCs migrate a short distance to the basal side of the INL and maintain their bipolar morphology with apical and basal attachments in the OPL and IPL. Figure taken from (Chow et al. 2015).

1.2.4. Molecular guidance cues

There is a great deal of polarity in the developing neuroepithelium and extracellular cues are likely to influence cell migration and lamination. One of the earliest platforms for potential guidance cues established in the developing retina is the ILM, a large component of which is laminin.

Laminins are glycoproteins found in the basement membrane, or basal lamiae, of almost all tissues in vertebrates which underlie epithelial sheets, separating them from the surrounding connective tissue. Basal laminae, and laminins are involved in cell-cell and

cell-ECM communication. This aids in cell adhesion, proliferation, differentiation and movement, crucial for tissue morphogenesis. Mammals have been found to possess up to 15 different laminins, all formed from different combinations of subunits. Each tissue contains a different composition of ECM molecules and each type of laminin plays a slightly different role in development according to which other ECM components they interact with. Laminins are known to be involved in the patterning of epithelial tissues in zebrafish such as limbs and fins (Nagendran et al. 2015).

Laminin 1 is expressed at the basal lamina of the zebrafish retina (Lee & Gross 2007) and shown to provide a polarity cue to developing retinal cells (Randlett et al. 2011). Like other laminins, it is a heterotrimer, consisting of three subunits: α1, β1, and γ1. Although these studies focus on the role of laminin in orienting the axon emergence from developing RGCs, during these studies it was also seen in some samples that loss of the Lamα1 subunit of Laminin 1 led to a duplicated and mirrored layering of the retina, with RGCs in the middle, and the PR layers on the outside so that the cell types were in the following order: PRs, HCs, BPs, ACs, RGCs, ACs, BPs, HCs, PRs (Ryan MacDonald and Bill Harris, personal communication) indicating the loss of polarity in the lamination of the tissue. A recent study revealed a crucial role of laminin in optic cup morphogenesis. In this study, they use a lama1UW1 mutant to show that the loss of Lamα1 leads to loss of cell-cell adhesion and epithelial polarity. This in turn leads to defects in tissue architecture formation and results in a disorganised retina (Bryan et al. 2016).

There is an array of molecules that could be involved in retinal lamination, including other ECM-associated proteins such as integrins which mediate cell-cell and cell-matrix interactions. In fact, it has been shown that laminin mediates its signal through beta-integrin. Disruption of beta-integrin signalling leads to disruption of lamination and rosette formations in the xenopus retina (Li & Sakaguchi 2004). Integrins also work alongside other cell adhesion molecules such as cadherins. N-cadherin is commonly found in the nervous system and is expressed ubiquitously on retinal neurons. It has been shown to be important for retinal lamination although the mechanisms are not yet fully understood (Matsunaga et al. 1988; Masai et al. 2003; Malicki et al. 2003). A retina-specific cadherin, R-Cadherin has been shown to act in a similar way, and possibly also in concert with N-Cadherin (H Inuzuka et al. 1991; H. Inuzuka et al. 1991; Johnson et al.

2004; Babb et al. 2005). Both these molecules appear to be crucial to retinal cell adhesion and are expressed at temporally distinct times during retinal development, indicating a possible crucial role during the time of retinal histogenesis and lamination.

Some molecules involved in neural lamination are even secreted by particular cell types. The layering defect in the *reeler* mouse is due to the lack of the glycoprotein (Reelin), which is secreted largely by a single transient cell type, the Cajal Retzius cell; (D'Arcangelo & Curran 1998; Huang 2009). Although it seems Reelin does not play the same role in the zebrafish retina (Bill Harris, personal communication) this does highlight to us the need to investigate both cellular and molecular mechanisms together, in our investigations of neural lamination.

Other guidance cues common elsewhere in the nervous system, such as Semas, Sidekicks, Dscams and Contactins, have also been shown to provide cues during later stages of retinal lamination. (Matsuoka, Chivatakarn, et al. 2011; Matsuoka, Nguyen-Ba-Charvet, et al. 2011; Yamagata & Sanes 2008; Goodman et al. 2016; Yamagata & Sanes 2012). Many of these are involved in the fine-tuning stages of lamination, such as targeting of synapses within the synaptic plexiform layers. The list of molecules involved in these processes is estimated to be long, so I will not begin to list them all here as the topic of this thesis focussed on the earlier stages of lamination, the initial cellular arrangements.

1.2.5. Deciphering the mechanisms of lamination

It appears there are various cellular and molecular mechanisms involved in retinal lamination. These include an overlap of cell birth dates leading to significant interdigitation of cell types and a period of sorting out. There are also different modes of migration, in both the radial and tangential direction, illustrating that perhaps cells are not just responding to environmental cues, but that they rely on each other to seek their appropriate positioning. Finally, live imaging studies have revealed some dynamic cell-cell interactions that lead us to believe cell-cell communication may be key in correct lamination. However, it is also apparent that some external cues are influencing the correct layering of cells. Some provide polarity to the retina as a whole or are

involved in cell-cell adhesion and migration, or even in targeting of synapses to their appropriate synaptic layers. There are many potential mechanisms to explore in the retina as a neural system, but it is difficult to determine which are most important in such a complex system.

We must determine whether cells are laminating due to interactions between the different cell types, i.e. cell-cell interactions, or from different cell types responding to common environmental cues. The latter possibility is consistent with *in vivo* studies in which lamination is preserved even in the absence of specific cell types (Green et al. 2003; Kay et al. 2004; Randlett et al. 2013). However, other studies suggest that direct interactions between cell types are likely to be involved in normal layering. For instance, live imaging studies show that late-born RGCs migrate through earlier born Amacrine cells (ACs) to reach the RGC layer in the zebrafish retina and that dACs migrate through the forming IPL to find their position within the GCL (Chow et al. 2015). Even during unconstrained migration, some cells seem reliant on others to migrate. Clonal analysis from transplantation of wild type RPC cells into retinas where ACs are lacking revealed that HCs can only migrate away from ACs in WT clones with a sufficient number of ACs (Henrik Boije, Harris lab, personal communication). In addition, the involvement of cell-cell interactions is indicated by the formation of rosettes in retinoblastoma (Johnson et al. 2007) and retinal dysplasias in which cell adhesion molecules such as N-cadherin are compromised (Wei et al. 2006).

Although there are likely to be many interacting mechanisms governing retinal lamination, cell-cell interactions seem to be crucial to this process. I will therefore be focussing on the cellular mechanisms of lamination in this thesis.

1.3. Cellular mechanisms of lamination studied *in vivo*

As the retina develops, multiple cell types are being born from a common pool of progenitors and migrating to their final position. It is possible that some of these cell types are key to the lamination of the retina, by guiding other cells to their final position, through physical or molecular cues. Many studies have investigated the

cellular mechanisms of lamination and identified some of the key players. Here I will describe the development of these cell types during retinogenesis and discuss their possible role in lamination.

1.3.1. Retinal Pigment Epithelium

Retinal pigment epithelium (RPE) and neural retina (NR) arise from a common pool of bi-potential progenitors, but segregate during optic morphogenesis. It is thought that NR and RPE fates are segregated early, during optic vesicle development, depending on expression of Yap and Taz (Miesfeld et al. 2015). Cells facing the lens would later become NR and those on the opposite side, lens-averse cells, would become RPE (Fuhrmann 2010). However, a recent live imaging study has revealed that lens-averse cells are also contributing to NR fates due to a morphogenetic movement termed "epithelial flow" during optic vesicle invagination. Lens-averse cells move around the periphery of the hemispheric retinal epithelium and involute into the centre, to later become lens facing NR cells of the optic cup. The cells that remain on the outside after these movements later mature, and acquire the morphological shape and characteristics of RPE cells (Heermann et al. 2015). This highlights that the process by which RPE cells differentiate from retinal progenitors is perhaps not defined as early on as previously thought. In fact, further studies show that prospective RPE and NR fates share a lot of the same gene expression (Sinn & Wittbrodt 2013; Fuhrmann et al. 2014). It is also shown that RPE influence NR specification in mouse, through Notch-signalling (Ha et al. 2017).

RPE may play a role in lamination during this time, as several mutants lacking RPE or with disrupted RPE also display lamination defects. For example, in a zebrafish mutant called *mosaic eyes* RPE cells cannot properly signal to the NR. The nuclear layers of the neural retina are absent and NR cells can still differentiate, but are often misplaced (Jensen et al. 2001). Another study, where RPE integrity is disrupted due to the absence of the polarity protein Nagie oko (Nok) reveal that in the absence of RPE, retinas cannot laminate properly and that restoring RPE integrity rescues the defect (Zou et al. 2008). These studies highlight the possible influences of neighbouring tissues on retinal lamination, such as the RPE.

1.3.2. Müller Glia

MG differentiate from the same pool of retinal progenitors as all other retinal neurons but are the only glial cell type born in the retina. They are the last cell fate to specify and require high levels of Notch for their formation. Some speculate this may be the default retinal cell fate in the absence of other fate programmes, given that MG adopt a similar radial morphology to RPCs, have similar genetic signatures, and are able to de-differentiate into RPCs after retinal damage (Roesch et al. 2008). MG maintain an apical attachment to the outer limiting membrane (OLM) and a basal attachment to the inner limiting membrane (ILM) throughout their development and life. Upon specification, MG move their cell bodies, much like other retinal neurons, from the apical surface in a basal direction, eventually residing in the INL, amongst the Amacrine Cells (ACs) and Bipolar Cells (BPs). They then undergo a series of maturation steps. After nuclear migration the MG tile across the retina, a process whereby MG become evenly spaced within the retina so as to ensure full coverage, and avoid overlapping of processes (MacDonald et al. 2017). This appears to be an active process governed by homotypic interactions between MG. For instance, in the zebrafish retina, when MG are laser ablated, others fill the gap with their processes (Williams et al. 2010). The next maturation step involves MG extending processes into all of the retinal cell layers to make contact with all the retinal cell types as well as some blood vessels (MacDonald et al. 2017). This ensures they can carry out their many functions during the development and maintenance of retinal tissue, including metabolic, physical, and functional support, as well as guiding light onto the photoreceptor layer (Jadhav et al. 2009; Reichenbach & Bringmann 2013; MacDonald et al. 2015; Franze et al. 2007).

A recent paper investigating the role of MG in retinogenesis has also revealed a potential role of MG in retinal lamination. MacDonald and colleagues removed MG from the retina using a pharmacological approach to prevent MG from differentiating during retinogenesis. For this, they used a γ-secretase inhibitor called DAPT to inhibit Notch signalling during MG specification. Notch signalling is involved in the genesis of all retinal cell types, but MG are amongst the last cell type to differentiate in the retina. Thus, applying the drug at a very selective time, around 45-48hpf onwards, MG can be selectively eliminated from the retina, without affecting the genesis of other cell types

(MacDonald et al. 2015). By doing this the authors show that retinas void of any Müller Glia still laminate correctly, although the layers are less tightly packed, and occasionally they found tearing in the RGC layer. They then carried out laser cut experiments whereby they cut either the apical or basal process and observe it recoiling, as though under tension. This revealed that MG are held under a certain level of tension within the retina, and that when they are removed, there is a loss of retinal tension.

1.3.3. Retinal Ganglion Cells

Retinal Ganglion Cells (RGCs) are amongst the first retinal cell type to be specified and laminate during retinogenesis. Like all other retinal neurons, they are born at the apical side, but move basally until they reach their cell layer, next to the inner limiting membrane (ILM). They do this by attaching apical and basal processes to the OLM and ILM respectively and moving their cell bodies basally. Once they reach the ganglion cell layer (GCL) they detach their apical process and send out a basal axon which will eventually form part of the optic nerve.

Since they are the first to differentiate and laminate, and form the most basal layer of the retina, one might think that they would be important in setting up the cellular architecture, perhaps by providing a scaffold upon which other cell layers can form. In some live imaging studies it is seen that RGCs interact with neighbouring Amacrine Cells and prevent them from entering the ganglion cell layer, thereby influencing their lamination (Kay et al. 2004; Chow et al. 2015). However in Ath5 and Lakritz mutants, where RGCs are completely absent, the remaining cell types are still capable of laminating correctly in respect to each other, and even form the correct synaptic layers, such as the inner plexiform layer (Kay et al. 2004; Randlett et al. 2013). It is also seen that Amacrine cells interact with each other to establish an inner plexiform layer in the absence of RGCs, which leads one to think that perhaps RGCs guide ACs and help them to laminate but are not essential. Although RGCs may not be essential for lamination of other retinal cell types, they may be influential. A recent study has shown that when RGCs are translocated ectopically during development, i.e. more apically than usual, some other cells such as BPs will organise around them (Icha et al. 2016). It therefore

remains to be seen whether RGCs are necessary for retinal lamination, or just instructive.

1.3.4. Amacrine and Horizontal Cells

Amacrine and Horizontal cells are inhibitory neurons both specified by the same transcription factor – Pancreas transcription factor 1a (Ptf1a). Amacrine cells are the second retinal cell type be specified, although their birth date overlaps significantly with RGCs and BPs. They reside predominantly in the inner nuclear layer (INL), although some displaced ACs reside in the GCL. Previously, it was thought that normally placed Amacrine Cells (iACs) and displaced Amacrine cells (dACs) were segregated due to earlier born dACs becoming trapped by a nascent, forming IPL, followed by iACs being halted by a more mature formed IPL and synapsing on the apical side. However recent live imaging studies have revealed that these cells don't find their positioning simply due to the timing of their differentiation, but that more dynamic cell migratory behaviours are occurring, and cell types appear to communicate with each other to find their appropriate positioning. They also show that horizontal cells differentiate shortly after ACs and migrate to the outer nuclear layer (ONL), away from ACs (Chow et al. 2015). These studies revealed that first, iACs, dACs and HCs, termed retinal inhibitory neurons (RINs) all undergo a common migratory pattern characterised by a bipolar morphology, an apical process attached to the apical surface, and a persistent directional movement from the apical to the basal portion of the retina. This is followed by each cell type adopting multipolar morphology, migrating to the INL, then entering distinct phases of migration. HCs migrate apically to the ONL, adopting a more flattened morphology and further migrating tangentially to form the HC layer. iACs extend processes into the forming IPL on the apical side, and fine tune their soma position by moving tangentially. Finally, contrary to previous assumptions, dACs first synapse with the forming IPL between GCL and BP synapses, then move their soma through the IPL to reside in the GCL (Chow et al. 2015), providing further evidence of the active cell-cell communication occurring during retinal lamination.

All 3 RINs are born at roughly similar times, and initially migrate in similar ways, but later adopt distinct migratory behaviours, perhaps influenced by cell-cell

communication or other tissue cues allowing them to find different cell layers in the developed retina. Given their dynamic nature, and the evident cell-cell interactions occurring during these movements *in vivo* it would be interesting to decipher how important these cell-cell interactions are in the arrangement of these layers.

In the lakritz mutant, where RGCs are absent, interactions between ACs seem to be sufficient for generating the IPL (Kay et al. 2004) suggesting that perhaps they are key to setting up a scaffold for other cells to laminate upon. However, when ACs and HCs are eliminated from the retina all other cells still laminate in the correct order and an IPL still formed (Randlett et al. 2011). This suggests that either ACs and HCs are not necessary for lamination of other cells, or that other mechanisms *in vivo* are compensating in their absence.

1.3.1. Studying lamination *in vivo* vs *in vitro*

These studies have led to questions about whether any of these cells are key players in the process of lamination *in vivo*, but the environment in which they are laminating is subject to other molecular and physical signals which may be compensating for the loss of any particular cell type. To progress the study of lamination it is therefore becoming necessary to move away from the complicated environment *in vivo* and look at these mechanisms *in vitro* where we can begin to look at the cellular mechanisms in isolation, by removing factors such as pre-existing scaffolds and polarity cues often present during development. Only then will we begin to understand the roles of individual cell types and molecules in the process of lamination.

1.4. Organoids and Retinospheroids for studying lamination *in vitro*

1.4.1. Organoid Technology

The use of organoid technology to study developmental mechanisms in various tissues has boomed in recent years. Organoids have also allowed scientists to access the development of various tissues, including stomach (Noguchi et al. 2015), intestine (Sato

et al. 2009; Spence et al. 2011), liver (Broutier et al. 2016), pancreas (Greggio et al. 2013), and kidney (Takasato et al. 2015). They are also used to understand early embryogenesis in the mouse, a period of development that couldn't previously be accessed *in vivo* (Harrison et al. 2017). These organoids, although not perfect, closely model development of the organs they represent and provide researchers with a tool to look closer at the developmental events occurring during tissue morphogenesis. They even allow investigations of the physical mechanisms of morphogenesis (Dahl-Jensen & Grapin-Botton 2017). The work of Sasai and colleagues, who generated well-laminated retinal structures starting from mouse and human stem cells (Eiraku et al. 2011; Eiraku & Sasai 2012), and the cerebral organoids generated by Lancaster and Knoblich (Lancaster et al. 2013; Lancaster & Knoblich 2014) have been particularly exciting for the field of neural tissue organisation. These have provided human models of retinal and brain development whereby one can access the developmental mechanisms and diseases that are specific to humans. Organoids have opened a black box of development, allowing researchers to gain insights into various developmental events, however it is clear that these stem cell-derived organoids still laminate in the context of a great deal of early pattern. In these complex systems, early cues develop before lamination, such as the apicobasal cues, patterned extracellular matrix and localised signalling molecules. Thus, the mechanisms at play in these stem cell-derived organoids may be almost as complex as those in the tissues *in vivo*. It is therefore necessary to work on a more simplified *in vitro* system to understand the role of the cells in pattering, in the absence of pre-existing patterns and cues. The focus of this thesis is to investigate what role cell-cell communication plays in these processes, so we must first simplify the system down to the cellular level.

1.4.2. Reaggregation Studies and Retinospheroids

The reaggregation method involves dissociating cells into a single cell suspension and culturing them in a 3D format, allowing them to come back together as an aggregate of cells. Aggregation cultures, used since the early 20th century, have revealed the ability of various cell types to re-aggregate and re-organise into histotypic tissues in the absence of tissue scaffolds and extrinsic factors. This phenomenon was first seen in basic, monotypic tissues, such as sponge and sea urchin (Herbst 1900; Wilson 1907), when

cells were separated through a fine mesh and allowed to reaggregate, revealing an innate ability of certain cell types to reaggregate and self-organise. These studies provided a platform on which investigations of cell-cell interactions involved in histogenesis began.

In the mid-century, Aron Moscona and colleagues used aggregation studies to investigate tissue formation in a variety of multi-cellular tissues such as limb bud (Moscona & Moscona 1952). These studies revealed the self-organising properties of cells during co-cultures of mesoderm and endoderm cells. Each cell type preferentially bound to its own kind, organising in a manner to promote homotypic interactions, resulting in one cell type organising in the centre of aggregates, and the other surrounding it. Later, it was revealed that even complex, multitypic tissues could self-organise in aggregation culture. Moscona and colleagues were experimenting with aggregation cultures of various tissues when they discovered that the retina, one of the few multi-cellular tissues, was capable of reaggregating into a histotypic arrangement of cells (Moscona 1961). To achieve this, they cultured cells in conical flasks on a gyratory shaker at controlled speeds and temperatures. They tested different cell concentrations, and speed of rotation to reveal differences in cell-cell adhesiveness and patterning within aggregates. Using this method, they discovered that 7-day chick retinal cells were able to aggregate within hours and begin to establish patterning within 24 hours.

A large portion of Moscona's studies focused on the initial cell-cell adhesion involved in this reaggregation and reorganization process. These studies revealed that retinal progenitors can reaggregate in the absence of any scaffolds, and that this is dependent on a molecule called R-Cognin (Moscona 1961; Sheffield & Moscona 1969). This was first identified as a cell reaggregation-promoting factor that played a role in "conferring upon embryonic cells the properties of "selective affinities" and "surface specificities" that are essential for histogenesis" (Lilien & Moscona 1967), describing the homotypic interactions preferred by these cells due to the cell-specific expression of this factor. It was found to be expressed on the surface of retinal cells, but also secreted into the medium as a diffusible factor. Supernatant from previously cultured retinal cells also promoted the reaggregation of cells. This factor was later cloned and identified as retinal cognin (R-Cognin) (Hausman & Moscona 1976) and found to be expressed

uniformly, on the surface of all chick retinal cell types, during early retinal development until retinal stratification (Dobi et al. 1986). Furthermore, it was shown that trypsinisation of the cells induced a time lag in the recovery of the cells ability to reaggregate, due to a delayed re-expression of R-Cognin, also corresponding with previous findings that protein synthesis was required in reaggregation (Hausman & Moscona 1979). These reaggregation studies revealed an important molecular player in the ability of retinal cells to come back together after dissociation and that it had to be actively re-transported to the cell surface. Interestingly, the same study also revealed the age-dependant manner in which these cells were able to reaggregate. Those cultured from younger stages recovered from trypsinisation more quickly and were more capable of reaggregating than those from older stages, suggesting that the expression of this protein changes over developmental time.

Other studies using electron microscopy revealed the ability of retinal cells to aggregate and pattern and characterised the initial stages of aggregation. They revealed that after an initial adhesion of cells into small clusters, cells polarise into their normal polarity, and small clusters of cells fuse together to form larger clusters (Sheffield & Moscona 1969). They also showed that these aggregates comprised features of the cells during development *in vivo.* For instance, aggregates of cells from younger stages contained rosettes with lumens in the centre, termed "lumicentric rosettes", whereas those from older stages contained rosettes with axonal projections in the centre, "axocentric rosettes" representing the more mature state of the cells. They also described that the cells displayed typical cellular polarity in terms of organelle positioning and adherens junction locations (Sheffield & Moscona 1970). These studies highlighted the importance of cell-cell communication in multi-cellular tissue organisation, but aggregates were of an inconsistent size and patterning consisted of rosettes of cells within each aggregate, rather than the aggregate being organised as a whole.

1.4.1. Revealing the cellular mechanisms of lamination using reaggregation studies

Following on from Moscona's studies, Paul Layer and colleagues were able to generate fully stratified retinal aggregates, termed retinospheroids, from embryonic chick retinal

cells in rotary culture (Layer & Willbold 1993; Layer & Willbold 1994; Rothermel et al. 1997), thus revealing the intricate level of organisation these reaggregates can achieve, in the right conditions. These studies highlighted how well these cells can organise in the absence of extrinsic cues and scaffolds, but they also revealed various features of retinal aggregates and began to elucidate some of the developmental, cellular and molecular mechanisms of lamination. Whereas Moscona observed a general organisation within the retinal aggregates, Layer began to describe how these cells organised themselves during the process of lamination and began to reveal some of the mechanisms governing this process.

Layer and colleagues began to investigate the roles of particular cells by removing them and/or replacing them back into the cultures and assessing the effect on lamination. These studies revealed that RPE cells induced a higher order of organisation in chick retinal aggregates in gyratory culture, such as inner plexiform layer (IPL) formation (Vollmer et al. 1984). The cells also layered in a similar order to that *in vivo* and the degree of organisation of these layers was dependant on developmental age of the cells prior to seeding. Cells from younger stages generated better organised aggregates than those from older stages (Vollmer & Layer 1986).

RPE cells were deemed necessary to achieve this stage-dependent higher order of lamination, and they appeared to do this by polarising the cells correctly. Cells cultured without RPE formed aggregates containing rosettes, whereas cells co-cultured with RPE formed fully laminated aggregates (Layer & Willbold 1989). Even culturing aggregates above a monolayer of RPE cells could induce correct lamination (Rothermel et al. 1997), indicating that the mechanism by which RPE cells influence lamination is through a diffusible factor.

These studies also revealed a potential role of MG in lamination, which wasn't revealed in *in vivo* studies. *In vivo* MG typically arrange in a radial spoke-like pattern throughout the retina and make connections in every cell layer. Layer and colleagues revealed this is also the case in retinospheroids but that they play a role in stabilizing retinal cell columns, crucial for lamination in the retinospheroids. When selectively removing Müller Glia with a gliotoxin, other cell types migrated away from the column and

retinospheroids were less organised (Willbold et al. 1995). They also showed that MG, like RPE played a role in whole tissue organization through a diffusible factor. Cells cultured above a monolayer of MG were more capable of forming fully stratified retinospheroids as compared to those cultured without, which displayed inverted internal rosettes throughout (Willbold et al. 2000). This diffusible factor is currently unknown, but some candidates have been explored in reaggregate cultures such as Wnt2-b. Adding Wnt2-b to reaggregate cultures drastically improves the ability of cells to laminate (Nakagawa et al. 2003) but there is no current evidence to suggest that it is MG themselves producing Wnt2-b.

1.5. Reaggregation techniques

Reaggregation cultures have been used for over a century and techniques have varied over time, with the advancement of different technologies, and adaptions to address different issues. For my studies, I want cells only to interact with each other, and not with their surrounding environment. Here I discuss the different techniques used in previous studies to promote reaggregation of cells in a non-adhesive format, and the corresponding benefits and caveats.

The first aggregation studies on sponge and sea urchin simply allowed cells to reaggregate in a drop of medium on a coverslip as they were observed under a microscope (Herbst 1900; Wilson 1907). Later aggregation studies incorporated agitation of the cells in culture dishes to increase chances of cell-cell encounters and improve their likeliness of cells aggregating. Gyratory cultures prevent cells from settling to the bottom of the dish, and provide a centrifugal force to encourage cells together in the centre of the dish (Moscona 1961). Rotary cultures rotate the cultures in tubes, allowing culture of cells in microgravity, however these are more appropriate for tissue explants, rather than cells in suspension (Hoff et al. 1999; Mitteregger et al. 1999; Rzeczinski et al. 2006). More recent advances in technology allow researchers to establish aggregation cultures using a spinning method in so-called “bioreactors” where cells in suspension are constantly spun using a magnetic stirrer and culture medium can be easily exchanged, and growth factors and drugs added or removed (Sutherland et al.

1970; Kim 2005; Lancaster & Knoblich 2014). In all of these methods speed must be closely controlled - not too high as to damage the cells by shear stress, but not too low that they will settle on the bottom and adhere to the surface of the culture dish. They also encourage good transport and exchange of nutrients and oxygen over a long period of time, allowing for production of large aggregates. However, aggregate size and shape is not easily controlled, and aggregates cannot be monitored during culture.

While these methods allow for maximum cell aggregation, some culture methods are simpler, and don't require complex equipment and constant agitation. The hanging drop assay consists of small droplets (10-30μm) of cells in suspension being seeded onto the coverslip of a culture dish which is then inverted to allow the drops to hang. Cells fall to the bottom of the drop with gravity, where they come into close contact with each other due to the curvature of the drop, and begin to aggregate (Foty 2011). Aggregate size can be controlled by adjusting cell concentration before seeding and the process of aggregation can be monitored by imaging the dish from above, through the coverslip with a long working distance lens. The downside to this method is that media exchange is difficult, and certainly impossible before cells have aggregated, so often aggregates need to be transferred to an alternative format for longer term culture. It is also hard to scale up production with this method due to production of only one aggregate per drop, however there are some formats which improve production yield, such as the GravityPLUS™ Hanging Drop System 96-well plate. This allows precise seeding of similar sized drops, followed by harvesting into the GravityTRAP™ plate which allows longer term culture and storage of spheroids (InSphero AG, Zürich, Switzerland) (Amann et al. 2014).

Cells don't always have to be cultured in suspension to achieve aggregation in a non-adhesive format. Aggregates can also be produced in a traditional multi-well plate format if it is coated with a non-adhesive substance to prevent cells from attaching to the plate itself. Lipidure® coated plates (Amsbio) are lined with a biocompatible polymer containing phosphorylcholine, which repels cells. This prevent cells from adhering to the surface of the well, thereby increasing the chances of cell-cell interactions. Aggregates can also be produced using microwell agarose plates, cast from a PDMS mould (Microtissues). Cells do not adhere to agarose, and the small size of the

round-bottomed wells increases cell-cell proximity. These plates are discussed in more detail in the results section.

All methods of aggregation culture have different benefits and caveats, so it must be determined which is most appropriate for the cells being examined and what questions are being addressed. Each study may have different experimental priorities, whether these are mass production for drug screening, visualisation of the aggregation process, or precision of size and shape for quantitation. Reaggregation of retinal cells has led to a big advancement in our understanding of retinal lamination, but many of these studies used gyratory or rotary culture to encourage cells to aggregate in the first instance (see Chapter 1), which meant that it was difficult to control aggregate size and shape. It also meant that cells couldn't be viewed until harvested at the end of culture. On top of this, culture protocols were often time-consuming, and access to the process of aggregation and lamination was limited by the need to fix, section and label the cells after culture. Finally, identification and manipulation of the cells and molecules involved in these processes was limited by the genetic tools available for the model organisms used at the time. These are the challenges I aim to overcome in this thesis to allow the advancement of these studies.

1.6. Research objectives

Aggregate studies provide a platform upon which to investigate some of the fundamental mechanisms of retinal lamination. Previous studies have revealed the importance of developmental stage on the ability of cells to reaggregate, and the role of certain cell types in the full reconstitution of retinal layers. They have even led to physical and theoretical considerations of how tissues might self-organise including differential adhesion or tension between cells (Steinberg 2007; Heisenberg & Bellaïche 2013). While these reaggregation studies began to reveal the fundamental mechanisms of retinal lamination that couldn't be investigated so easily *in vivo*, many of the techniques used were still time consuming, and limited by the genetic tools available at the time. This limited the extent to which researchers could manipulate cells or molecules of interest to explore their role in lamination.

Many of these challenges can be addressed using the zebrafish retina as the model of lamination. Zebrafish have been used in many studies of retinal development due to their transparency during development, relatively short developmental time, and the range of genetic tools available to label cells and manipulate cells and molecules of interest. Thanks to this, we now know a lot about zebrafish retinal development *in vivo* which provides a strong platform on which to continue our investigations of the mechanisms of lamination. We know roughly when the different cell types are born, and when they become laminated (Randlett et al. 2013; Almeida et al. 2014; Chow et al. 2015), therefore we know which times in development to look at in our system. In fact, retinal lamination occurs between 24hpf and 72hpf, a relatively short time window in comparison to other organisms. We also understand some of the genetic components of cellular differentiation, making it possible to manipulate cell populations (Kay et al. 2001; Agathocleous & Harris 2009; Jusuf & Harris 2009) Finally, we have various tools available, including various transgenic lines and antibodies for labelling, to allow us to visualise and manipulate the different cell types or molecules in either fixed or live tissue (Kay et al. 2001; Bernardos & Raymond 2006; Jusuf & Harris 2009; Almeida et al. 2014).

Aggregate studies are useful for investigating the roles of particular cells or molecules in lamination, but we still don't know precisely which are the mechanisms governing this. In this thesis, I aim to address some of these questions by establishing a novel zebrafish retinal reaggregation model with which to accelerate and expand these investigations.

1.6.1. Establishing a Novel Zebrafish Retinal Reaggregation Model

Zebrafish cells are not commonly used in cell culture and there are not many established techniques available. Zebrafish retinal neurons have only previously been cultured on laminin coated plates in a simple culture medium over a short period of time (Zolessi et al. 2006; Randlett et al. 2011; Chen et al. 2013). They have never been cultured as a reaggregation culture.

In Chapter 3 I present the development of a novel zebrafish retinal reaggregation model with which to investigate the mechanisms of retinal lamination. This involved establishing the best methods to dissociate and culture zebrafish retinal cells in a non-adhesive environment, imaging the resulting reaggregates to examine the position of the different retinal cell types and development of a novel method for quantifying the lamination in these aggregates. I also describe some of the developmental mechanisms involved in the reaggregation and lamination of retinal cells, including the role of R-Cognin in reaggregation, and the importance of developmental stage in the ability of the cells to laminate.

1.6.2. Investigating the Cellular and Molecular Mechanisms of Zebrafish Retinal Lamination

In Chapter 4 I investigate the roles of several cell types in retinal lamination, using this new reaggregation model. Cell types that are investigated include Retinal Pigment Epithelial Cells, Müller Glial Cells, Retinal Ganglion Cells, and Amacrine and Horizontal Cells. To do this I generated cell-type deficient aggregates and assessed any changes in the ability of the remaining cell types to organise as an indicator of whether they are key players in the process of retinal lamination.

Finally, in the discussion chapter I summarise what I have learned during the course of this thesis and discuss future directions to continue these investigations.

CHAPTER 2

Methods

2. Methods

A large portion of this project comprised finding the optimal conditions for culturing zebrafish retinal cells in a 3D format and analysing the resulting organisation within these aggregates. Here I will describe the final protocols used to gain the data shown later in the thesis, but the process of optimisation of these conditions is discussed in Chapter 3.

2.1. Animals

Adult zebrafish were maintained and bred at 26.5°C. Embryos were collected on the morning of the day before the start of culture. Embryos were maintained in embryo medium at 28.5°C and staged in hours post fertilisation (hpf) according to morphological features, as previously described (Kimmel et al. 1995). Embryos were treated with 0.003% N-Phenylthiourea (PTU) from 8hpf onwards to prevent pigment formation.

2.2. Transgenic lines and mutants

Transgenic lines Ptf1a:cytGFP (Godinho et al. 2005), Crx:gapCFP (Almeida et al. 2014) and GFAP:GFP (Bernardos & Raymond 2006), and the polytransgenic SoFa1 line (Atoh7:gapRFP/Ptf1a:cytGFP/Crx: gapCFP) (Almeida et al. 2014) have all been previously described. Ptf1a: cytGFP/Crx:gapCFP embryos were obtained by crossing homozygous Ptf1a:cytGFP and Crx:gapCFP lines.

2.3. Embryo injections

Morpholinos and RNA constructs were injected into embryos at the one or two cell stage. Morpholinos were prepared and injected at the following concentrations: 4ng of Ath5 MO (5'-TTCATGGCTCTTCAAAAAAGTCTCC-3', Gene Tools); 12ng each of Ptf1a MOs (translation blocking Ptf1a MO1 (5'-CCAACACAGTGTCCATTTTTTGTGC-3', Gene Tools)) and splice blocking Ptf1a MO 2 (5'-TTGCCCAGTAACAACAATCGCCTAC-3', Gene Tools)) if

injected independently, or 8ng of each if co-injected; 2ng or 4ng of Su(H) 5'MO (5'-CGCCATCTTCACCAACTCTCTCTAA-3' Gene Tools); 2ng of Her2 MO2 (5'-CTGGAAAGAGAAGGTAAAAGTTTGG-3', Gene Tools, kind gift of the Cheng lab) 6ng Lhx2b MO (5'-GCTTTTCTCCTACCGTCTCTGTTTC-3', Gene Tools); 4ng of P53 MO (5'-GCGCCATTGCTTTGCAAGAATTG-3', Gene Tools). Her2 dominant negative RNA (her2ΔWRPW) (kind gift of the Cheng lab) was prepared on ice and injected at 2ng (Cheng et al. 2015).

2.4. Preparation of solutions and cell culture medium

2.4.1. Stocks and Solutions

The following stocks and aliquots were prepared and stored for long-term use:

1. L-15 (Leibowitz's L-15 Medium with L-glutamine, Thermo Fisher Scientific) stored at 4°C.
2. PSF (Antibiotic-Antimycotic (100x), Thermo Fisher Scientific). Aliquoted and stored at -20°C.
3. PTU (N-Phenylthiourea, Sigma) 40x concentrated stock stored at 4°C.
4. FBS (Fetal Bovine Serum, Thermo Fisher Scientific): Aliquoted (100µl) and stored at -20°C.
5. MS-222 (Tricaine methanesulfonate, Sigma): 100x concentrated stock aliquoted (1ml) and stored at -20°C.
6. Trypsin-EDTA 0.25% (Sigma). Aliquoted (1ml) and stored at -20°C.
7. N2 supplement (Thermo Fisher Scientific). Aliquoted (100µl) and stored at -20°C.
8. Calcium-free medium, as previously described (Harris & Messersmith 1992). The final working concentrations (1x) were: 116.6 mM NaCl, 0.67 mM KCl, 4.62 mM Tris, 0.4 mM EDTA. Dissolved in water to make a 10x concentrated stock, pH adjusted to 7.8 and stored at 4°C for up to 6 months.
9. Heparin solution (Heparin sodium salt, Sigma): The final working concentration (1x) was 100µg/ml. Dissolved in water to make a 10x concentrated stock and stored at 4°C for up to 6 months.

10. Calcium-free Ringer's solution: 116 mM NaCl, 2.9 mM KCl, 5.0 mM HEPEs, dissolve in water. (1M working concentration, pH 7.2, stored at 4°C for up to 6 months).
11. Embryo extract (see below)

2.4.2. Embryo extract

Embryo extract was made using the following protocol, as adapted from ZFin: (https://zfin.org/zf_info/zfbook/chapt6.html) :

1. Grow wild type zebrafish embryos until 72hpf.
2. Dechorionate the embryos then chill them on ice
3. Transfer the embryos to a Dounce homogeniser, remove most of the embryo medium and rinse with 0.5% bleach for 2 min (re-suspending the embryos a few times), then with calcium-free Ringer's solution for 2 min.
4. Remove as much liquid as possible and homogenize thoroughly.
5. For every 200 embryos, add 1 ml L-15 supplemented with 1% PSF.
6. Aliquot and store at -20°C for up to 1 month, or at -80°C for up to 6 months.

2.4.3. Preparation of dissection and culture mediums

The following solutions were prepared on the day of dissection and culture:

1. Dissociation medium: From the stocks and solutions previously prepared, the following volumes were mixed: 2ml Calcium-free medium, 2 ml Heparin solution, 200µl MS-222, 200µl PSF (Thermo Fisher Scientific) and 500µl PTU and filled up to 20ml with water.
2. Cell washing medium: L-15 supplemented with 3% FBS.
3. Cell culture Medium L-15 supplemented with 10% embryo extract, 3% FBS, 2% N2, 1% PTU, 1% PSF. Enough was made for 750 µl per culture dish.

2.5. Isolation of Zebrafish Retinal Cells

Retinas were isolated from embryos of various stages. RPE was left attached in all experiments, unless otherwise stated. For all stages the solutions used were the same, but incubation times and dissection technique varied.

The following equipment was prepared prior to dissection:

1. Dissecting stereo microscope with transmitted light base.
2. Sylgard dissecting dish: Dishes prepared prior to starting the protocol using the Sylgard 184 Silicone Elastomer Kit (Dow Corning). The base and curing agents were mixed together in a 10:1 ratio and poured into the bottoms of 3cm culture dishes and baked at 65°C overnight to set.
3. Two dissecting pin holders with 0.125mm tungsten needles (Fine Science Tools).
4. Two glass pasteur pipettes, narrowed using a Bunsen burner: one wide enough for transferring embryos and one narrower, for dissociating with. New pipettes were prepared for each dissociation.
5. 10ml petri dishes.
6. Three-well glass dish (Pyrex, Corning).
7. 1.5ml tubes.
8. Table top centrifuge, accurate at low speeds (around 300 g).
9. Cell counter (Improved Neubauer).
10. Large bucket of ice.
11. Waste container with bleach.

2.5.1. Dissection of Retinas from 24hpf/36hpf Zebrafish Embryos

The following protocol is adapted from a previously published protocol (Zolessi et al. 2006) but with significant modifications. A maximum of 5 embryos at a time were transferred using a wide bored glass pipette, in a minimal amount of embryo medium, to a dish containing washing medium. After swirling the dish, they were then transferred to the dissecting dish. Retinas were dissected using two dissecting pins by gently teasing apart the tissues surrounding the retinas, making sure to not cut into the retinas and to leave the RPE attached. Where RPE was removed, this was done by making a small incision in the RPE layer, and gentle teasing/rolling of the retina away from the RPE layer. Debris was discarded from the dish in the waste container before transferring the retinas in dissecting medium to the glass dish on ice. The above steps were repeated as necessary until the desired number of retinas were collected.

2.5.2. Dissection of Retinas from 48 and 72hpf Zebrafish Embryos

Retinas from 48hpf and 72hpf embryos were dissected using slightly different techniques. The tissues were not as soft as in 24hpf embryos, so a pair of forceps was used to hold the embryo in position while a dissecting pin was used to make an incision in the outer layer covering the retina, then the retina was pushed out by applying pressure from the opposite side.

2.5.3. Dissociation of Retinas into a Single Cell Suspension

For 24hpf retinas the glass dish containing retinas and a trypsin aliquot were removed from the ice and allowed to come to room temperature. As much dissociation medium as possible was removed from the dish, without disturbing the retinas. Retinas were incubated with 200µl Trypsin-EDTA per 20 eyes for 12 minutes at room temperature. 48hpf and 72hpf retinas were incubated with the trypsin at 28°C for 15 minutes. Trypsin-EDTA was then replaced with 200µl dissociation medium per 20 eyes.

Retinas were first disrupted by gentle trituration using a narrow-bore glass pipette until mostly dissociated then triturated more vigorously using a P-200 pipette until a single cell suspension was achieved. The cell suspension was transferred to a 1.5ml tube and supplemented with washing medium to stop any further reaction. Cells were then washed twice more with washing medium followed by centrifugation at 300 *g* for 7 mins to form a loose pellet. Cells were concentrated appropriately by removing the desired amount of supernatant. Cells were left no longer than 20-30 minutes on ice to prevent them from re-aggregating before seeding.

2.6. Cell counting, viability and cluster analysis

Cells were counted, and percentage viability and cluster sizes were calculated using the LUNA-FL Dual Fluorescence Cell Counter (Logos Biosystems). Cells in suspension were mixed with an Acridine Orange/ Propidium Iodide mix (Logos Biosystems) and analysed in fluorescence mode. Cells are counted by identification of signal above an average size threshold. Percentage viability is calculated as a proportion of Acridine

Orange/ Propidium Iodide signal. Cell clusters are calculated using the area of each cluster / average size of a single cell.

2.7. Preparation of agarose microwell culture dishes

Agarose micro-well dishes were prepared as previously described (Napolitano et al. 2007), from 3D Petri Dishes (Microtissues), but with some modifications. Some moulds were also modified to reduce the size of the moulds to produce just 15 wells, rather than 35. The moulds were sterilised in 70% culture dish grade ethanol for 20 mins then allowed to air dry in a culture hood. Aliquots of sterile agarose were heated to 65°C for at least 20 minutes, mixed thoroughly, then 330µl agarose was pipetted into each 35-well mould, or 350µl into the modified 15-well mould. Agarose was allowed to set for 20 minutes and the formed microwell dishes pushed out from the moulds into a 4-well culture plate. 750µl Equilibration medium was added to each dish and left for at least 20 minutes to allow the dishes to equilibrate. Just before seeding, equilibration medium was replaced once more.

2.8. Culture of Zebrafish retinal cells

After cell isolation, cells were resuspended well in the culture medium and seeded into the agarose dishes. If the 35-well plates were being used, 75µl cell suspension was prepared at a concentration of roughly 5.3 x 10^5 cells per ml and the full amount seeded. If the 15-well plates were being used, 45µl cell suspension was prepared at a concentration of roughly 3.8 x 10^5 cells per ml and the full amount seeded.
Cells were seeded in a drop-wise fashion from directly above the dish to allow even dispersion of cells. After allowing cells to settle for 20 minutes, 750µl culture medium was added via the medium exchange port to prevent disruption of the cells. Cells were cultured at 28°C for 48 hours.

2.9. Drug application

For the Müller Glia experiments, embryos were incubated with 25 µM DAPT (Sigma) or the equivalent volume of DMSO starting from 45-48 hpf, or 63 hpf. Cells were also

incubated with 25 μM DAPT or the equivalent volume of DMSO starting from the equivalent time of 45-48 hpf, or 63 hpf. The drug was applied to the cells by removing 500μl culture medium from the dishes already in culture, adding the DAPT, mixing thoroughly, then replacing to the culture dishes carefully, to avoid disrupting the aggregates. For the R-Cognin experiments, cells were incubated with 5, 50, 100 or 200 μM PACMA31 (Sigma) or the highest equivalent volume of DMSO from the time of cell seeding onwards.

2.10. Fixation and mounting

Aggregate fixation and staining were all carried out within the agarose micro-well dishes. Media was exchanged via the medium exchange ports to avoid flushing out the aggregates. Aggregates were first rinsed with PBS then fixed with 4% PFA at room temperature for 15 minutes. From this point, aggregates were kept away from light to avoid photo-bleaching of fluorophores. After fixation, aggregates were washed 3 x 5 min with PBS. Aggregates were mounted using Vectashield hard-set mounting medium with DAPI, on microscope slides protected between reinforcement rings, and covered with 13mm round coverslips (no.0). Samples were either imaged immediately or stored at 4°C for up to one month, depending on stability of the fluorophores.

2.11. Immunostaining

Aggregates were stained whole-mount within the agarose micro-well dishes. They were first fixed as described above, but the washing steps were replaced with those outlined below, keeping dishes away from light between each step. Aggregates were washed once quickly and then incubated for 10 min with 0.1% PBS-T. Aggregates were then washed for 10 min with PBS. Aggregates being stained with Zn5 antibodies were subjected to an extra blocking step: they were blocked for 20 mins at room temperature (10% HIGS, 1% BSA, 0.5% Triton, diluted in 1x PBS) then washed with PBS. PBS was removed, and aggregates incubated with 200μl primary antibodies diluted in PBS, added just to the seeding chamber of the microwell dishes. Culture plates were sealed with parafilm to prevent the dishes drying out and left at 4°C overnight. Primary antibodies were removed, and aggregates washed for 10 min with 0.05% PBT.

Secondary antibodies were added, and dishes placed on a rocker at a very slow speed for 2 hrs at room temperature. Aggregates were then washed for 10 min with PBS with rocking. After one final quick wash with PBS, aggregates were mounted using the same protocol as above. Primary antibodies used were as follows: mouse anti-Zn5 (1:100, ZIRC); mouse anti-GFAP (1:100, ZIRC); Secondary antibodies were diluted 1:500 in PBS and DAPI was diluted 1:1000.

2.12. Time-lapse of cells aggregating in microwell dishes

Time-lapse movies were taken using a Nikon Eclipse 80i upright microscope with a Nikon Plan Fluor 10x (N.A.=0.3) phase DIC objective and a Hamamatsu ORCA-ER C4742-80-12AG cooled CCD camera. Images were acquired using a Volocity Acquisition package (Improvision). Images were taken in 2µm slices, every 2 mins for 15 hours. The movie shows the first 3 hours of aggregation played at 10 frames per second. It is shown as a compressed stack to visualize the aggregates in 3D.

2.13. Imaging of aggregates with Laser Scanning Confocal Microscopy

Aggregates were imaged under an oil-immersion 60× objective (NA=1.30) using an inverted laser-scanning confocal microscope (Olympus FV1000). The centre point of aggregates was found by looking for the start and end-point in the DAPI channel. Images were acquired for seven z-slices at the centre of each aggregate as 1µm optical sections using the same settings throughout: 1024x1024 resolution, 12.5 µs/pixel scanning speed. Data were acquired using Olympus FV1000 software and analysed using Volocity Software (Perkin Elmer).

2.14. Analysis of patterning by Isocontour Profiling

Aggregates were analysed for patterning using isocontour profiling calculated using custom-made Matlab scripts made in collaboration with Dr Leila Muresan from the Cambridge Advanced Imaging Centre in the department of Physiology, Development and Neuroscience. These scripts have been deposited at: http://caic.bio.cam.ac.uk/dataanalysis/projects/aggregateimages/scripts

To analyse the patterning of these aggregates, isocontour profiles were computed using integrated fluorescence along concentric bands up to a maximal radius (Centre to Periphery: CtoP) or starting from the perimeter towards the centre, along shrinking bands (Periphery to Centre: PtoC). The average fluorescence intensity is computed for each band (sum of pixel intensity for all the pixels inside the band divided by the number of pixels in the band) and plotted against the distance of the band from the barycentre of the selected polygon. For the computation of bands in the CtoP case the image was transformed into polar coordinates, while for the PtoC case the Matlab distance function was used.

The script "ComputePatterns" computes both versions. The width of the band can be set as parameter w in line 13 (by default w = 5 pixels). The input image files were multipage Tiff stack format. The order of the images in the stack was: CFP channel, GFP channel, RFP channel, brightfield, DAPI. If DAPI was missing, the script replaced it with the brightfield image for the subsequent computations.

Upon opening the "ComputePatterns" Script it prompts the user to select the first Tiff stack file for analysis. It will then prompt the user to draw the outline of the aggregate to be analysed. The centre point and outline of the aggregate are then shown superimposed to the DAPI image.

Fluorescence profiles are computed and saved as csv files. When all samples of that condition have been analysed another script called "MakeFigures" is run. The user is prompted to select the source folder, where all the csv files are saved for that condition and the script will produce the following graphs:

- [filename]. Showing the fluorescence profiles for each individual sample

By default, this part of code is commented out but removing comments from lines 79 - 98 will generate the figures.

- [FigAll_samples_profiles]. Showing all fluorescence profiles on the same graph.
- [Figfilename_ecdf]. This shows the fluorescence profiles plotted as an empirical cumulative distribution function (ecdf) for each individual sample. By default,

this part of code is commented out but removing comments from lines 110 – 126 will generate the figures.

- [FigAll samples_profiles_with error]. This shows the fluorescence profiles for all samples in that condition, with sample error. Shown only if at least two profiles available.
- [FigAll samples_ecdf_with error]. This shows the ecdf plots for all samples in that condition, with sample error. Shown only if at least two profiles available.

Choosing one of two options for the parameter "CorP" in line 8 of this script will select if the figures are generated based on either CtoP isocontours (CorP =1), or PtoC isocontours (CorP =2). This script will then produce a csv file called [Area_measurements.csv] containing the areas measured under the ecdf curves for the RFP, CFP and GFP channels for each aggregate and the area between the CFP and GFP ecdf curves. This is the measure of organisation of the aggregates. Data in the final column (AUC CFP- AUC GFP) was used to compare one condition to another. The differences between each condition were analysed using the nonparametric Mann-Whitney U test to gain a measure of statistical significance.

CHAPTER 3

Zebrafish Retinal Cells Self-Organise in 3D Culture

3. Zebrafish Retinal Cells Self-Organise in 3D Culture

3.1. Focus of this chapter

This chapter focusses on the development of a novel culture method for zebrafish retinal cells in a 3D format. I explain the optimisation processes for the dissociation and culture of the cells and the testing of two different 3D culture formats. I also explain how I identified these cells, revealing how they are capable of self-organising into distinct layers. During this process, it was also revealed that developmental stage is important for the ability of these cells to self-organise, and that they appear to be organising in the same order as they do *in vivo*. Finally, I explain the development of a method to analyse the organisation in these aggregates as a metric of lamination for comparison of this layering within later experiments.

3.2. Optimisation of dissociation

The aim of this thesis is to investigate how zebrafish retinal cells form their layers in the absence of extrinsic scaffolds and cues from surrounding tissues. To do this I first needed to establish a cell dissociation protocol that allowed me to gain a single cell suspension containing cells healthy enough for culture.

3.2.1. Dissociation of 72hpf and 48hpf retinas

A dissociation protocol has been used previously in the lab to dissociate retinal cells from 72hpf retinas (Almeida et al. 2014) so I started with that protocol and adapted it for my own needs. As described in the previous protocol, embryos were grown under normal conditions, then for dissection, transferred to a calcium-free dissociation medium supplemented with heparin and MS-222 anaesthetic (see methods) and retinas, plus attached RPE, were collected in this medium (see Figure 3.1). Similarly, retinas were then incubated with Trypsin-EDTA for 10 min at 37°C, replaced with ca-free medium and dissociated by trituration using a fire-pulled glass pipette.

While this protocol allowed collection of a single cell suspension, I found that cell yield wasn't sufficient for cell culture, so I adapted the protocol to increase yield and viability. First, I tried replacing Trypsin with Papain, a gentler digestive enzyme, but cell numbers immediately after dissociation were roughly equal (numbers not shown) and aggregates cultured using cells from either protocol looked equally healthy. I therefore decided to stay with Trypsin, as the protocol required less steps. Cell counts immediately after dissociation of 72hpf retinas were roughly 12,000, as shown in Figure 3.1. Compared to an estimated 20,000 cells per 72hpf retina *in vivo* (He et al. 2012). Cell yield wasn't optimal but was deemed sufficient for culture.

3.2.2. Dissociation of 24hpf retinas

Later in this thesis I describe how the nature of the experiments led me to culture cells from 24hpf retinas. Retinas from 24hpf embryos are much smaller and the different layers of tissue are less tightly formed, meaning the cells disaggregate much easier than those in older retinas. Applying the previous dissociation protocol to these retinas seemed to be too harsh for the younger retinas, as relative cell yield decreased, and therefore needed to be optimised for this stage. I first tried changing the temperature of trypsin incubation. The optimal activation temperature for Trypsin is 37°C but it can be sub-optimally activated at lower temperatures as well. Since 37°C is much higher than the temperature at which zebrafish embryos normally grow, it is hypothesised that subjecting the cells to that temperature would stress them. I therefore wanted to find the lowest temperature at which trypsin was still active enough to aid in the dissociation of the cells. I tried 32°C, 28°C and room temperature (RT). Cells dissociated well after incubation at all temperatures, so I decided to continue incubation at RT, although incubation time had to be increased from 8 min to 12 min for effective dissociation. Another previously used protocol used to isolate RGCs from younger stage retinas (Zolessi et al. 2006) also describes adding 10% FBS to the cell suspension to inactivate any further Trypsin activity. Supplementing the L-15 in the final washing step with FBS also increased cell yield, as counted just before seeding.

During this time, I was also able to trial a Luna FL Automated Cell Counter. Samples were mixed with an Acridine Orange (AO)/ Propidium Iodide (PI) mix and loaded onto

a slide. Cells were automatically detected by the counter and a readout of cell count; clump analysis and cell viability were given. As shown in Figure 3.1 cell yield was consistently high, between 2000 and 3000 cells per 24 hpf retina, compared to an estimated 2000 cells in a 24hpf retina *in vivo* (He et al. 2012). This was therefore an extremely high yield, and in some cases shows that the retinas may have even been older that 24hpf (and therefore had incurred more cell divisions). Cluster analysis showed that over 95% of these dissociated cells were counted as single cells; and cell viability immediately after dissociation was over 96%. This dissociation protocol was therefore deemed sufficient for gaining cells for culture. A summary of all adaptations made during the optimisation process and the final protocol can be seen in Table 3.1.

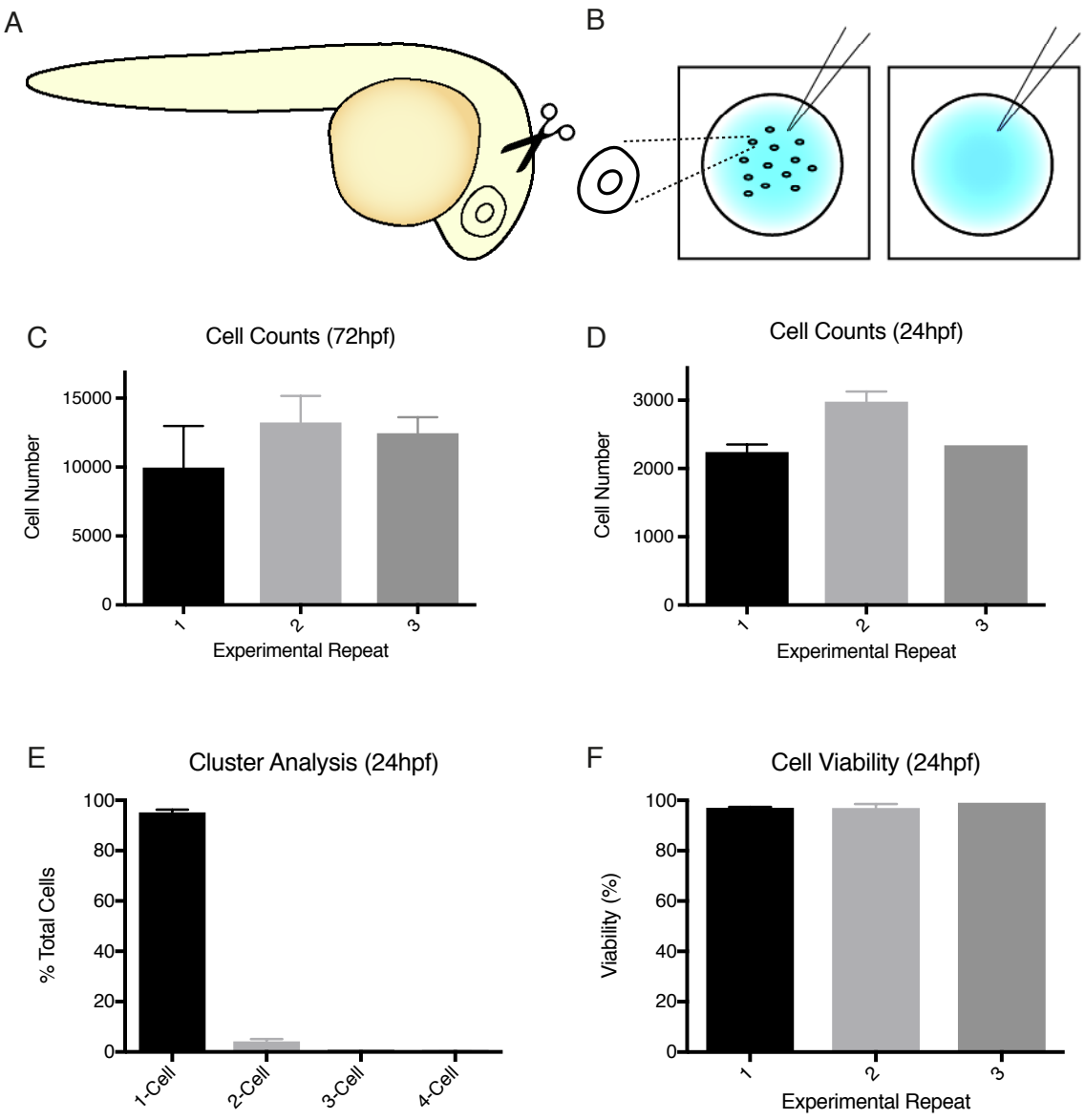

Figure 3-1: Dissociation of zebrafish retinal cells.

(A,B) Schematic representing retinas dissected from 24 hpf zebrafish (A), collected into glass dishes and dissociated into single cells (B). (C) Cell yield after dissociation of 72hpf retinas (cell number per retina) (n = 3 for each). (D) Cell yield after dissociation of 24hpf retinas (cell number per retina) (n = 3 for each). (E) Cluster analysis for the same experiments as in (D) (n = 9). (F) Percentage cell viability for the same 3 experimental repeats as in (D,E).

Table 3-1: Adaptations of the dissociation protocol				
	Stage	**Enzyme**	**Incubation Temp**	**End of reaction**
Zolessi et al. 2006	28hpf	Trypsin-EDTA	28.5°C	L-15 + 10% FBS
Jonathan Tham	72hpf	Trypsin-EDTA	28.5°C / 32°C	Ca-free diss. med.
Me	48/72hpf	Trypsin-EDTA	28.5°C / 32°C	Ca-free diss. med.
Me	48/72hpf	Papain	28.5°C / 32°C	Ca-free diss. med.
Me (Final Protocol)	24hpf	Trypsin-EDTA	RT / 28.5°C / 32°C	Ca-free diss. med. then L-15 + 10% FBS

3.3. Optimisation of culture

To investigate how these cells, behave in an environment void of other influencing factors such as scaffolds or molecules I next turned to finding an appropriate 3D culture format.

3.3.1. The Hanging Drop Technique

One of the most common methods for culturing cells in a non-adhesive 3D environment is using the hanging drop technique (Foty 2011). Cells are cultured within a drop of culture medium suspended from a surface such as the coverslip of an inverted culture dish. After the drop is seeded the dish is inverted and cells fall to the bottom of the drop by gravity. The round shape of the drop increases proximity between cells and minimises interactions with any surface. This method has been used as a non-adhesive culture of various cell types due to its simple design. For my experiments, I dissected roughly 20 eyes per condition and cultured cells at a concentration of 7×10^5 cells per ml, as 10ul drops. I adapted this method slightly as I was finding the drops were drying out before the end of culture. To remedy this, I added a humidity chamber to the dish consisting of a shallow dish filled with PBS added into the bottom of the culture dish to keep the environment humid. Using this method, I found that zebrafish retinal cells can aggregate within 24-48 hours in vitro (hiv) in a minimal culture medium, however the level and rate of aggregation varied from one experiment to another. As seen in Figure 3.2 B some cells formed one large aggregate, whereas others formed multiple smaller aggregates. This made it difficult to quantify any patterning seen in aggregates, as later described in this thesis, so I looked for an alternative 3D culture format to produce aggregates of a more consistent size and shape.

3.3.2. The 3D Petri Dish

The 3D Petri Dish is a commercially available PDMS mould containing several rounded pegs from which agarose micro-well dishes can be cast (Napolitano et al. 2007). This dish was originally developed to overcome some of the challenges associated with other non-adhesive 3D culture techniques such as low throughput and limitation in tissue

shape. The dish supports the culture of various cell types including human breast cancer cells, human fibroblasts, rat hepatoma cells and rat glioblastoma cells and have also been previously used to culture dissociated primary zebrafish ectoderm and mesoderm germ layer progenitor cells (Klopper et al. 2010).

Being made from agarose, cells do not adhere to the surface of these dishes, thereby creating a micro-environment which encourages cells to adhere to each other. Agarose is also porous, meaning nutrients and oxygen can diffuse easily through the dish. The dishes cast from the PDMS mould fit into the wells of a 24-well plate which contains the culture medium, allowing for easy medium exchange, and the wells within these dishes have a diameter of just 800μm and a depth of 800μm with a rounded bottom, increasing the proximity between the cells in each well. There are a variety of dishes with different sizes, shapes and numbers of wells, but for these experiments I used the "24-35 Large Spheroid" dishes which fit into 24 well plates and have 35 wells each (5 x 7 array). The number of wells in these dishes was quite high for my experiments, given the limited number of cells used as a starting material, so I customised these dishes by removing the outer rows and columns of pegs with a sharp scalpel to reduce the capacity of the dishes to just 15 wells (3 x 5 array).

Culturing the cells in these 3D Petri Dishes produced drastically more consistent results, both within and between experiments. Figure 3.2 shows the comparison between cells cultured using the hanging drop technique and those cultured with the 3D Petri dish after 48hic. Cells in the 3D Petri Dish (Fig 3.2 D) have mostly all aggregated into one, round aggregate of similar size in each well, whereas those in the hanging drops (Fig 3.2 B) are of varying sizes and shapes. I decided to continue my experiments in the 3D Petri Dish as these gave more reproducible, quantifiable results.

3.3.3. Culture Medium and Supplements

Finally, I needed to find the best culture medium for these cells to allow them to remain as healthy as possible during culture, so they would behave as normally as possible. I started with a basic medium of L-15 supplemented with PSF. Within 24 hours the cells were mostly aggregated into one aggregate at the centre of the well. Next, I tried the

addition of FBS and zebrafish embryo extract. FBS is a supplement commonly used in cell culture due to the rich variety of proteins available which aid in cell survival and stimulate growth. As shown in Figure 3.3, aggregates cultured with additional FBS (Fig 3.3 B) appear to be larger than those cultured without (Fig 3.3 A). This could be due to the role of FBS in cell growth and survival, however this was not tested. Another supplement that can be added to cell culture is Embryo Extract. Extract from embryos of chick or trout have been used previously in various cell culture protocols as a rich source of growth factors (Stemple & Anderson 1992; Bradford et al. 1994). A recipe deposited on ZFin and in the Zebrafish Book (Westerfield 2007) also suggested the addition of zebrafish embryo extract to dissociated cell culture. The extract is prepared ahead of time and stored at -80°C. It is made from crushed 72hpf zebrafish embryos and added directly to the culture medium, before it is filtered. As shown in Figure 3.3, aggregates cultured with Embryo Extract (Fig 3.3 C) were yet again larger and more compact than those without (Fig 3.3 A). Aggregates cultured with both FBS and Embryo Extract (Fig 3.3 D) were the largest and most compact so it is assumed they were healthier. I decided to continue with both supplements in the culture medium.

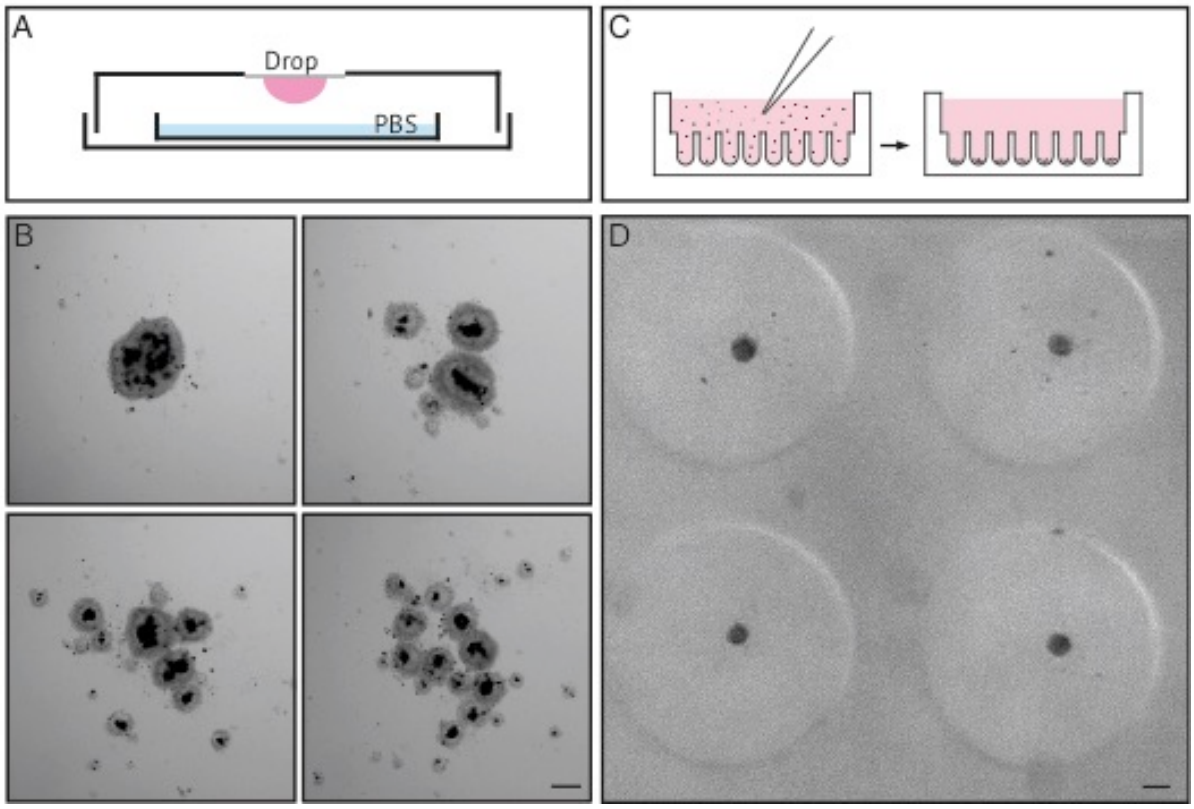

Figure 3-2: Comparison of Zebrafish retinal cells cultured using the Hanging Drop method vs The 3D Petri Dish

(A) Schematic representing the hanging drop setup. Cells were seeded on the coverslip of a culture dish and inverted. A smaller dish containing PBS was placed inside to maintain a humid environment to prevent the drop drying out. (B) Representative examples of aggregates produced using the hanging drop method. Note the varying degrees of aggregation, some generating 1 whole aggregate, and others generating multiple smaller aggregates. Scale bar = 100µm. (C) Schematic representing the seeding chamber of the 3D Petri dish. After seeding, cells settle into individual wells. (D) A representative example of 4 wells of a culture in an agarose microwell dish cast from the 3D Petri Dish PDMS mould. Note the consistent size and shape of each aggregate. Dark cells are RPE, which reside in the centre of almost all aggregates. Scale bar = 100µm.

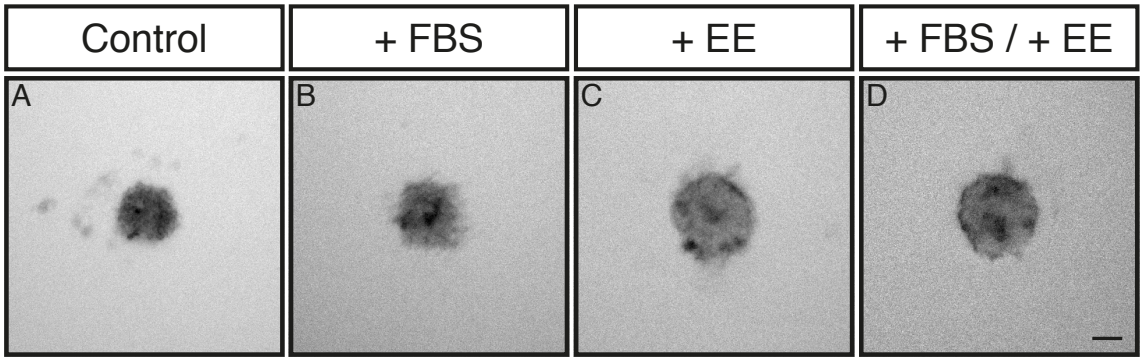

Figure 3-3: Optimisation of supplements added to the culture medium

Comparison of cells cultured in the absence or presence of various supplements (n=3). (A) Cells cultured in control conditions (L-15 + PSF). (B) Cells cultured in control conditions and supplemented with FBS (+FBS). (C) Cells cultured in control conditions and supplemented with embryo extract (+EE). (D) Cells cultured in control conditions and supplemented with FBS and embryo extract (+FBS/+EE). Dark cells are RPE. Scale bar = 50µm.

3.4. Mechanisms of retinal reaggregation

Once I established the culture protocol I first began investigating the mechanisms of reaggregation. This involved looking at the behaviour of the cells as they aggregated and whether there were any important factors involved in this process.

3.4.1. Zebrafish retinal cells reaggregate quickly, within 3 hours of dissociation

To characterise the reaggregation process a time-lapse movie was taken starting immediately after cells were seeded and continuing for 15 hours. As shown in Figure 3.4 and Movie 1, after seeding, cells quickly settled to the bottom of the dish in the centre (due to its rounded shape) (Fig 3.4 D) and began to actively reaggregate within just 60 minutes (Fig 3.4E). After 3 hours, the cells were mostly aggregated (Fig 3.4 F), and by 15 hours the cells had undergone what looks like compaction (Fig 3.4 H).

3.4.2. Retinal Cognin is required for zebrafish retinal cell reaggregation

R-Cognin is expressed uniformly across the retina (Dobi et al. 1986) and has been shown to play a role in retinal reaggregation in chick (Moscona 1961; Lilien & Moscona 1967; Sheffield & Moscona 1969) so we hypothesised it might also be important for retinal reaggregation in zebrafish. R-cognin is a member of the protein disulphide isomerase (PDI) family (Pariser et al. 2000) and its activity can be inhibited using a small-molecule inhibitor PACMA31, a selective inhibitor of proteins in the PDI family. It works by binding irreversibly to the cysteines in the active site of PDI (Xu et al. 2012). To assess whether the same factor was involved in the reaggregation of zebrafish retinal cells, PACMA31 was added to cultures starting from the point of cell seeding. We found a dose-dependent effect on aggregation; cells treated with 5μM of PACMA31 generated slightly loose aggregates after 24 hours in vitro (hiv), whereas those treated with 50-200μM were completely unable to aggregate (Figure 3.5) suggesting R-Cognin plays an important role in zebrafish retinal cell reaggregation. This effect was not quantified; however, the same experiment effect was observed in 3 experimental repeats carried out on different days.

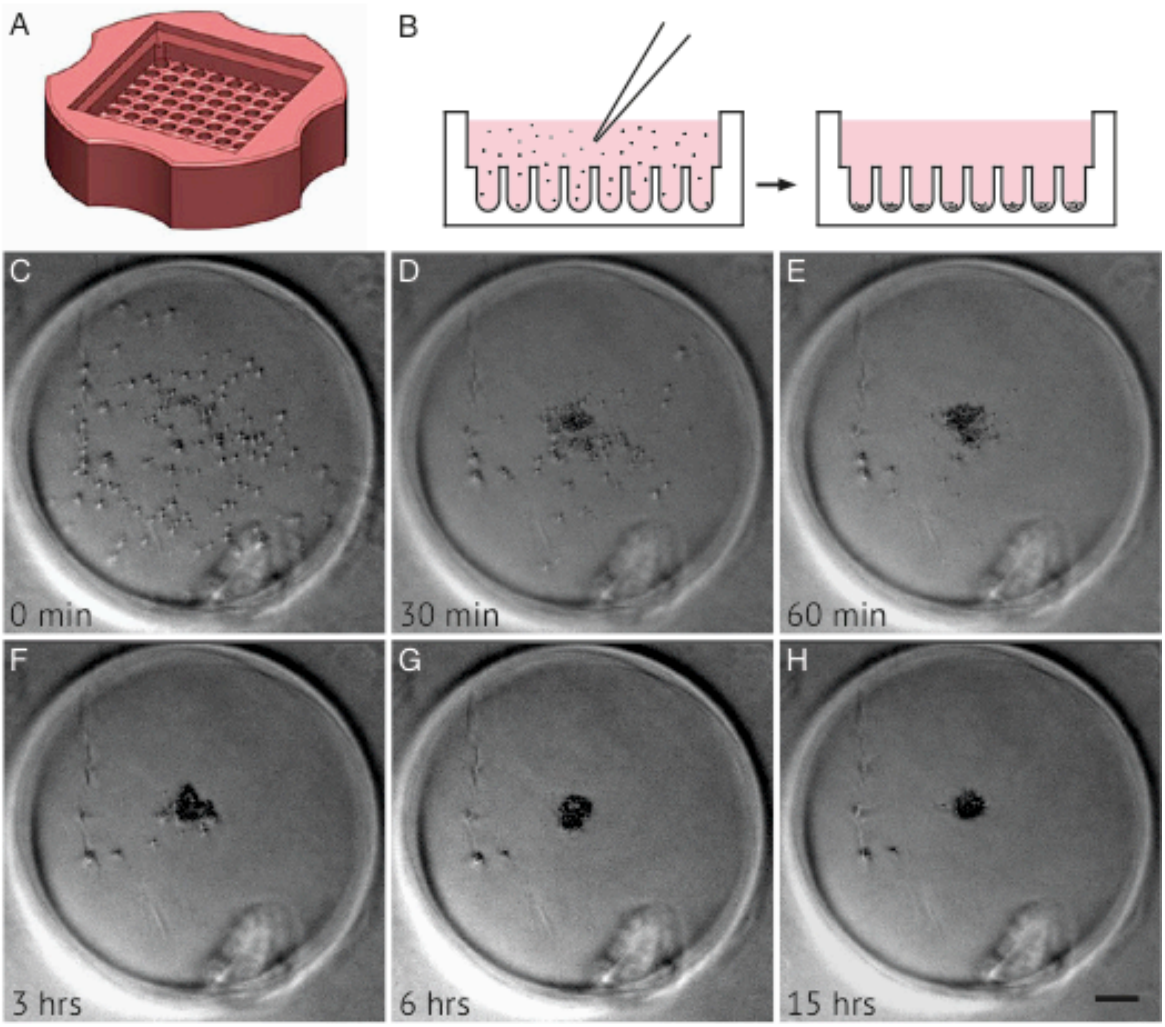

Figure 3-4: Timepoint of aggregation of cells in one of the microwells of the 3D Petri Dish

(A) Agarose microwell dish cast from the 3D Petri Dish PDMS Mould (adapted, with permission, from http://www.microtissues.com). (B) Schematic representing the seeding chamber of the 3D Petri dish. After seeding, cells settle into individual wells (n=3). (C-H) Time-lapse images of a single well from the 3D Petri dish showing 24 hpf cells re aggregating. (F) Cells are almost fully reaggregated 3 h after seeding. (H) Cells have undergone compaction 15 h after seeding. Time is in minutes and hours after seeding. Dark cells are RPE. Scale bar = 100 μm.

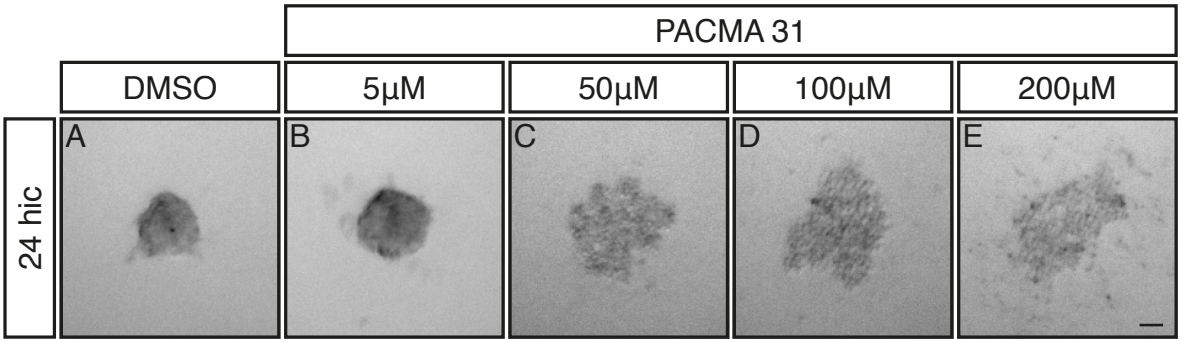

Figure 3-5: R-Cognin is important for embryonic zebrafish retinal cell reaggregation after dissociation.

24hpf cells after 24 hours in vitro (24hiv). Cells were treated with either (A) DMSO or (B) 5µM (C) 50µM (D) 100µM or (E) 200µM of PACMA 31, a small molecule inhibitor of R-Cognin. Cells cultured in 5µM PACMA31 (B) generated slightly looser aggregates. Cells cultured with 50µM - 200µM PACMA31 (C-E) were completely unable to aggregate (n= 3 for each condition). Dark cells are RPE. Scale bar = 50µm.

3.5. Visualising lamination with the Spectrum of Fates transgenic line

To visualise the cells within these aggregates we used cells from the Spectrum of Fates polytransgenic zebrafish line. This line (Atoh7:gapRFP/Ptf1a:cytGFP/Crx:gapCFP) (SoFa 1) (Almeida et al. 2014) allows visualisation of the 5 main retinal neurons: Retinal Ganglion Cells (RGCs), Amacrine Cells (ACs), Horizontal Cells (HCs), Bipolar Cells (BPs) and Photoreceptors (PRs). Expression of three different fluorescent proteins: CFP, GFP and RFP are driven by cell fate-specific promoters so that, in particular combinations, each main cell type can be identified, as shown in Figure 3.6. Atoh7:gapRFP expression begins at around 28-30hpf in some retinal progenitors. This spreads throughout the retina and expression remains in some cell types into adulthood. Expression of Crx:gapCFP begins shortly after in newly born BCs and PRs, followed by Ptf1a:cytGFP in newly born HCs and ACs. At 72hpf, when all cell types have been born, it can be seen that RGCs are labelled with just membrane RFP (Fig 3.6 C), ACs and HCs with membrane RFP and cytoplasmic GFP (Fig 3.6D), BPs with membrane CFP (Fig 3.6 E) and PRs with membrane CFP and RFP (Fig 3.6F). This line highlights the beautiful, striking layering of the zebrafish retina *in situ* and allows us to identify individual cells when dissociated.

3.5.1. Fixation and mounting procedure

At first, aggregates from both the hanging drop technique and the 3D Petri Dish were transferred to glass-bottomed culture dishes for imaging with an inverted laser-scanning confocal microscope. At first, aggregates could be visualised, and all FPs distinguished in their respective channels, but distinguishing between some individual cell types was difficult. To resolve this, I decided to optimise the technique for mounting and imaging the aggregates in the hope that it would improve clarity.

There were several possible reasons for this low image quality, and which could be altered to improve it. Firstly, aggregates were sitting on the bottom of a culture dish and could be disrupted by vibrations during imaging. Secondly, aggregates were being imaged within culture medium that was supplemented with Phenol Red, which may interfere with the laser stimulation and light emission. Thirdly, some aggregates cultured with the hanging drop technique were quite large, meaning there was quite a

lot of tissue for the lasers to penetrate through when imaging the central portion. Finally, pigmented cells in the centre of the aggregate may have been either absorbing some of the excitation or emission light, preventing some of the excitation of surrounding cells. I therefore decided to address each of these potential problems to improve imaging quality.

First, I incorporated PTU (N-Phenylthiourea) into the culture medium to prevent pigment formation in RPE cells. Figure 3.7 clearly shows the reduced amount of pigment in aggregates cultured with PTU. I continued optimisation with PTU in the culture medium from the beginning of culture. I also made sure that embryos were kept in PTU from 24hpf onwards, and throughout dissection.

To address the issue of aggregates moving around and to remove them from the coloured culture medium I decided to fix and mount the aggregates. I tried several mounting formats, but eventually settled with a simple format whereby aggregates were mounted in DAPI Vectashield hard-set mounting medium between a microscope slide and a number 0 coverslip, separated with a reinforcement ring to prevent the aggregates from being crushed. This mounting medium sets in just 20 minutes at room temperature allowing for immediate imaging, or slides can be stored at 4°C for preservation of samples for about a month, depending on fluorophore stability.

After adopting these changes, I was much better able to distinguish between individual cell types in aggregates imaged using the same confocal microscope, as shown in Figure 3.8. Another observation of transitioning from the hanging drop technique to the 3D Petri Dish at the same time was that smaller aggregates generated with the 3D Petri Dish were more easily imaged, further improving imaging quality.

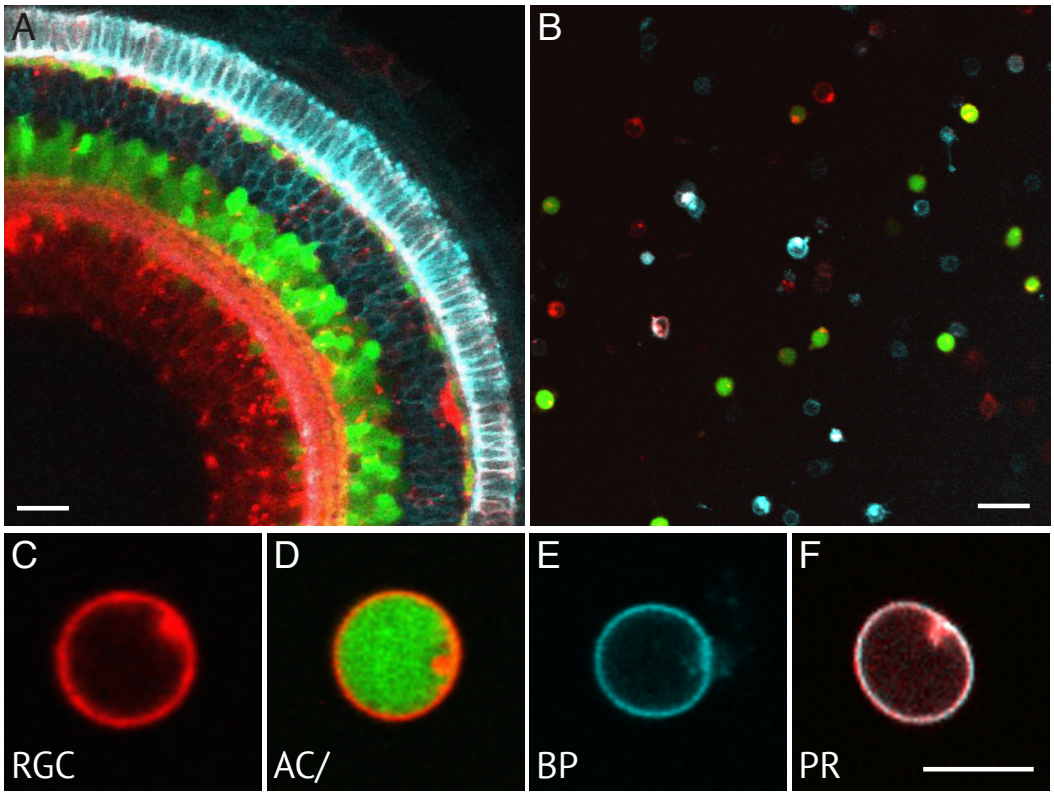

Figure 3-6: Identification of zebrafish retinal cells.

The main cell types of the retina can be identified in the SoFa1 transgenic line (Almeida et al., 2014) using a combination of genetically tagged cell fate markers: Atoh7:gapRFP labels RGC, AC/HC and PR cell membranes; Ptf1a:cytGFP labels AC/HC cytoplasm; and Crx:gapCFP labels BP and PR membranes. (A) Central sagittal section of a region of the SoFa1 retina. Scale bar = 20 µm. (B) Dissociated cells of the SoFa1 line. Scale bar = 20 µm. (C-F) Individual cells are identified based on their spectral expression: (C) RGCs express membrane RFP; (D) AC/HCs express cytoplasmic GFP and membrane RFP; (E) BPs express membrane CFP; and (F) PRs express membrane CFP and RFP. Scale bar = 5 µm.

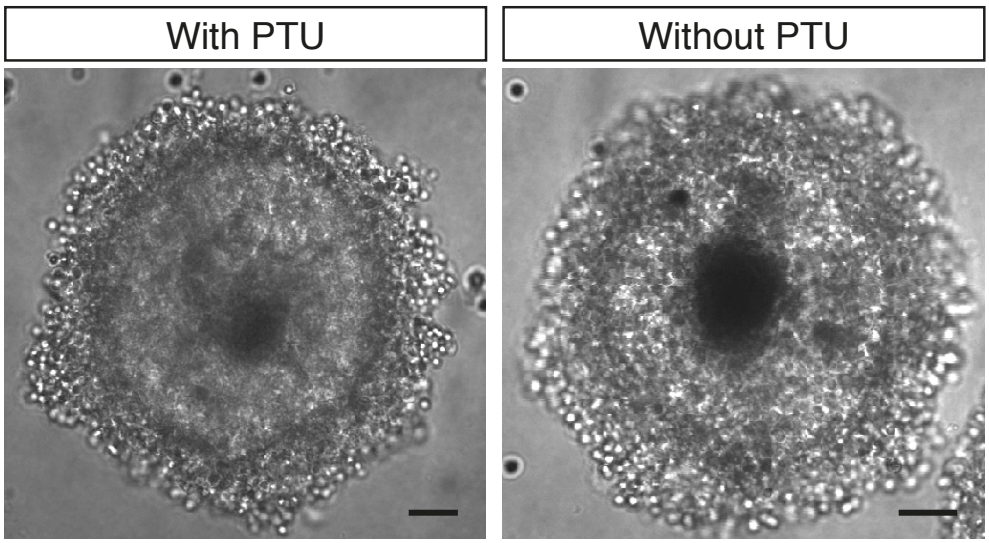

Figure 3-7: Comparison of aggregates with or without PTU

Aggregates cultured with and without PTU (n=3). Imaged with brightfield at 60x magnification. Dark cells are RPE. Scale bars = 20µm.

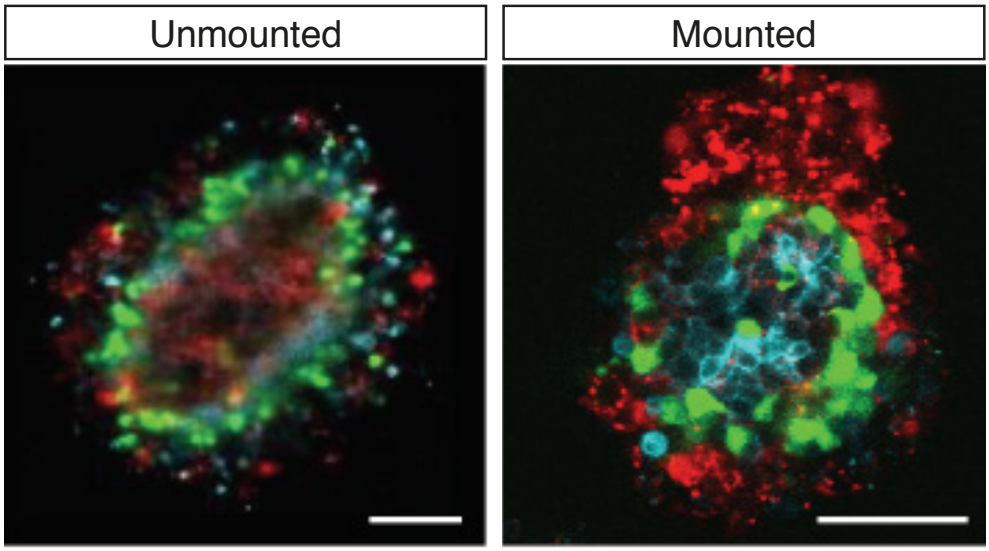

Figure 3-8: Comparison of aggregates before and after mounting

Comparison between larger, unmounted aggregates produced using the Hanging Drop Method and smaller, mounted aggregates produced using the 3D Petri Dish method. Aggregates imaged on a confocal microscope at 60x. Red label = Atoh7:gapRFP, Cyan label = Crx:gapCFP, Green label = Ptf1a:cytGFP. Scale bars = 40µm.

3.6. Validating the model

Having finally optimised the dissociation, culture and imaging of the aggregates I next moved onto validating the aggregates as a reaggregate model of zebrafish retinal development. Using the SoFa1 line I wanted to check whether the correct cell types were generated in the right developmental time frame, and in the correct proportions.

3.6.1. Transgenic markers are expressed in aggregates at a similar time to *in vivo*.

In the spectrum of fates (SoFa1) line Atoh7 is the first promoter to turn on at around 28hpf, driving the expression of gapRFP in all retinal progenitors. This is followed shortly by expression of Crx:gapCFP (expressed in BPs and PRs) and then Ptf1a:cytGFP (expressed in ACs and HCs), increasing up until 72hpf (Almeida et al. 2014). Figure 3.9 shows an aggregate after 24 hours in vitro, equivalent to a 48hpf retina. It can be clearly seen that Atoh7:gapRFP is expressed in many of the cells and Crx:gapCFP and Ptf1a:cytGFP are beginning to be expressed in just a few cells. This is slightly delayed in comparison to *in vivo*, where a higher proportion of cells are already expressing Crx:gapCFP and Ptf1a:cytGFP, but this is a modest delay, and by 48 hic, the equivalent of a 72hpf retina, all fluorophores are expressed, as they are *in vivo*.

3.6.2. Cell numbers in 48hic aggregates are similar to the 72hpf retina

Although it was evident that all three transgenic markers were expressed by 48hic, I decided to check whether all cell types were present in the aggregates and whether their proportions were representative of those *in vivo*. I did this with the help of an undergraduate dissertation student, Sara Conde, from Barcelona University, who counted cells using the Point function in the Volocity Visualisation software. Cells were counted as a proportion of total cell nuclei counted in the DAPI channel. In this format, using the SoFa1 line, RGCs couldn't be easily distinguished, since RFP was also expressed in many other cell types. So, we considered the number of RGCs and RPE cells as those remaining after all other cells were counted. We also couldn't distinguish ACs from HCs without the positional information normally found *in vivo*, as they express the

same transgenic markers, so these were also counted together. This is also the case for BPs and PRs as they cannot easily be distinguished from each other. Finally, we counted MG cell numbers in aggregates cultured from the GFAP:GFP transgenic line. The GFAP:GFP reporter is expressed at high levels in MG and lens cells (Bernardos & Raymond 2006). We therefore only counted those cells with bright GFP expression and with the appropriate position and morphology for MG (i.e. elongated cells that were incorporated with other retinal cells rather than smaller cells in the centre or peripheries of the aggregate). All cell counts are shown in Table 3.2.

It was therefore deemed that these aggregates modelled the development of retinal cells *in vivo* in terms of when the transgenic markers turn on, and therefore when each cell type begins to differentiate. However, it must be noted that we did not investigate the extent to which these cells differentiate or mature.

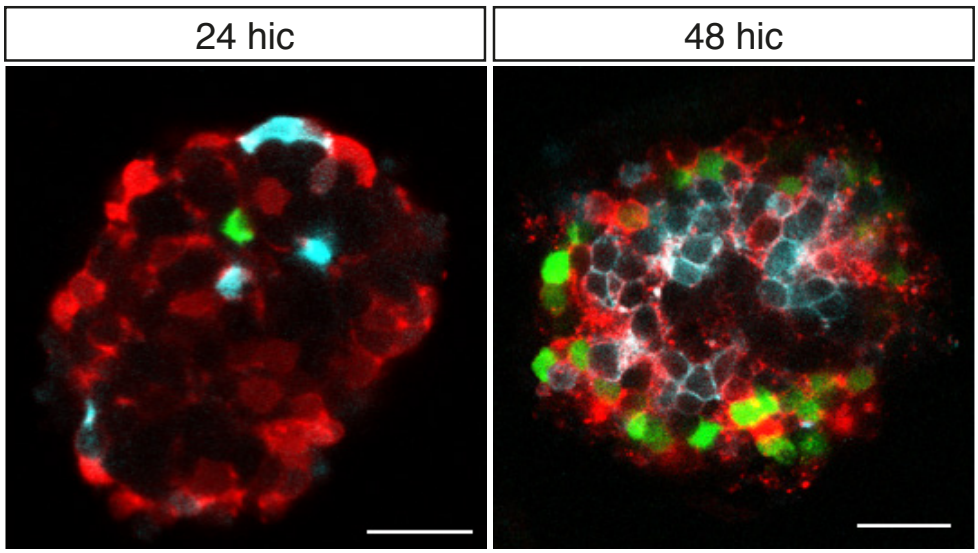

Figure 3-9: Expression of fluorophores in 24hic aggregates vs 48hic

In the 24hic aggregate (equivalent to 48hpf in vivo) Atoh7:gapRFP expression can be seen in almost all cells. Crx:gapCFP expression is seen in some cells, and Ptf1a:cytGFP is seen in just one cell. In the 48hic aggregate (equivalent to 72hpf in vivo) all three transgenes are expressed in various cells in the aggregate. (n = 9) Scale bars = 20μm.

Table 3-2: Proportions of cell types in aggregates are similar to the retina					
	% Total Retinal Cells				
	dAC, AC, HC	BC, PR	RGC	RPE	MC
in vivo	22.5	56.7	10.8	nc	10
in vitro	25.2	44.6	18.4		11.8

Table 3.2 shows the proportion of cell types counted in our aggregates (*in vitro*) compared to a previously published in vivo study (Boije et al. 2015) and our own counts of MCs *in vivo*. dACs, ACs and HCs are counted together in SoFa1 samples in the GFP channel (n=15, s.e.m. 1.72). BCs and PRs are counted together in SoFa1 samples in the CFP channel (n=15, s.e.m. 2.21). MCs are counted in GFAP:GFP samples (n=19 s.e.m. 0.81). RGC and RPE counts in the aggregates are calculated as the remaining cell types not counted in the GFP or CFP channels of the SoFa1 samples.

3.7. Lamination of retinal aggregates is dependent on developmental stage

Having validated the aggregates as a representative model of zebrafish retinal development *in vivo*, I began my first experiments to understand the developmental mechanisms of retinal lamination. First, I wanted to find out at which developmental stage zebrafish retinal cells were most capable of self-organising, if at all. Retinas, plus attached RPE, were dissected from embryos of different stages and subjected to the same preparation and culture protocols as described previously in this chapter. The stages chosen ranged from 24hpf, when retinal progenitors are just beginning to differentiate, to 72hpf, when most of the cells of the retina have differentiated and the retina is fully laminated.

As shown in Fig 3.10, cells from retinas dissected at 24hpf (Fig 3.10 A-E) were quite organised by 48hic. At this stage, a ring of GFP expressing cells, namely the ACs and HCs, (Fig 3.10 C) can clearly be seen surrounding a cluster of CFP expressing cells (Fig 3.10 B), the BPs and PRs. RFP expressing cells were found throughout the aggregates (Fig 3.10 D). Cells from retinas dissected at 48hpf (Fig 3.10 K-O) were somewhat able to organise. The GFP expressing cells (Fig 3.10 M) were also found as a ring, but the CFP expressing cells (Fig 3.10 L) were not always found as one cluster, often found throughout the aggregate. RFP expressing cells were found throughout the aggregate (Fig 3.10 N). Cells from retinas dissected at 72hpf (Fig 3.10 P-T) were the least organised and most inconsistent from one experiment to another. Sometimes GFP expressing cells (Fig 3.10 R) were found as a defined ring, but other times the ring was not so well defined. CFP expressing cells (Fig 3.10 Q) were either found throughout the aggregate or even as a rough ring around the outside of the aggregate. RFP expressing cells were always found throughout (Fig 3.10 S).

As described later in this thesis, it was necessary to also culture cells from retinas dissected at 32hpf. Therefore, aggregates cultured from cells from 32hpf retinas were compared to cells from 24hpf retinas. These are slightly less organised than cells from 24hpf retinas, however the same general pattern can be seen: GFP expressing cells organised in a ring around a cluster of CFP expressing cells, and RFP expressing cells throughout.

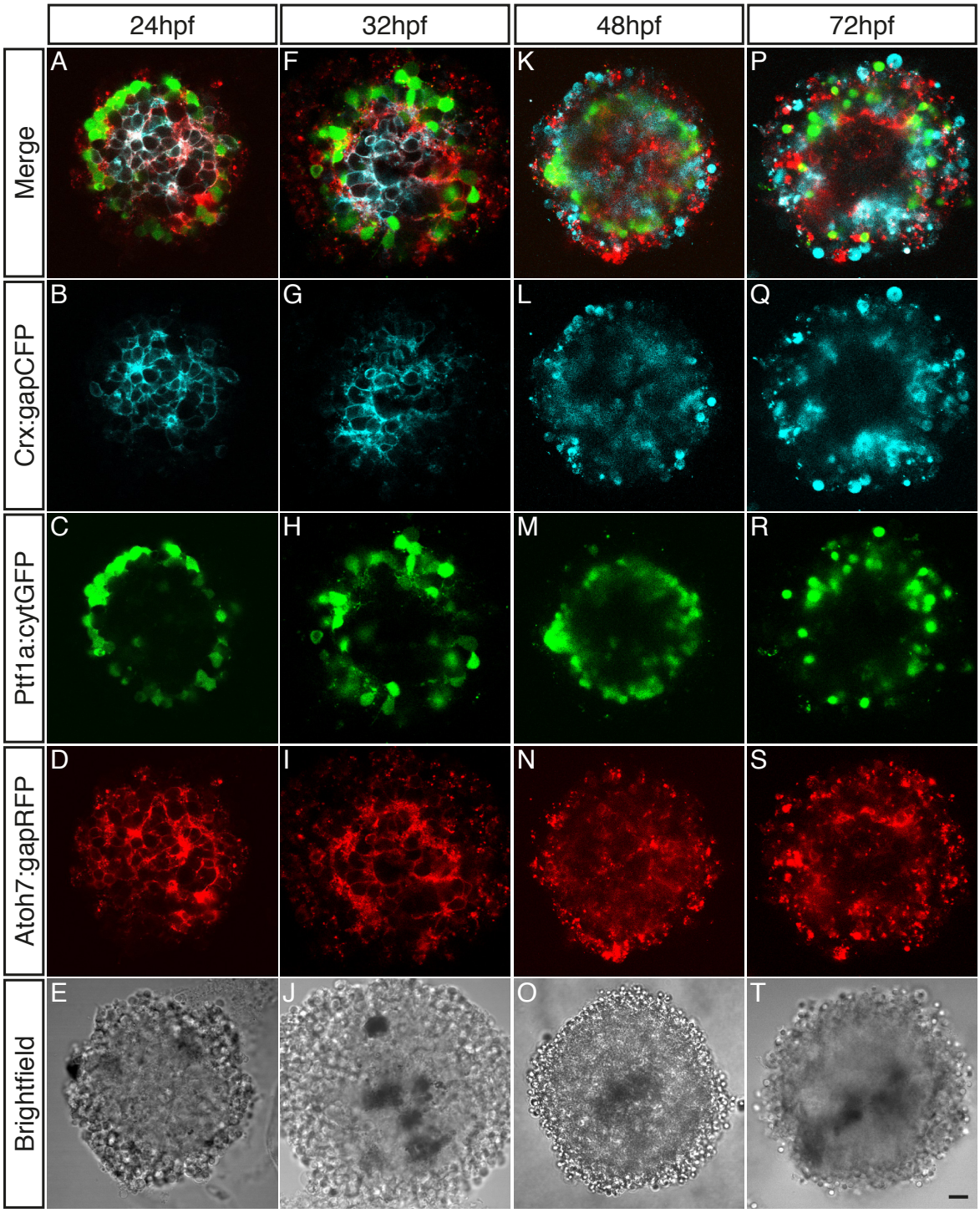

Figure 3-10: Cells cultured from younger embryonic zebrafish stages are most capable of organising.

Cells from varying embryonic stage zebrafish (24hpf – 72hpf) cultured for 48 hours (n = 5 for each condition). Expression of the various transgenes begins at different times starting from 24hpf, but all are expressed by 72hpf, as seen in these cultures. (A-E)

Central sagittal section of a SoFa1 aggregate cultured from 24hpf cells. (A) Merge of all channels. (B) Crx:gapCFP expressing cells are found in the centre of the aggregate. (C) Ptf1a:cytGFP expressing cells are found in a distinct ring around the outside of the aggregate. (D) Atoh7:gapRFP expressing cells are found throughout the aggregate. (E) Brightfield. (F-J) Central sagittal section of a SoFa1 aggregate cultured from 32hpf cells. (F) Merge of all channels. (G) Crx:gapCFP expressing cells are found in the centre of the aggregate. (H) Ptf1a:cytGFP expressing cells are found in a distinct ring around the outside of the aggregate. (I) Atoh7:gapRFP expressing cells are found throughout the aggregate. (J) Brightfield. (K-O) Central sagittal section of a SoFa1 aggregate cultured from 48hpf cells. (K) Merge of all channels. (L) Crx:gapCFP expressing cells are found throughout the aggregate. (M) Ptf1a:cytGFP expressing cells are found in a ring around the outside of the aggregate. (N) Atoh7:gapRFP expressing cells are found throughout the aggregate. (O) Brightfield. (P-T) Central sagittal section of a SoFa1 aggregate cultured from 72hpf cells. (P) Merge of all channels. (Q) Crx:gapCFP expressing cells are found towards the outside of the aggregate. (R) Ptf1a:cytGFP expressing cells are found in a ring around the outside of the aggregate. (S) Atoh7:gapRFP expressing cells are found throughout the aggregate. (T) Brightfield. Dark cells are RPE. Scale bar = 10μm

3.8. Cells are self-organising in the same order as the layers *in vivo*

Having decided that cells from 24hpf retinas are most organised in these aggregates I next wanted to characterise their organisation. As shown in Figure 3.11, it is clear in these aggregates that Crx:gapCFP expressing cells (Fig 3.11 A) (namely the PRs and BPs) are positioned most centrally, surrounded by the Ptf1a:cytGFP expressing cells (Fig 3.11B) (the ACs and HCs). I wanted to know whether all cell types were organising in distinct layers.

In the SoFa l line, it is difficult to distinguish the RGCs *in vitro,* without the positional information found in the intact retina, due to the Atoh7:gapRFP label also being expressed in many other cell types. To look at the position of the RGCs I stained aggregates with Zn5, a monoclonal antibody against DM-GRASP/alcama, a cell adhesion molecule specific to RGCs (Zolessi et al. 2006). Figure 3.12 shows that the RGCs were positioned on the outside of the aggregate (Fig 3.12 A), among the Ptf1a:cytGFP expressing cells (Fig 3.12 E).

This confirms that the cells in these aggregates are layered roughly in the same order as *in vivo*: RPE in the centre, next to photoreceptors and bipolar cells, next to horizontal and Amacrine cells, next to RGCs on the outside.

3.8.1. Extending culture time

Following this interesting result, I wanted to see if this was the final organisation of the cells or just the early patterning behaviour. I decided to try to culture the cells for longer to see if they would organise further, or even re-invert their layering as they do in chick retinal reaggregates at later stages (Rothermel et al. 1997; Willbold et al. 2000). I found that cells cultured past 48 hours didn't organise differently, and also started dying, meaning there would need to be further optimisation, such as changing the culture medium regularly. Since the aggregates were becoming laminated within the same time window as *in vivo*, I decided this was representative of what was going on *in vivo* during lamination and was sufficient for me to investigate the basic cellular and molecular mechanisms of lamination.

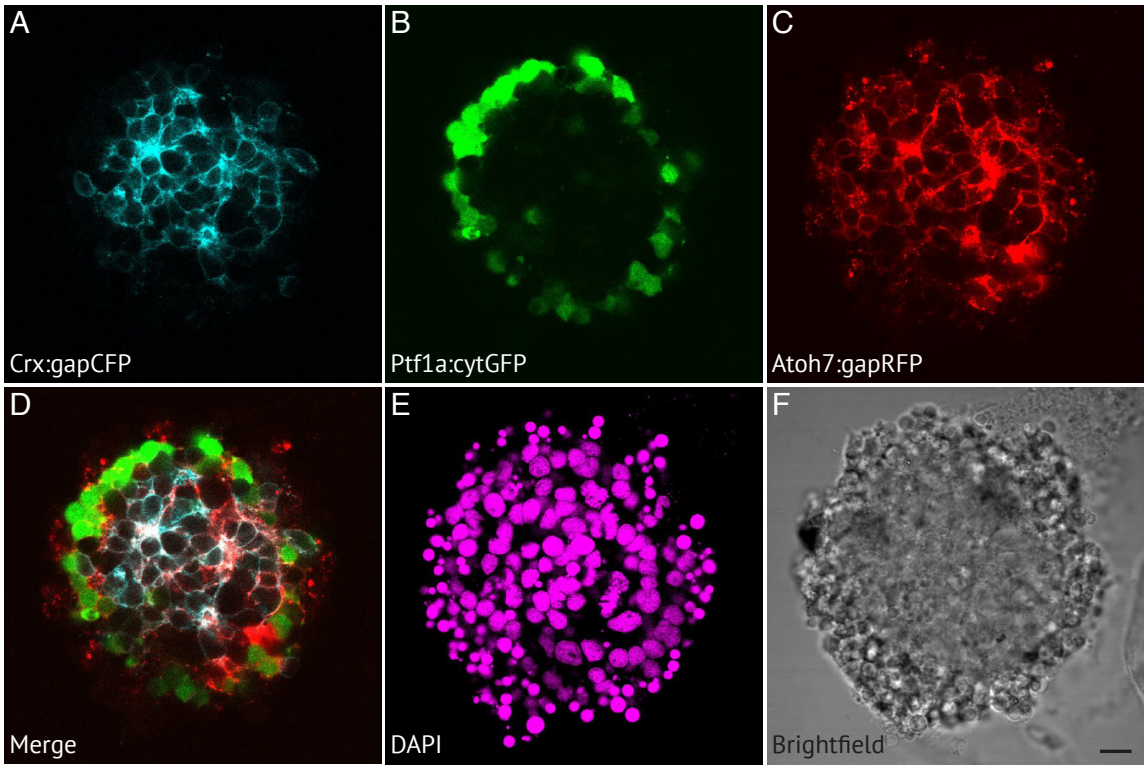

Figure 3-11: Central sagittal section of a retinal aggregate cultured using the SoFa1 line.

A representative sample to illustrate basic layering of aggregates after 48hic. (A) Crx:gapCFP-expressing cells are found in the centre of the aggregate. (B) Ptf1a:cytGFP-expressing cells are found in a distinct ring around the Crx: gapCFP population. (C) Atoh7:gapRFP-expressing cells are found throughout the aggregate. (D) Merge of channels represented in G-I. (E) DAPI. (F) Brightfield image. Dark cells are RPE. Scale bar = 10 µm.

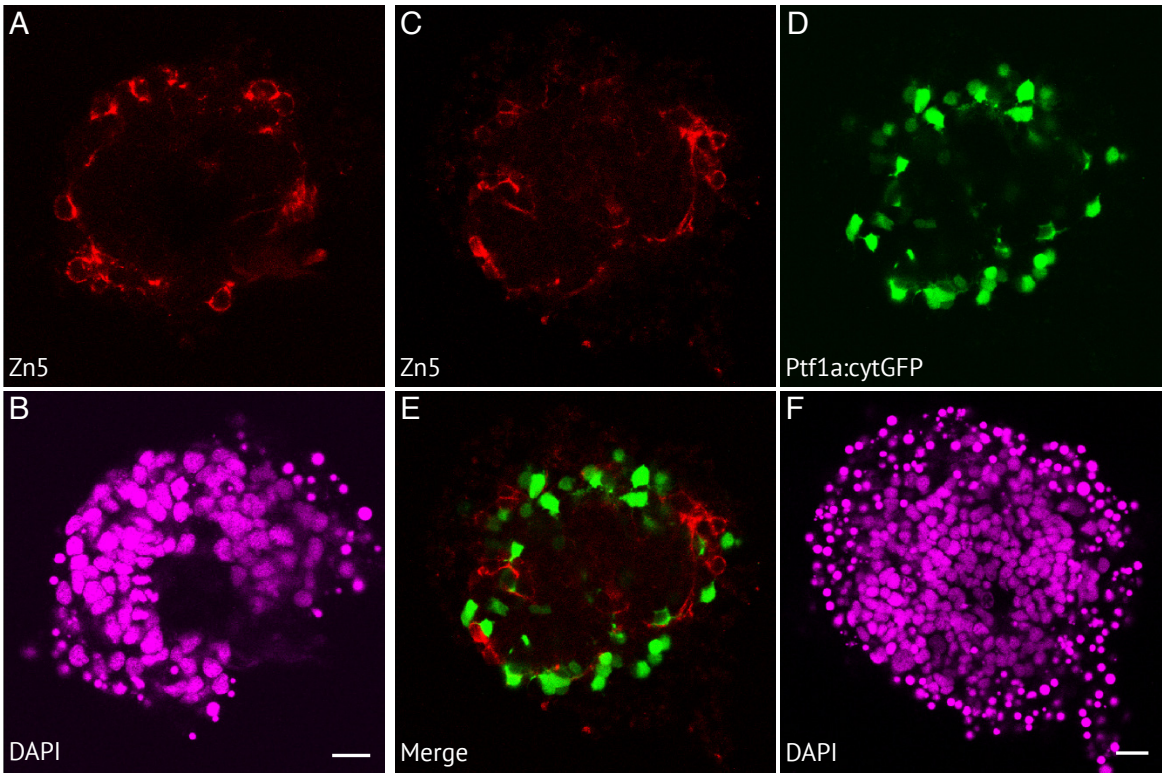

Figure 3-12: RGC cells are positioned in the outer layer of zebrafish retinal aggregates.

(A-B) Aggregates cultured using the WT zebrafish strain and stained with Zn5 primary antibody (marking RGCs) and DAPI (n = 5). (A) RGCs can be seen positioned in the outer layer of the aggregate and are extending axonal projections into the aggregate (arrows). (B) DAPI. Scale bar = 10μm. (C-F) Aggregates cultured using the Ptf1a:cytGFP zebrafish line and stained with Zn5 primary antibody (marking RGCs) and DAPI (n = 6). (C) RGCs can be seen positioned in the outer layer of the aggregate and are extending axonal projections into the aggregate. (D) Ptf1a:cytGFP cells (namely ACs) are positioned in a ring around the outside of the aggregate. (E) Merge of (C and D) showing Zn5+ RGCs positioned in the outer layer, amongst the Ptf1a:cytGFP expressing cells. (F) DAPI. Scale bar = 10μm.

3.9. Metrics of organisation of zebrafish retinal reaggregates

Now that we could see how these aggregates were organising I started to explore possible ways to analyse the patterning as a measure of organisation. I needed to find a way to quantify this organisation to be able to compare one condition to another when I began to explore the mechanisms of lamination.

3.9.1. Semi-quantitative pattern analysis

First, I decided to do a rough assessment of organisation of the aggregates cultured from retinas of different stages using a semi-quantitative approach. I noticed that the different populations of cells were organising in one of three patterns, as shown in the diagrams in Figure 3.13 These were: a cluster in the centre "Centre" (Fig 3.13 A), an inner ring of cells "Inner Ring" (Fig 3.13 B) or an outer ring of cells "Outer Ring" (Fig 3.13 C). Alternatively, cells could be found throughout the aggregate, so I classified the patterning of these as "None" (Fig 3.13 D). Aggregates were scored by channel (CFP, GFP and RFP) and each colour was scored by placing into one of the four categories. As described earlier in this thesis, aggregates from the 24hpf condition are clearly most organised. In Figure 3.14 it can be seen that in almost all aggregates, GFP was scored as an inner ring, CFP in the centre, and RFP as "None". As developmental age increases, the scores of organisation become less clear and the patterning even changes in some cases. Most notably, the CFP changes from being positioned mostly in the centre, to mostly in the outer ring. When the same data is rearranged and ordered with fluorescent channel on the x-axis, rather than developmental stage (Figure 3.15), it is quite clear that GFP expressing cells (ACs and HCs) are almost always found in an inner ring. This robustness suggests these cells can self-organise independent of developmental stage, whereas the other cells are perhaps dependent on mechanisms that change with developmental time.

3.9.2. Possible measures of organisation

The semi-quantitative approach gave me some insight into the organisation of these aggregates and the possible importance of developmental time in the ability of the cells

to organise. However, the results were not clear enough to be able to compare one condition to another in future experiments and I wanted to develop a more robust, quantifiable measure of organisation. There are several possible ways to measure organisation such as analysing cell clustering or measuring the area occupied by different cell populations, but they give no indication as to how the cells are patterned, i.e. where in the aggregate cells are positioned, and in what shape.

3.9.3. Concentric pattern analysis (isocontouring)

Given the circular nature of the patterning, I decided to build a new method of quantitation based on whether the cells were organising in a concentric pattern or not. In collaboration with Dr Leila Muresan in the Cambridge Advanced Imaging Centre (CAIC) we built a Matlab script that measures the average fluorescence of each fluorescent channel in concentric rings at 2-pixel intervals throughout the aggregates and plots these as a graph of average fluorescence against radial position.

As explained in the methods section, first an outline is drawn around the aggregate to select the area of measurement, then isocontours are fit at 2-pixel intervals from the periphery to the centre of the aggregate, along which the fluorescence is measured. An example of this is shown in Figure 3.16 where the original images of the different fluorescent channels of the aggregate are shown (Fig 3.16 A-F), together with a schematic showing how the isocontours were fit (Fig 3.16 H), and an example of the output graph showing the fluorescence profile for that aggregate (Fig 3.16 I). The CFP expression is high near the centre of the aggregate, tailing off towards the periphery, whereas the GFP expression is low in the centre, but peaks near the periphery, corresponding roughly with Crx:gapCFP and Ptf1a:cytGFP-expressing cell positions, respectively. At first, we designed the script to fit circular contours starting in the centre of the aggregate and moving outward, toward the periphery, but we found that this was unforgiving for slight changes in aggregate shape, i.e. any that weren't perfectly round, and the output data was very noisy. Ultimately, we decided to fit isocontours from the periphery to the centre instead which take account of aggregate shape, and found results to be much more consistent, and less noisy.

3.9.4. Empirical cumulative distribution function analysis

The fluorescence profiles showed us qualitatively what the organisation looked like, but it didn't yet give us a quantitative measure. We decided to apply an empirical cumulative distribution function analysis to this data to show us how far these patterns of expression deviated from a normal distribution of expression, that being, the expression being equally likely at any position along the radius. This gives us a readout graph that shows common properties, regardless of the pattern distributions, making it easy to compare populations. For instance, distributions will always lie between 0 and 1. This allows us to see at any given point along the x-axis (radial position), the y-value is the probability of a value < X (to the left of x) as shown in (Fig 3.16 J). The black dashed line represents a normal distribution of fluorescence expression where the ECDF score increases linearly with radial position. In other words, fluorescence is evenly distributed throughout the aggregate and equally likely to appear at any point along the radius. (Fig 3.16 J) shows that the ECDF curve representing distribution of Atoh7:gapRFP is close to such a straight line (dotted line). An even patterning of fluorescent marker across the aggregate represents a complete failure of patterning, which is consistent with the fact that Atoh7:gapRFP is expressed in most of the cell types. The ECDF for Crx:gapCFP-expressing cells is clearly shifted to the left of this line, indicating an increased likeliness that Crx:gapCFP-expression will appear in the centre of the aggregate. This is consistent with the fact that these cells are predominantly distributed in the centre of the aggregate. On the other hand, the ECDF for Ptf1a:cytGFP-expressing cells is shifted to the right, indicating an increased likeliness that Ptf1a:cytGFP-expresion will appear near the outer radius. This is consistent with the cells being predominantly distributed nearer the outer periphery of the aggregate.

ECDF curves that overlay each other would indicate cell populations that are not spatially distinct, or intermingled, therefore exhibiting a failure of patterning. Theoretically, the further apart these ECDF plots are, the more spatially distinct, and therefore organized, the two populations are. By measuring the area between the ECDF curves for the CFP and GFP-expressing cells in each aggregate we can gain a quantitative measure of organization which we can then use to compare the level of organization in two or more experimental conditions.

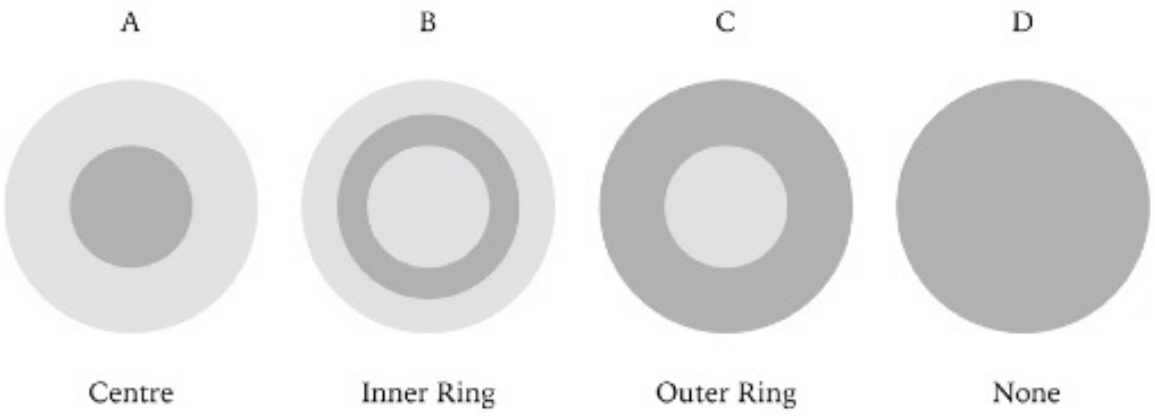

Figure 3-13: Categories of pattern for scoring organisation

Schematic to illustrate patterns of grouped cell positions observed in aggregates and categories used to score the organization of each sample.

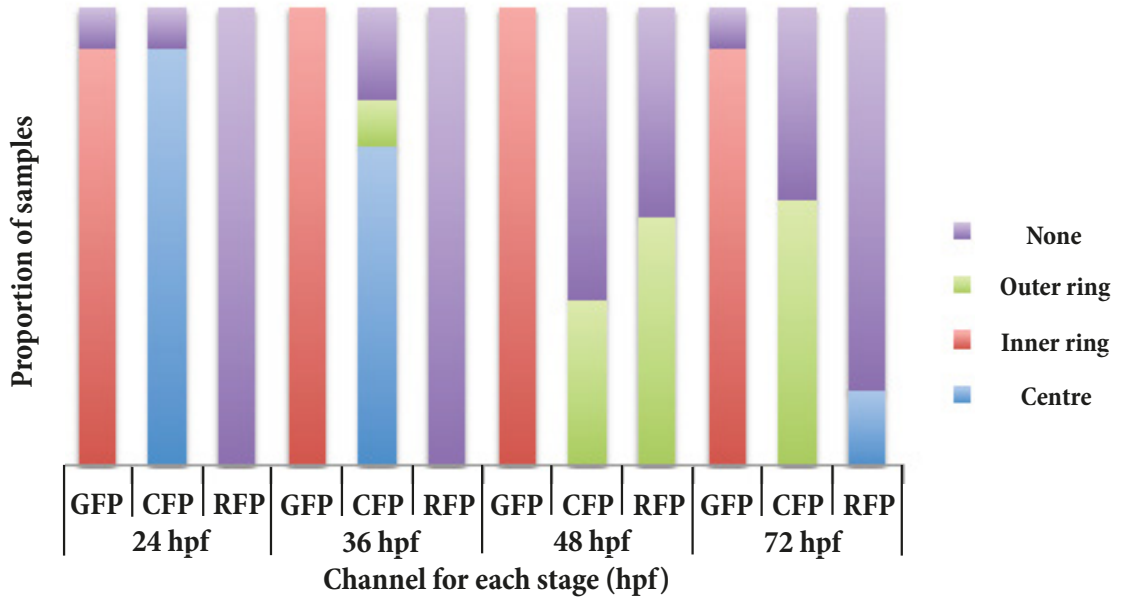

Figure 3-14: Scoring of aggregates by stage

Cumulative counts of samples displaying cellular organization patterns that fit one of four categories: organized in the centre, in an inner ring, an outer ring, or no organisation. Data arranged to display organization of cells by channel for each stage. 24hpf (n=12), 36hpf (n=10), 48hpf (n=11), 72hpf (n=12) all data is grouped from 3 independent experiments.

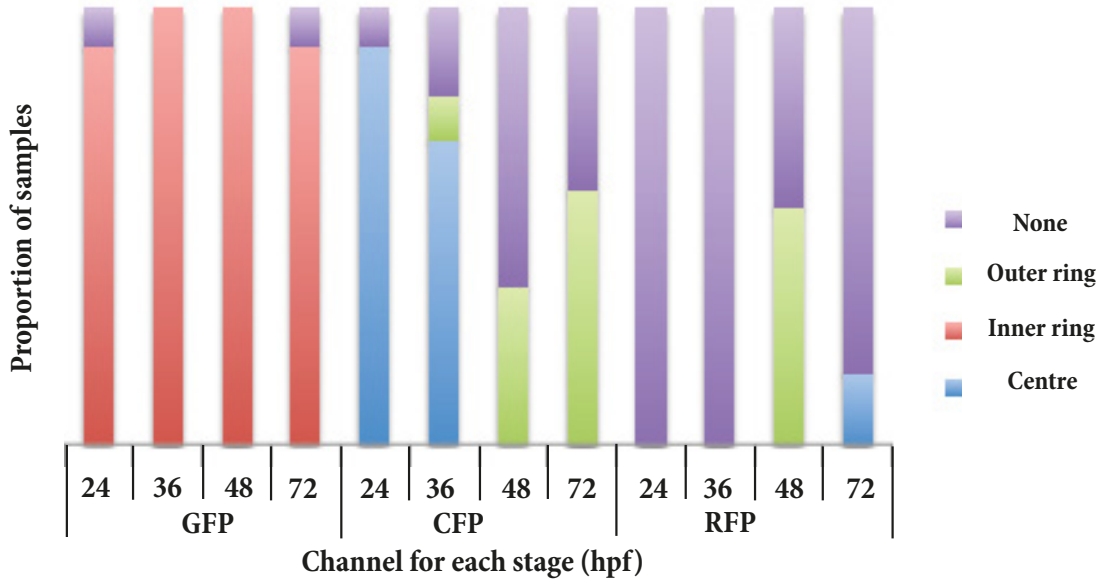

Figure 3-15: Scoring of aggregates by channel

Cumulative counts of samples displaying cellular organisation patterns that fit one of four categories: organised in the centre, in an inner ring, an outer ring, or no organisation. Data arranged to display organisation of cells by stage for each channel. 24hpf (n=12), 36hpf (n=10), 48hpf (n=11), 72hpf (n=12) all data is grouped from 3 independent experiments.

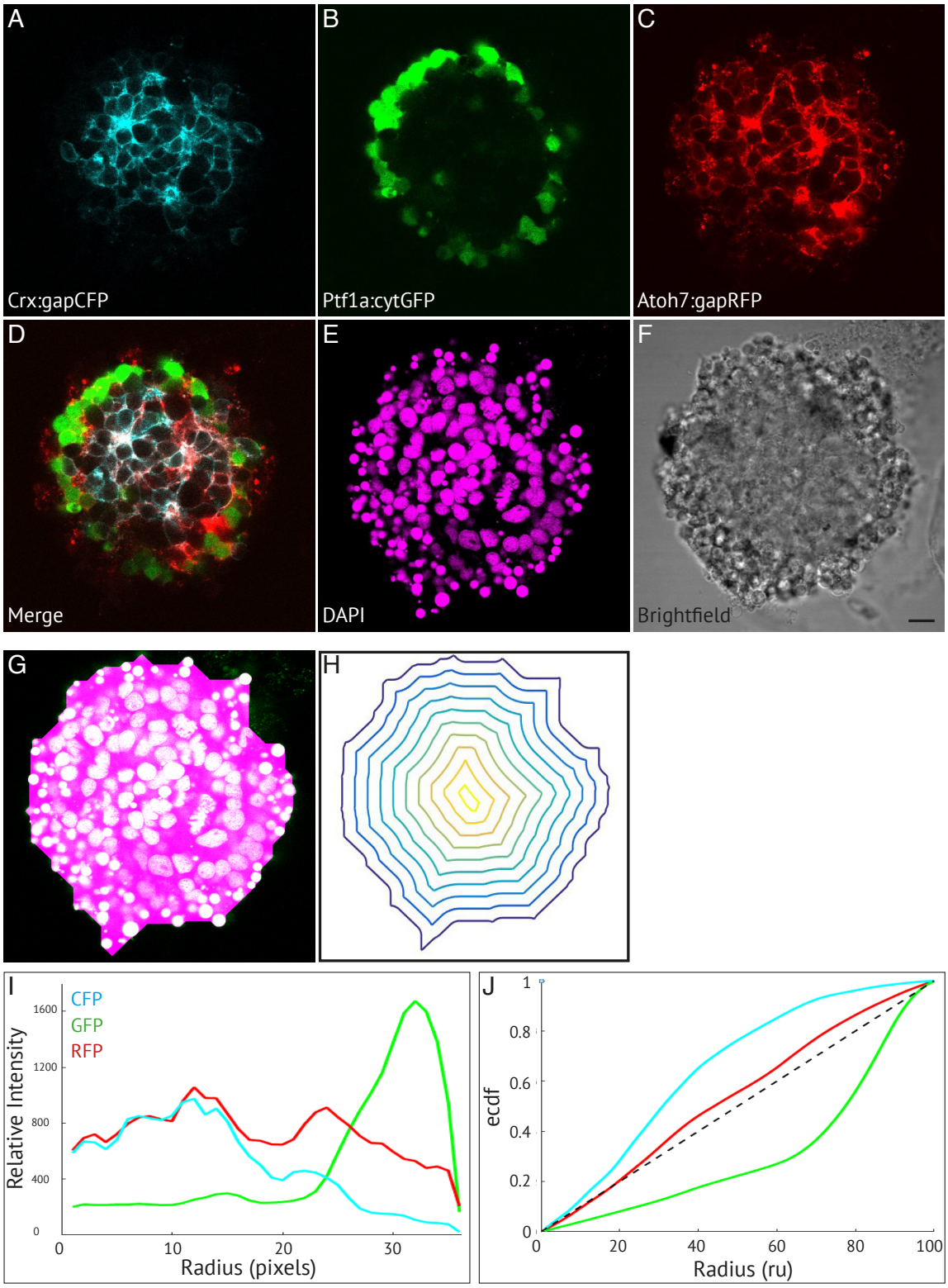

Figure 3-16: Characterisation of organisation.

(A-F) Representative central sagittal section of a retinal aggregate cultured using the SoFa1 line. (A) Crx:gapCFP-expressing cells are found in the centre of the aggregate. (B)

Ptf1a:cytGFP-expressing cells are found in a distinct ring around the Crx:gapCFP population. (C) Atoh7:gapRFP-expressing cells are found throughout the aggregate. (D) Merge of channels represented in A-C. (E) DAPI. (F) Brightfield image. Dark cells are RPE. Scale bar = 10 μm. (G-J) Generation of analysis of cellular organisation using custom made Matlab scripts. (G) A mask is fitted to the aggregate using the DAPI channel. (H) Successive isocontours are fitted from the periphery to the centre of the aggregate. (I) Fluorescence is measured along each contour and plotted as relative fluorescence intensity (y-axis) against radial position (in pixels) (x-axis). (J) Fluorescence profiles for each channel are plotted as an empirical cumulative distribution function (ECDF) (y-axis) against radial position [radial units (ru)] (x-axis). The dotted diagonal line represents a theoretically even distribution of fluorescence from centre to periphery.

3.10. Summary

In this chapter I present details of a novel protocol for culture of zebrafish retinal cells in a non-adhesive 3D format. This involved optimisation of retinal dissection and dissociation, optimisation of the culture medium in which cells were cultured and finding an appropriate 3D culture format in which cells could reaggregate and self-organise in the absence of extrinsic cues and scaffolds. Finally, I present details of the process of devising a method to analyse the organisation of these self-organised aggregates as a metric of lamination. During the development of this novel retinal reaggregation model I also uncovered several developmental mechanisms of retinal lamination, which are discussed in the discussion chapter of the thesis.

CHAPTER 4

The Roles of Individual Retina Cell Types in Self-Organisation

4. The Roles of Individual Retina Cell Types in Self-Organisation

4.1. Focus of this chapter

In this chapter I will explain my investigations of the role of various cell types in the self-organisation of these zebrafish retinal reaggregates. I eliminated individual cell types using a variety of techniques including manual dissection before culture, pharmacological inhibition, and genetic ablation. I then analysed the organisation in the resulting cell type-deficient reaggregates to assess their role in the layering of the other cell types. First, I discuss the role of two supporting cell types to the neural retina: Retinal Pigment Epithelium and Müller Glial Cells. Next, I discuss the role of Retinal Ganglion Cells and Amacrine Cells.

4.2. Retinal Pigment Epithelium *is not* required for self-organisation

Given that in some RPE mutants, retinal lamination is disrupted (Jensen et al. 2001; Zou et al. 2008) and RPE are important for lamination in chick retinal reaggregates (Vollmer et al. 1984; Vollmer & Layer 1986; Layer & Willbold 1989; Rothermel et al. 1997) I decided to investigate their role in my zebrafish reaggregates by looking at the lamination of RPE-deficient aggregates. Currently there are no known techniques for removing RPE, other than manual segregation. Some studies are making good progress in understanding the genetic mechanisms behind RPE genesis which could provide the basis for genetic ablation of RPE, but these studies are not yet complete enough to develop a tool to ensure complete removal (Miesfeld et al. 2015).

4.2.1. Removing RPE for aggregates - Manual dissection at 32hpf

Since there are no known genetic or biochemical techniques for completely removing RPE cells in zebrafish I decided to remove the RPE layer with manual dissection before culture. I decided to do this at around the 32hpf stage, as this is when RPE cells develop enough pigment for me to visually distinguish RPE from neural retina. The layer

surrounds the retina and the cells themselves are held together under tension. I realised that when I cut into the layer, releasing the tension, the rest of the RPE cells recoiled together, coming away from the retina cells as they do so. This allowed for complete separation by gently rolling the retina away from the RPE layer. The RPE layer was completely removed without causing too much damage to other cells. Earlier work, described in Chapter 3 showed there wasn't much difference in the organisation of cells taken from retinas at the 24hpf or 32hpf stage, so I was confident the different stage for the starting material of the culture shouldn't be a big factor in the results of the experiment.

4.2.2. RPE is not required for self-organisation

In this experiment, I cultured cells in the same conditions as described in the optimised protocol in Chapter 3, but in one condition, RPE cells were removed at the dissection stage. For one experiment, PTU was not used at any stage to allow pigment to form in RPE cells so I could check for presence or absence of RPE in each condition (as shown in (Fig 4.1 F,N)).

Aggregates with and without RPE were analysed for organization using the isocontour profiling method described in Chapter 3. It is clear that the fluorescence profiles of cultures with RPE (Fig. 4.1 G) and without RPE (Fig. 4.1 O) are in the same order, with the Crx:gapCFP profile peaking towards the centre of the aggregate and the Ptf1a:cytGFP profile peaking towards the periphery. This pattern is consistent across all aggregates analysed (Fig. 4.1 Q,R). This is also represented in the ECDF plots in which, for aggregates with RPE (Fig. 4.1 H) and without RPE (Fig. 4.1 P) the Crx:gapCFP curve is shifted to the left of the Atoh7:gapRFP curve, and the Ptf1a:cytGFP curve is shifted to the right. The somewhat different shapes of the curves near the centre of the aggregate for the condition with RPE is due to the pigment epithelial cells, which are themselves not fluorescent, being present in the centre of these aggregates. Areas measured between these curves for both conditions show no significant difference (Fig. 4.1 S-U). These results, together with the fact that in both conditions the aggregates show a similar degree of ordering in the same relative patterns, suggest that in these experiments, RPE cells may not have an appreciable influence on the ability of

developing zebrafish retinal tissue to self-organise in aggregate culture. Due to this result it was deemed unnecessary to exclude RPE from any further experiments and it should be assumed that all other cultures described in this thesis are including RPE, unless otherwise stated.

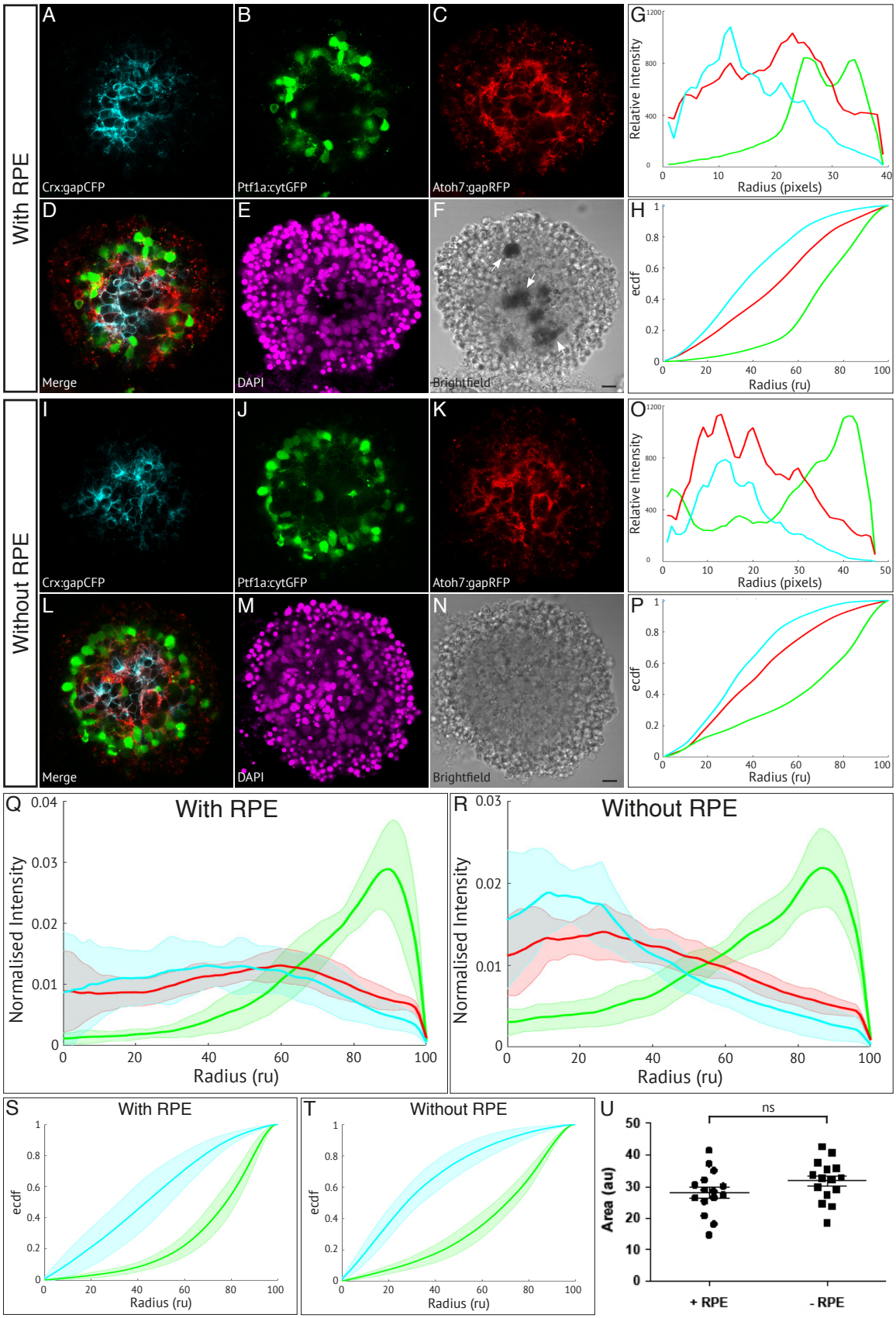
With RPE
A
Crx:gapCFP
B
Ptf1a:cytGFP
C
Atoh7:gapRFP
G
Relative Intensity
Radius (pixels)
D
Merge
E
DAPI
F
Brightfield
H
ecdf
Radius (ru)
Without RPE
I
Crx:gapCFP
J
Ptf1a:cytGFP
K
Atoh7:gapRFP
O
Relative Intensity
Radius (pixels)
L
Merge
M
DAPI
N
Brightfield
P
ecdf
Radius (ru)
Q
With RPE
Normalised Intensity
Radius (ru)
R
Without RPE
Normalised Intensity
Radius (ru)
S
With RPE
ecdf
Radius (ru)
T
Without RPE
ecdf
Radius (ru)
U
ns
Area (au)
+ RPE
- RPE

Figure 4-1: Retinal pigment epithelium is not required for zebrafish retinal self-organisation.

Fluorescence profiles are generated for SoFa1 aggregates cultured either with or without RPE cells. (A-F) Central sagittal section of a SoFa1 aggregate with RPE. (A) Crx:gapCFP-expressing cells are found in the centre of the aggregate. (B) Ptf1a:cytGFP-expressing cells are found in a ring around the edge of the Crx:gapCFP population. (C) Atoh7:gapRFP-expressing cells are found throughout the aggregate. (D) Merge of channels represented in (A-C). (E) DAPI. (F) Bright-field image. Pigment-expressing RPE cells can be seen near the centre of the aggregate (arrows). Scale bar: 10 μm. (G) Fluorescence profiles for the aggregate represented in A-F. (H) ECDF plot for the aggregate represented in A-F. (I-N) Central sagittal section of a SoFa1 aggregate without RPE. (I) Crx:gapCFP-expressing cells are found in the centre of the aggregate. (J) Ptf1a:cytGFP-expressing cells are found in a ring around the edge of the Crx:gapCFP population. (K) Atoh7:gapRFP-expressing cells are found throughout the aggregate. (L) Merge of channels represented in I-K. (M) DAPI. (N) Bright-field image. No pigment-expressing RPE cells can be seen. Scale bar: 10 μm. (O) Fluorescence profiles for the aggregate represented in I-N. (P) ECDF plot for the aggregate represented in I-N. (Q) Average fluorescence profiles with shaded error for aggregates with RPE (n=15, three experimental repeats). (R) Average fluorescence profiles with shaded error for aggregates without RPE (n=15, three experimental repeats). (S) Average ECDF plots for aggregates with RPE. (T) Average ECDF plots for aggregates without RPE. (U) Area (in arbitrary units) is calculated between the ECDF for the Crx:gapCFP population and the ECDF for the Ptf1a:cytGFP population of cells and compared between aggregates with RPE (+RPE) and without RPE (–RPE) (n=15 for each condition, Mann–Whitney two-tailed U test, $P>0.05$).

4.3. Müller Glia *are* required for self-organisation

Given that Müller Glia are important for lamination in chick retinal reaggregates (Willbold et al. 1995; Willbold et al. 2000) I decided to investigate their role in my zebrafish reaggregates by looking at the lamination of Müller Glia-deficient aggregates. Firstly, I wanted to make sure that Müller cell numbers were roughly representative of that *in vivo* and found that they are similar in my aggregates (Table 3.2, Chapter 3). I also checked that Müller cells appear at approximately the same time in the aggregates as they do *in vivo* (Figure 4.2) which is important to know due to the method by which I removed MG in the experiment. I was happy that the MG population in these aggregates was representative of that *in vivo.*

4.3.1. Methods for eliminating Müller Glia

Currently, the only proven method for removing Müller Glia in zebrafish is through the inhibition of Notch signalling in a time dependant manner, as previously described (MacDonald et al. 2015) . It is possible to try to use the same strategy of removing Müller Glia by apply the drug DAPT to cells in the same time-dependent manner as done *in vivo*. However, instead of adding it to embryo medium, it would have to be added to culture medium, and this had to be optimized.

4.3.2. Removing MG in aggregates with DAPT

DAPT is typically applied to the embryo medium of embryos at 45-48 hours onwards to selectively block the differentiation of Müller Glia without affecting the differentiation of any of the neural cell types (MacDonald et al. 2015). As I was taking the cells from the embryos before this time window for my cultures I needed to adapt this approach, by applying DAPT to the culture medium from the time equivalent of 45-48 hpf in the embryo onwards. To test the success of the drug the GFAP:GFP reporter line (Bernardos & Raymond 2006) was used to confirm the presence or absence of Müller Glia in the aggregates as shown in Figure 4.3. DMSO-treated controls show a high expression of GFAP:GFP, with Müller Glia extending processes throughout the aggregate (Fig. 4.3 A),

whereas aggregates treated with 25 μM DAPT displayed vastly reduced expression of GFAP:GFP and no mature MG processes (Fig. 4.3 C).

4.3.3. MG are required for self-organisation

I then analysed the effect of removing Müller Glia on the ability of all other cell types to organise using the SoFa1 line (Figure 4.4). The morphology of the aggregates (Fig. 4.4 A-F) and fluorescence profiles of DMSO-treated aggregates (Fig. 4.4 G) are similar to previous control aggregates, with the Crx: gapCFP profile peaking towards the centre of the aggregate and the Ptf1a:cytGFP profile peaking towards the periphery. This is consistent across all aggregates analysed for this condition (Fig. 4.4 Q). This is also represented in the ECDF plot (Fig. 4.4 H) where the Crx:gapCFP curve is shifted to the left of the Atoh7: gapRFP curve, and the Ptf1a:cytGFP curve is shifted to the right. The DAPT-treated cultures show disorganised aggregates (Fig. 4.4 I-N) and the corresponding fluorescence profiles clearly differ from the controls (Fig. 4.4 O); the lack of pattern is seen in all aggregates analysed for this condition (Fig. 4.4 R). The Crx:gapCFP curve does not peak in the centre of the aggregate, but rather shows more of a plateau, with two smaller peaks (one nearer the centre and one nearer the periphery), while the Ptf1a:cytGFP profile still peaks towards the periphery but the gradient is much reduced. These trends are reflected in the ECDF plots for the DAPT-treated culture, where it is clear that both the Crx:gapCFP and the Ptf1a:cytGFP have both been shifted towards the Atoh7:gapRFP curve (Fig. 4.4 P), representing an almost complete failure of patterning. Areas measured between these curves for both conditions show a significantly higher order of organisation for the DMSO-treated controls as compared with the DAPT-treated cultures (Fig. 4.4 S-U). These results suggest that Müller Glia may play an important role in the laminar organisation of zebrafish retinal aggregates.

4.3.4. Removing MG in aggregates using a Notch-independent method

These results clearly show there is an effect on lamination in aggregates treated with DAPT, but since Notch has been implicated in many other cellular processes I could not

exclude the possibility that lamination defects resulted from Notch inhibition rather than only the absence of MG. Thus, I attempted to remove the MG without affecting Notch signalling. Although there are no known genetic targets for eliminating Müller Glia in the zebrafish retina, a recent gene expression analysis performed in the lab by Dr Mark Charlton-Perkins has highlighted several candidate genes, found to be specific to MG. One such candidate is LIM homeobox domain 2b (Lhx2b). A conditional knock-out in mouse reveals Lhx2 to be essential for all stages of MG development (de Melo et al. 2016). Given it is expressed specifically in MG in zebrafish, we anticipated we may be able to target it using a readily available morpholino (Peukert et al. 2011) to eliminate the MG. An alternative gene highlighted in these gene analysis studies is Hairy/E(spl)-related 2 (*her2)*. This gene is known to play a role in gliogenesis through regulation of Notch signaling. MG differentiation can be blocked using either a morpholino, or through overexpression of a dominant negative Her2 construct lacking a WRPW domain (essential for Her2 function) using *her2ΔWRPW* cRNA (Cheng et al. 2015). Again, this gene is expressed specifically in MG in zebrafish, so we anticipated it could be targeted in order to eliminate them.

I tried to eliminate MG by targeting either Lhx2b, or Her2. Unfortunately, targeting Lhx2b with a morpholino did not have the desired effect of specifically eliminating MG. Low doses (2-6ng) did not eliminate MG (Figure 4.5) while higher doses (above 8ng) led to embryo lethality before 24hpf. Targeting Her 2 using either a morpholino or the dominant negative construct also had the same results. Low doses such as 2ng Her2MO or 2ng Her2MO + 2ng *her2ΔWRPW* cRNA did not have the desired effect of reducing MC numbers (Figure 4.5), and higher doses (4ng and above) caused almost complete lethality of the embryos before 24hpf. This suggests that zebrafish MG likely require different genes/gene orthologues for viability and/or specification than those previously reported in the mouse.

Since none of these approaches were successful at removing Müller Glia without badly affecting retinal development or causing lethality before 24hpf, the only way to address the issue of whether this phenotype could be due to effects of inhibiting Notch during the later stages of organisation, was to provide further evidence of the correlation between presence of MG and extent of lamination of the aggregates. I decided to

compare the organisation of cultures treated with DAPT to eliminate MG to cultures where DAPT was applied at a later time-point to allow some Müller Glia to differentiate. Aggregates in which DAPT was added at 63 hpf onwards appear to organise better than those in which DAPT was applied from 48 hpf onwards (Fig. 4.6 G-M), indicating that the ability to organise correlates with the presence of Müller Glia in the cultures [shown with GFAP staining (Fig. 4.6 A-F)].

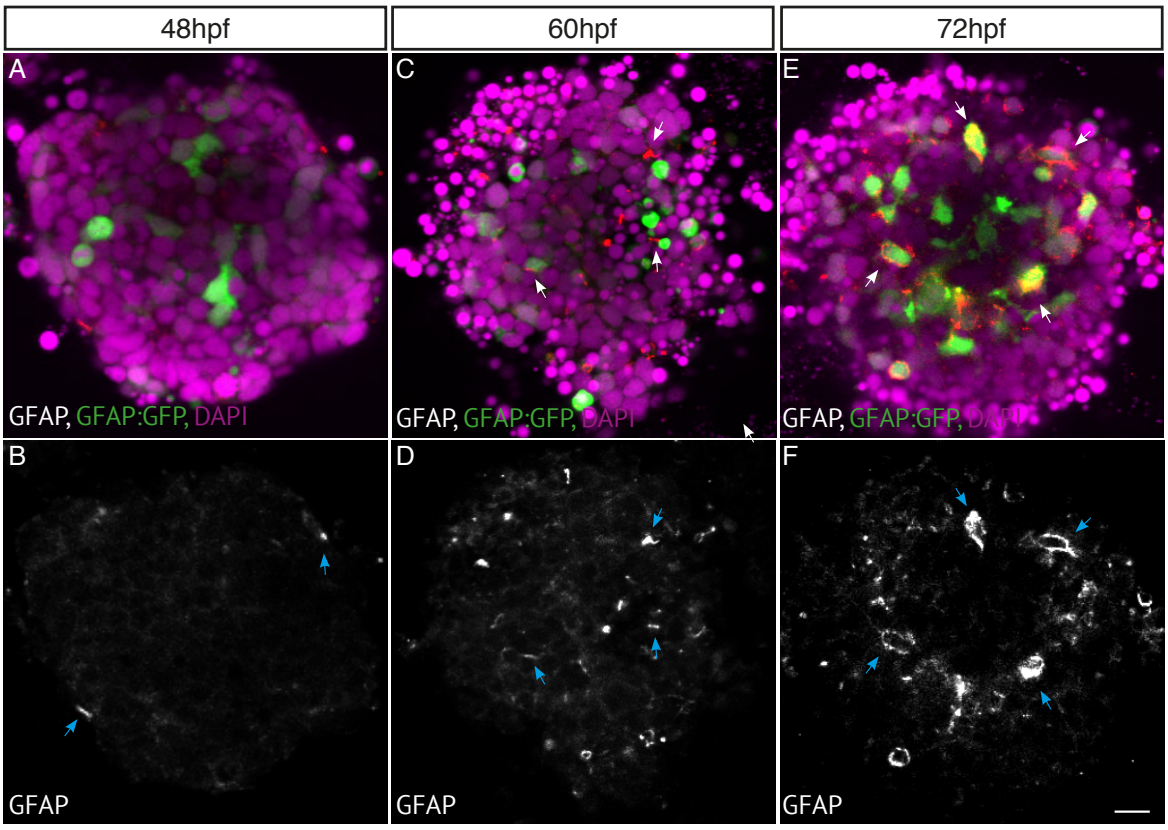

Figure 4-2: Müller Glia development is similar in aggregates as *in vivo*.

(A-B) GFAP expression starts to be seen in very few cells at 48hpf. (C-D) As Müller cells mature GFAP is expressed in more cells by 60hpf. (E-F) By 72hpf GFAP expression is seen in most, if not all, mature Müller cells (n = 5 for each condition). GFAP positive cells indicated with arrows. Scale bar = 10μm.

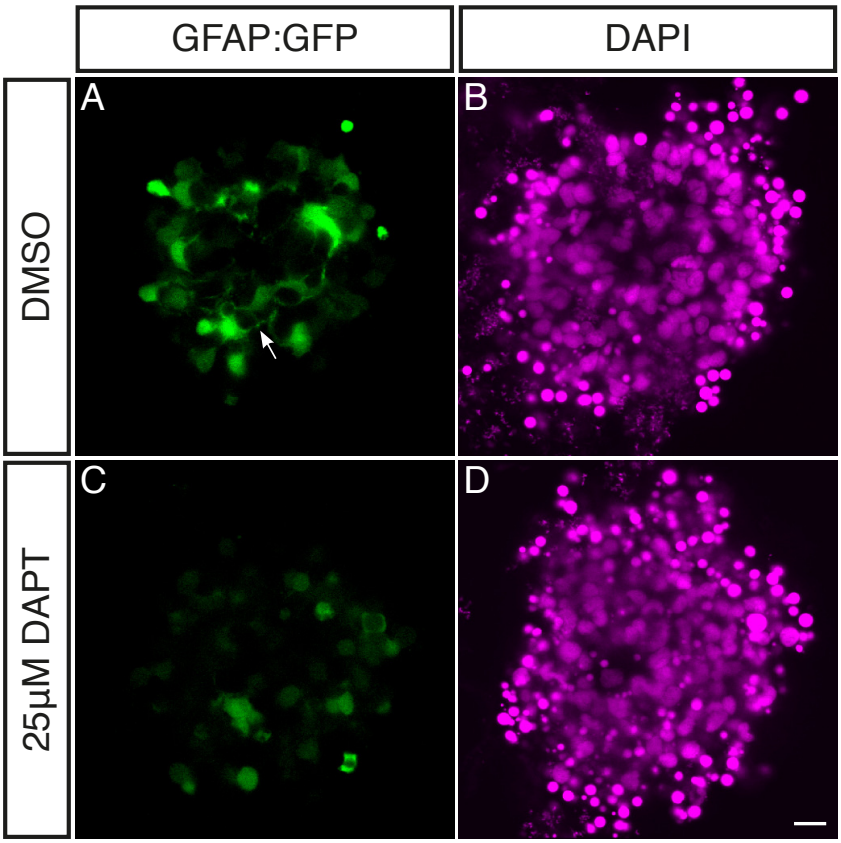

Figure 4-3: Müller Glia are absent in aggregates treated with 25µM DAPT.

Zebrafish retinal cells were cultured using the GFAP:GFP transgenic line which strongly labels Müller Glia (but is also expressed in undifferentiated cells at low levels). Aggregates were treated with either DMSO or 25µM DAPT from the equivalent of 45hpf onwards. (A-B) Aggregates treated with DMSO as a control. (A) GFAP:GFP expressing MG can be seen throughout the aggregate, extending axonal like projections into the aggregate (arrow). (B) DAPI. (C-D) Aggregates treated with 25µM DAPT. (C) GFAP:GFP can only be seen at low levels, and no axonal projections can be seen indicating a lack of MG present. (D) DAPI. (n =15 for each condition) Scale bar = 10µm.

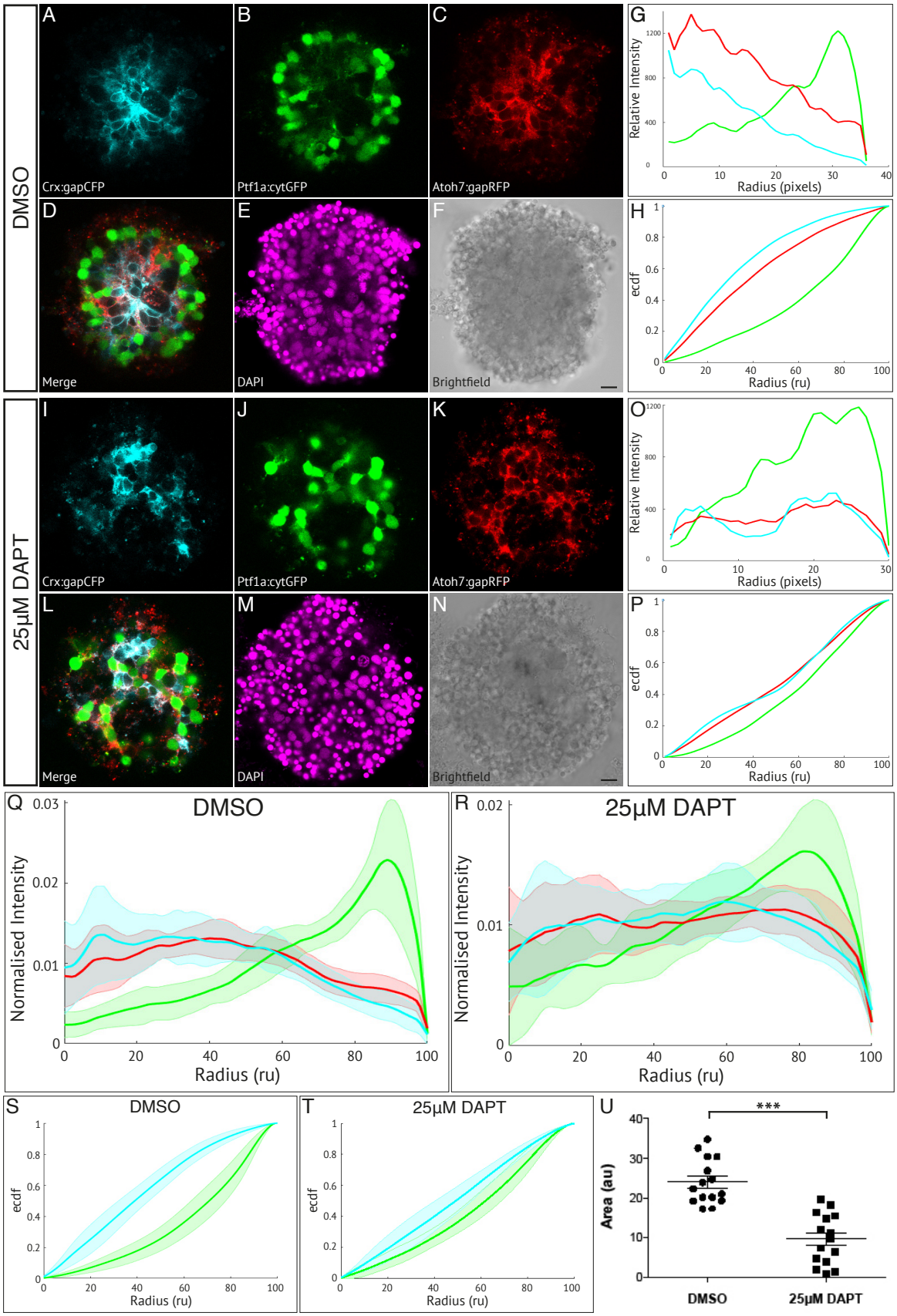
DMSO
A
Crx:gapCFP
B
Ptf1a:cytGFP
C
Atoh7:gapRFP
G
Relative Intensity
Radius (pixels)
D
Merge
E
DAPI
F
Brightfield
H
ecdf
Radius (ru)
25µM DAPT
I
Crx:gapCFP
J
Ptf1a:cytGFP
K
Atoh7:gapRFP
O
Relative Intensity
Radius (pixels)
L
Merge
M
DAPI
N
Brightfield
P
ecdf
Radius (ru)
Q
DMSO
Normalised Intensity
Radius (ru)
R
25µM DAPT
Normalised Intensity
Radius (ru)
S
DMSO
ecdf
Radius (ru)
T
25µM DAPT
ecdf
Radius (ru)
U
***
Area (au)
DMSO
25µM DAPT

Figure 4-4: Müller glia are important in zebrafish retinal self-organisation.

Fluorescence profiles are generated for SoFa1 aggregates treated either with 25 μM DAPT to prevent the differentiation of Müller glia or with DMSO as a control. (A-F) Central sagittal section of a SoFa1 aggregate treated with DMSO. (A) Crx: gapCFP-expressing cells are found in the centre of the aggregate. (B) Ptf1a:cytGFPexpressing cells are found in a ring around the edge of the Crx:gapCFP population. (C) Atoh7:gapRFP-expressing cells are found throughout the aggregate. (D) Merge of channels represented in A-C. (E) DAPI. (F) Bright-field image. Scale bar: 10 μm. (G) Fluorescence profiles for the aggregate represented in A-F. (H) ECDF plot for the aggregate represented in A-F. (I-N) Central sagittal section of a SoFa1 aggregate treated with 25 μM DAPT. (I) Some Crx:gapCFP-expressing cells are found in the centre of the aggregate, and some are found nearer the edge. (J) Ptf1a:cytGFPexpressing cells are found throughout the aggregate. (K) Atoh7:gapRFP-expressing cells are found throughout the aggregate. (L) Merge of channels presented in I-K. (M) DAPI. (N) Bright-field image. Scale bar: 10 μm. (O) Fluorescence profiles for the aggregate represented in I-N. (P) ECDF plot for the aggregate represented in I-N. (Q) Average fluorescence profiles with shaded error for aggregates treated with DMSO (n=15, three experimental repeats). (R) Average fluorescence profiles with shaded error for aggregates treated with 25 μM DAPT (n=15, three experimental repeats). (S) Average ECDF plots for aggregates treated with DMSO. (T) Average ECDF plots for aggregates treated with 25 μM DAPT. (U) Area (in arbitrary units) is calculated between the ECDF for the Crx:gapCFP population and the ECDF for the Ptf1a:cytGFP population of cells and compared between aggregates treated with DMSO and aggregates treated with 25 μM DAPT (n=15 for each condition, Mann–Whitney two-tailed U-test, $P<0.0001$).

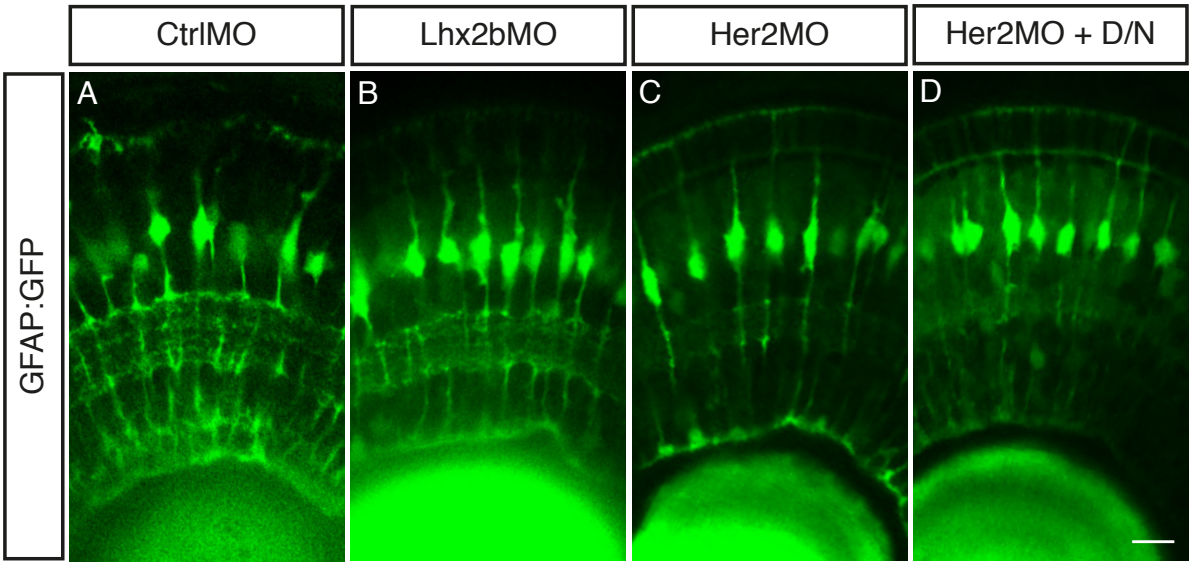

Figure 4-5: Attempted removal of MG in aggregates using Notch-independent methods

Central sagittal sections of 72hpf retinas of embryos from the GFAP:GFP transgenic line. (A) Embryo injected with 6ng control morpholino. (B) Embryo injected with 6ng Lhx2b morpholino. (C) Embryo injected with 2ng Her2 morpholino. (D) Embryos co-injected with 2ng Her2 morpholino and 2ng her2ΔWRPW cRNA. Müller Glia can be seen in all conditions. (n = 9 for each condition) Scale bar = 10μm.

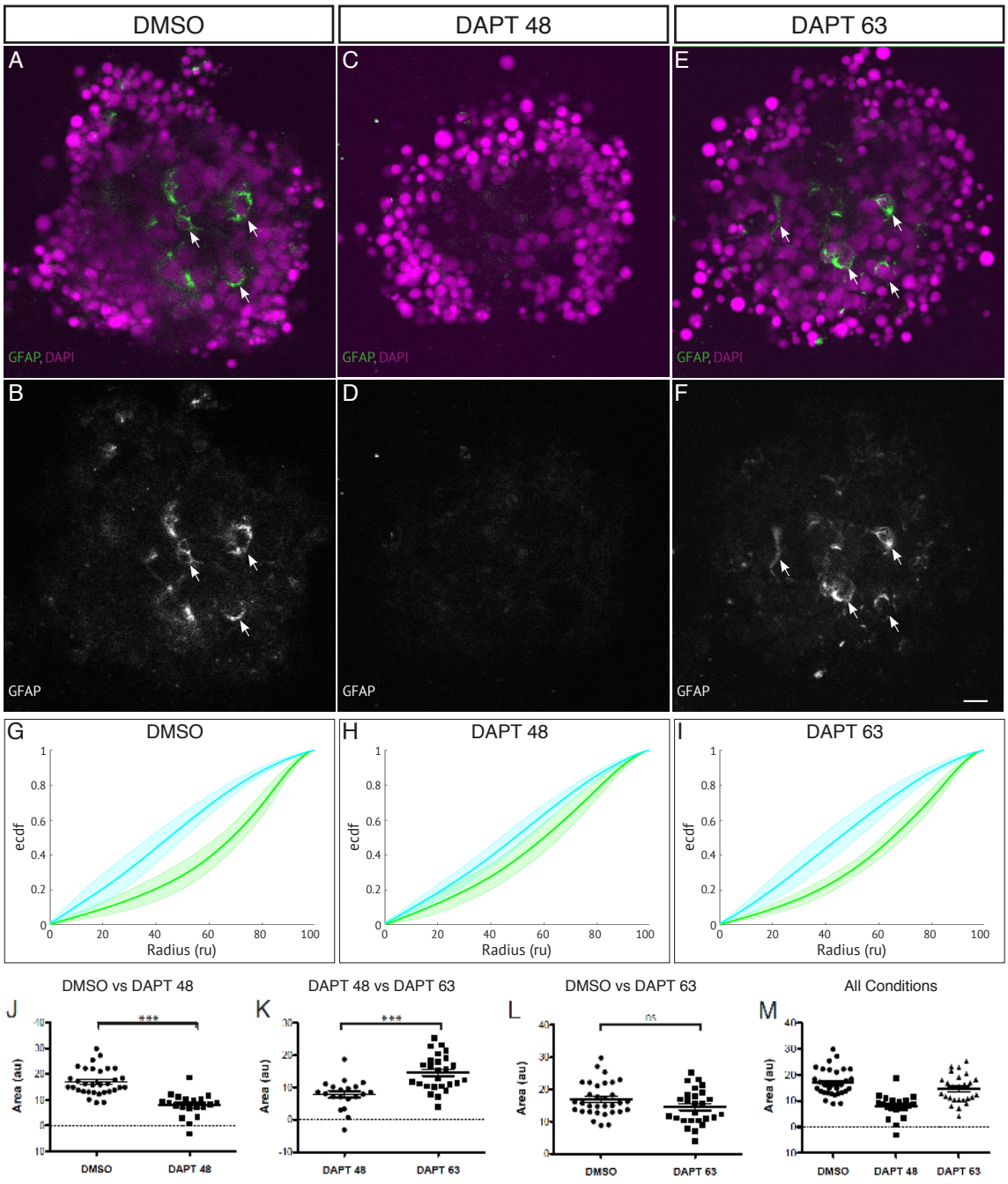

Figure 4-6: Late application of DAPT allows Müller glia to be generated and aggregates to self-organise.

Aggregates are cultured in the presence of DAPT applied at 45-48 hpf onwards to block the differentiation of Müller glia or at 63 hpf onwards to allow the differentiation of some Müller glia compared with DMSO control. (A,B) Aggregates cultured in the presence of DMSO show several GFAP positive cells (indicated by arrows). (C,D) Aggregates cultured in the presence of DAPT from 45-48 hpf onwards have little or no

GFAP-positive cells. (E,F) Aggregates cultured in the presence of DAPT from 63 hpf onwards have several GFAP-positive cells (indicated by arrows). Scale bar: 10μm. (G) Average ECDF plots for aggregates treated with DMSO. (H) Average ECDF plots for aggregates treated with DAPT from 45-48 hpf onwards. (I) Average ECDF plots for aggregates treated with DAPT from 63 hpf onwards. (J) Area (in arbitrary units) is calculated between the ECDF for the Crx:gapCFP population and the ECDF for the Ptf1a:cytGFP population of cells and compared between aggregates treated with DMSO and aggregates treated with DAPT from 45-48 hpf onwards (n=32 for DMSO, n=20 for DAPT at 45-48 hpf, Mann–Whitney two-tailed U-test, $P<0.0001$). (K) Area (arbitrary units) compared between the ECDF plots of aggregates treated with DAPT from 45-48 hpf onwards and aggregates treated with DAPT from 63 hpf onwards (n=20 for DAPT at 45-48 hpf, n=26 for DAPT at 63 hpf, Mann–Whitney two-tailed U-test, $P<0.0001$). (L) Area (arbitrary units) compared between the ECDF plots of aggregates treated with DMSO and aggregates treated with DAPT from 63 hpf onwards (n=32 for DMSO, n=26 for DAPT at 63 hpf, Mann Whitney two-tailed U-test, $P>0.05$). (M) Areas of data from all conditions.

4.4. Retinal Ganglion Cells are *not* required for self-organisation

RGCs are the first cell type to differentiate and laminate in the retina and so it could be hypothesised that they provide a scaffold upon which other cell layers can form, however previous studies have not been able to clearly decipher whether RGCs are crucial for retinal lamination or not. Live imaging studies show that they interact with neighbouring Amacrine Cells as they are finding their correct layer (Kay et al. 2004; Chow et al. 2015), however retinas void of RGCs are still capable of laminating correctly (Kay et al. 2004; Randlett et al. 2013). It is unknown whether RGCs are necessary for lamination, or whether they are simply instructive, given that RGCs that are translocated ectopically during development influence BPs to organise around them (Icha et al. 2016). The novel reaggregation model presented in this thesis provides the opportunity to begin to decipher whether RGCs are necessary or instructive to retinal lamination.

4.4.1. Methods for eliminating RGCs

RGCs can be removed from our culture in two ways. One is by culturing cells from the Lakritz mutant. This mutant is null for the Atoh7 gene (also known as Ath5), which prevents differentiation of all RGCs. This line is well established, but there are some difficulties that must be overcome in using it for my experiments. To analyse the organisation of these aggregates, I must cross this mutant to the SoFa1 line, so I can identify the cell types. Ideally this would be done by crossing a homozygous fish from each line. However, the homozygous Lakritz mutant fish is blind and as a consequence will not mate. I would therefore need to cross a heterozygous Lakritz fish with the SoFa1 fish, but this would need to be crossed and bred through several generations before establishing a line, which would still need to be screened before each culture. Unfortunately, the fish cannot be screened for the Lakritz mutation at the early stage we need to dissect the eyes. I therefore decided that I couldn't use this mutant for my cultures, and so decided to take an alternative approach, to inject embryos with an Ath5 morpholino. This morpholino is very efficient and prevents the differentiation of almost all RGCs. Although this morpholino works efficiently *in vivo* we don't yet know how well it works when the cells are cultured *in vitro* so this needed to be tested in my cultures.

4.4.2. Eliminating RGCs with the Ath5 morpholino

Embryos were injected between the 1-2 cell stages with either 4ng Ath5 morpholino (Ath5MO) or a standard control morpholino (CtrlMO) (see methods for more details). Embryos were then allowed to grow to 24hpf as usual and the culture carried out as previously described. Sibling embryos were grown until 72hpf to check the morpholino injections were successful in that the retinas were void of RGCs (Figure 4.7). Embryos injected with the CtrlMO (Fig 4.7 A-D) show all retinal cell layers, as seen with the SoFa1 transgenic line. Embryos injected with the Ath5MO (Fig 4.7 E-H) had an absent RGC cell layer (Fig 4.7 H) (denoted by the dashed white line) and a slightly expanded Amacrine cell layer (Fig 4.7 G), which correlates with findings in previous studies (Kay et al. 2001; Almeida et al. 2014). Roughly 80% of embryos showed this phenotype so I was confident that there would be a sufficient knock down of RGCs in my cultures. I also stained some cultures with Zn5 to show presence or absence of RGCs (Figure 4.8). In the CtrlMO condition (Fig 4.8 A-B), RGCs can be seen clearly, around the outside of the aggregate, whereas in the Ath5MO (Fig 4.8 C-D) condition, the numbers of RCGs are significantly reduced.

4.4.3. RGCs are not important for self-organisation

Cells from embryos injected with either 4ng Ath5MO or 4ng CtrlMO were cultured in standard culture conditions and the organisation of aggregates in each condition was compared after analysis by Isocontour profiling, as previously described in Chapter 3. As seen in Figure 4.9, aggregates cultured from the Ath5MO condition appear to be better organised than those from the CtrlMO condition. The fluorescence profiles of cultures in the CtrlMO condition (Fig. 4.9 G) and the Ath5MO condition (Fig. 4.9 O) are in the same order, with the Crx:gapCFP profile peaking towards the centre of the aggregate and the Ptf1a:cytGFP profile peaking towards the periphery, however the spatial distinction between these two populations is reduced in the CtrlMO condition on average. This pattern is consistent across all aggregates analysed for the Ath5MO condition but varies considerably more in the CtrlMO condition (Fig. 4.9 Q,R). This is also represented in the ECDF plots in which for aggregates in the CtrlMO condition (Fig.

4.9 H) and Ath5MO condition (Fig. 4.9 P), the Crx:gapCFP curve is shifted to the left of the Atoh7:gapRFP curve, and the Ptf1a:cytGFP curve is shifted to the right, however the area between these curves is much reduced on average in the CtrlMO condition. Again, these results vary much more in the CtrlMO condition. Areas measured between these curves for both conditions show that aggregates cultured in the Ath5MO condition are not significantly more organized than those in the CtrlMO condition. (Fig. 4.9 S-U). These results, together with the fact that in both conditions the aggregates show a similar degree of ordering in the same relative patterns, suggest that in these experiments, RGC cells may not have an appreciable influence on the ability of developing zebrafish retinal tissue to self-organise in aggregate culture.

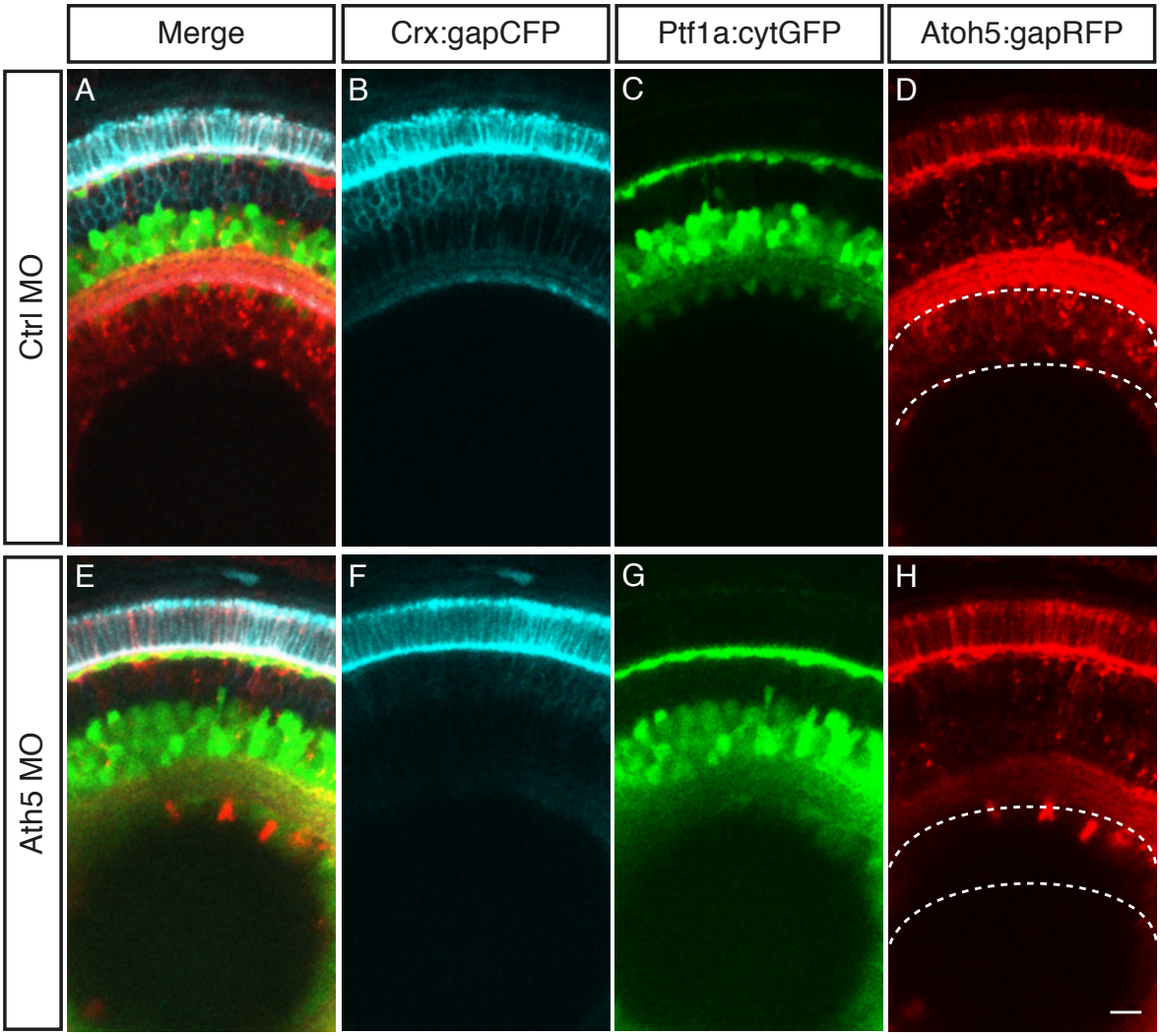

Figure 4-7: Retinal Ganglion Cells are absent in embryos injected with 4ng Ath5 morpholino

(A-H) Central sagittal section of the retina of a SoFa1 embryo injected with a control morpholino (CtrlMO) (A-D) where all retinal cell layers are present, or 4ng Ath5 morpholino (Ath5MO) (E-H) where the RGC cell layer is absent (indicated with the white dotted lines). (n = 9 for each condition) Scale bar = 10 μm.

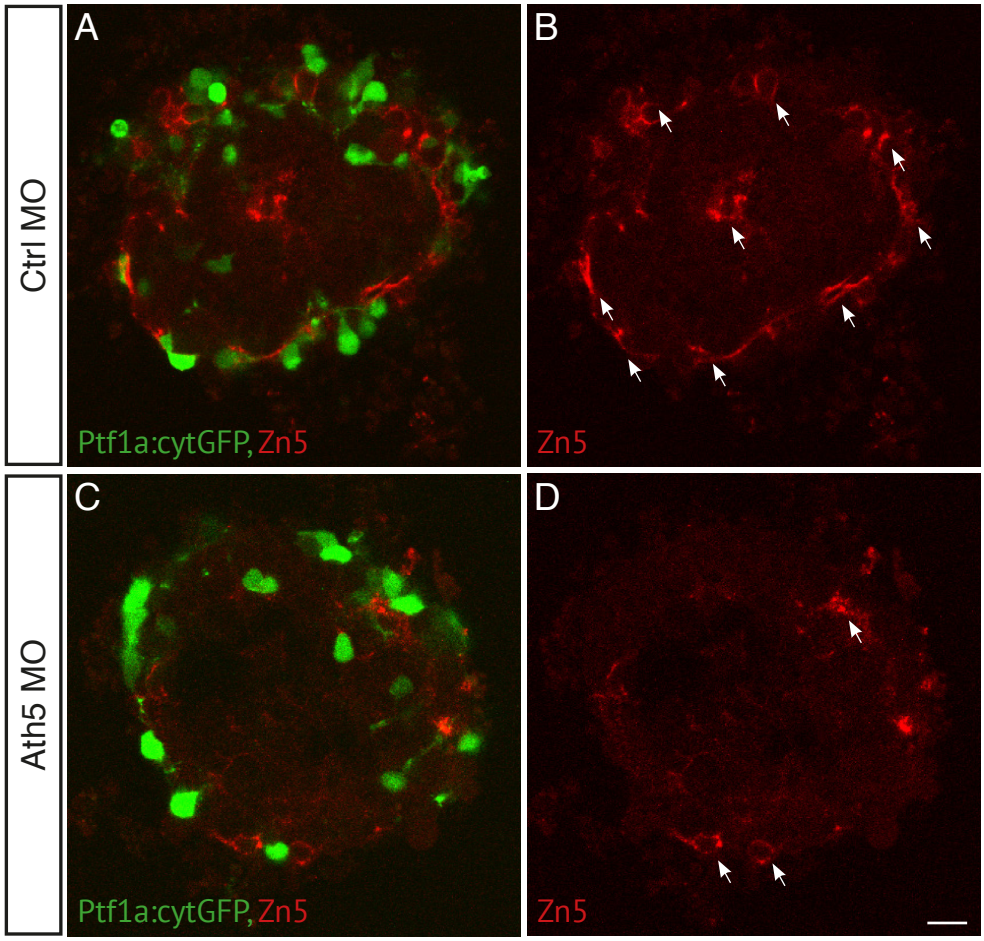

Figure 4-8: Retinal Ganglion Cells numbers are reduced in aggregates of cells from Ath5MO injected embryos

Aggregates cultured from embryos in the Ptf1a:cytGFP transgenic line and stained with Zn5. (A-B) Aggregates in the CtrlMO condition show multiple RGCs organised in the outer layer of the aggregate, amongst the Ptf1a:cytGFP positive cells as indicated by the white arrow heads. (C-D) Aggregates in the Ath5MO condition show far fewer RGCs, in the outer layer, amongst the Ptf1a:cytGFP positive cells. (n = 9 for each condition) Scale bar = 10 μm.

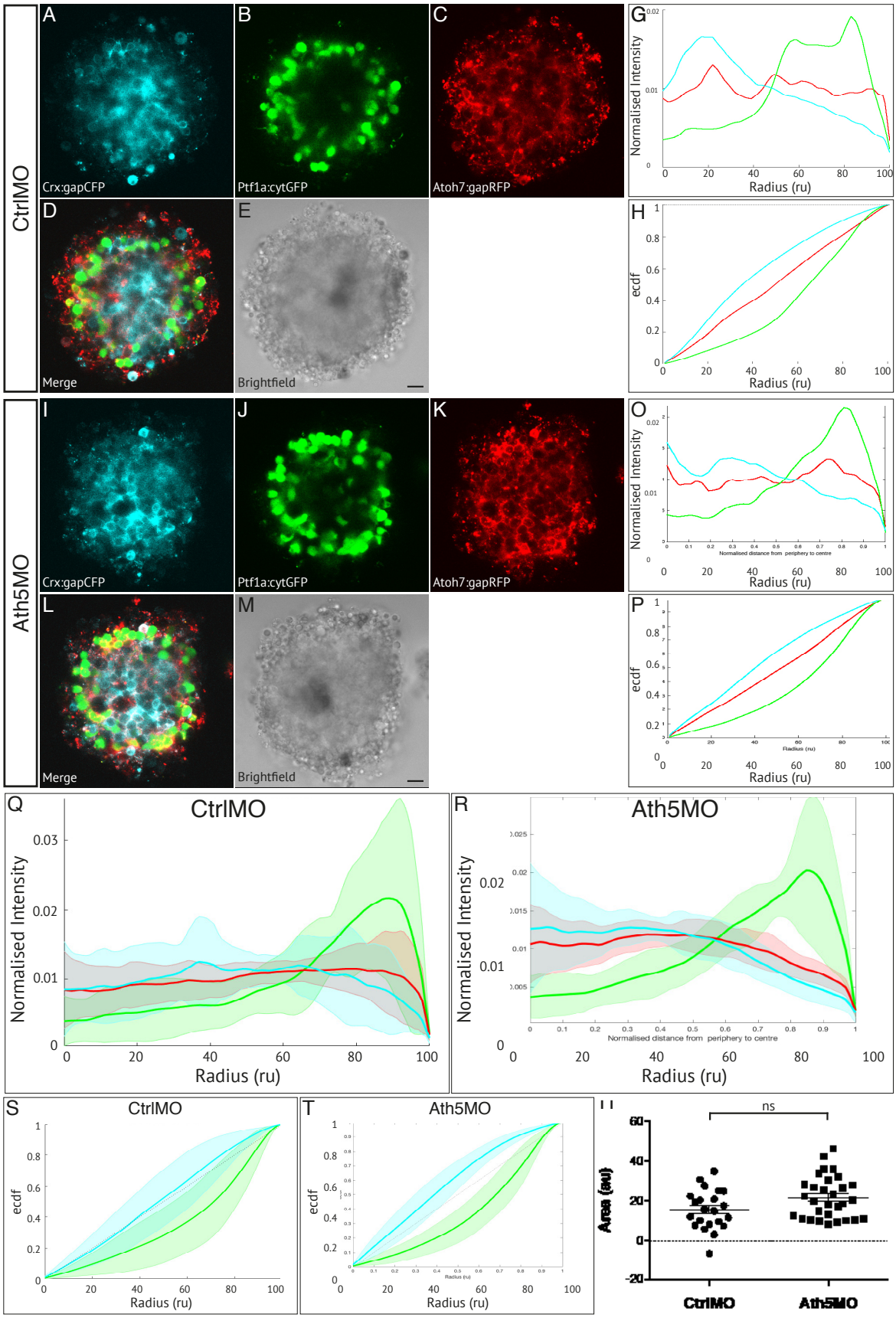
CtrlMO
A
Crx:gapCFP
B
Ptf1a:cytGFP
C
Atoh7:gapRFP
G
Normalised Intensity
Radius (ru)
D
Merge
E
Brightfield
H
ecdf
Radius (ru)
Ath5MO
I
Crx:gapCFP
J
Ptf1a:cytGFP
K
Atoh7:gapRFP
O
Normalised Intensity
Normalised distance from periphery to centre
Radius (ru)
L
Merge
M
Brightfield
P
ecdf
Radius (ru)
Q
CtrlMO
Normalised Intensity
Radius (ru)
R
Ath5MO
Normalised Intensity
Normalised distance from periphery to centre
Radius (ru)
S
CtrlMO
ecdf
Radius (ru)
T
Ath5MO
ecdf
Radius (ru)
U
ns
Area (au)
CtrlMO
Ath5MO

Figure 4-9: Retinal Ganglion Cells are not required for zebrafish retinal self-organisation.

Fluorescence profiles are generated for SoFa1 aggregates cultured from embryos that had either been injected with 4ng Ath5 morpholino (Ath5MO) or the same concentration of Control morpholino (CtrlMO). (A-E) Central sagittal section of a CtrlMO SoFa1 aggregate. (A) Crx:gapCFP-expressing cells are found in the centre of the aggregate. (B) Ptf1a:cytGFP-expressing cells are found in a ring around the edge of the Crx:gapCFP population. (C) Atoh7:gapRFP-expressing cells are found throughout the aggregate. (D) Merge of channels represented in (A-C). (E) Bright-field image. Dark cells are RPE. Scale bar: 10 μm. (G) Fluorescence profiles for the aggregate represented in A-E. (H) ECDF plot for the aggregate represented in A-E. (I-N) Central sagittal section of an Ath5MO SoFa1 aggregate. (I) Crx:gapCFP-expressing cells are found in the centre of the aggregate. (J) Ptf1a:cytGFP-expressing cells are found in a ring around the edge of the Crx:gapCFP population. (K) Atoh7:gapRFP-expressing cells are found throughout the aggregate. (L) Merge of channels represented in I-K. (M) Bright-field image. Scale bar: 10 μm. (O) Fluorescence profiles for the aggregate represented in I-O. (P) ECDF plot for the aggregate represented in I-O. (Q) Average fluorescence profiles with shaded error for CtrlMO aggregates (n=22, four experimental repeats). (R) Average fluorescence profiles with shaded error for Ath5MO aggregates (n=30, four experimental repeats). (S) Average ECDF plots for CtrlMO aggregates. (T) Average ECDF plots for Ath5MO aggregates. (U) Area (in arbitrary units) is calculated between the ECDF for the Crx:gapCFP population and the ECDF for the Ptf1a:cytGFP population of cells and compared between CtrlMO and Ath5MO aggregates (n=22 and 30 respectively for each condition, Mann–Whitney two-tailed U-test, $P>0.05$).

4.5. Amacrine and Horizontal Cells *may* play a role lamination

Amacrine and Horizontal cells exhibit dynamic cell migratory behaviours and appear to communicate with each other to find their appropriate laminar position during retinal development (Chow et al. 2015). Although there is no evidence to suggest they are crucial to retinal lamination *in vivo,* as retinas void of ACs and HCs are still able to laminate correctly (Randlett et al. 2013), they do seem to organise in a very distinct pattern in the aggregates of almost all conditions described so far in this thesis. It would therefore be interesting to investigate their role in this novel reaggregate system to see whether they are necessary for lamination or not in the absence of other scaffolds and cues.

4.5.1. Methods for eliminating AC/HCs

ACs/HCs can be eliminated from these cultures in two ways. The Ptf1a mutant fish has a nonsense mutation in the Ptf1a sa126 allele (Zebrafish Mutation Project; (Randlett et al. 2011)). This results in a knockdown of some, but not all ACs. An alternative method is to use a combination of two Ptf1a morpholinos, targeting different areas in the gene. Ptf1a-MO1 a splice-blocking morpholino which targets the 5'UTR of the Ptf1a gene sequence leads to a reduction in numbers of HCs but only a moderate reduction of ACs and dACs, whereas Ptf1a-MO2 a translation-blocking morpholino results in a complete loss of HCs and most ACs and dACs. Neither morpholino alone can knock down all ACs and HCs, however a combination of both can. A concentration of 8ng of each morpholino is deemed sufficient for almost a 100% knock down. (Jusuf & Harris 2009; Randlett et al. 2013; Almeida et al. 2014).

4.5.2. Eliminating ACs and HCs with the Ptf1a morpholino

Embryos were injected between the 1-2 cell stages with either a mix of 8ng Ptf1aMO1 and 8ng Ptf1aMO2 or a standard CtrlMO. Embryos were then allowed to grow to 24hpf as usual and the culture carried out as previously described. Sibling embryos were kept and grown until 72hpf to check the morpholino injections were successful in that the retinas were void of Amacrine and Horizontal (Ptf1a:cytGFP positive) cells (Figure

4.10). Embryos injected with the CtrlMO (Fig 4.10 A-D) had all retinal cell layers, as seen with the SoFa1 transgenic line. Embryos injected with the Ptf1aMO 1+2 combination (Fig 4.10 E-H) had absent Amacrine and Horizontal cell layers (Fig 4.10 G) (Ptf1a:cytGFP positive cells, denoted by the dashed white lines) and a slightly expanded Bipolar cell layer (Fig 4.10 F), which correlates with findings in previous studies (Jusuf & Harris 2009; Randlett et al. 2013; Almeida et al. 2014). Roughly 90% of embryos showed this phenotype so I was confident that there was a sufficient knock down of ACs and HCs in my cultures.

4.5.3. ACs and HCs *may* play a role in self-organisation

Unfortunately, during dissection of retinas from embryos and storage in calcium free medium, Ptf1a MO injected retinas frequently began to disintegrate in the dissection medium. This meant that once retinas had been incubated with trypsin and washed, many cells were already lost before dissociation, resulting in too little starting material for culture. Due to time constraints, I was unable to make adaptations to the dissection procedure to try to reduce loss of cells before dissociation to allow me to culture the cells enough times to get repeats for statistical analysis. The ways in which this could be done are discussed further in the discussion of this thesis. Nonetheless, one experiment was partly successful and 3 aggregates for each condition were cultured and imaged. Figure 4.11 shows a representative aggregate from each condition. Aggregates cultured from embryos injected with the control morpholino (Fig 4.11 A-D) display a similar pattern of organisation as previously seen in embryos injected with control morpholino, and uninjected embryos. The Crx:gapCFP-expressing cells are organised in one cluster in the centre (Fig 4.11 B), with the Ptf1a:cytGFP-expressing cells in a ring around them (Fig 4.11 C). In the Ptf1aMO 1+2 condition (Fig 4.11 E-H) the number of Ptf1a:cytGFP-expresisng cells (Fig 4.11 G) is clearly greatly reduced in the aggregates, indicating a much-reduced population of Amacrine and Horizontal cells. In this condition Crx:gapCFP-expressing cells (Fig 4.11 F) appear to be more spread out throughout the aggregate and clustered in several places rather than in one cluster in the centre, indicating a possible reduction in organisation.

At first glance the aggregates in the Ptf1aMO 1+2 condition appear to be less organised than those in the control condition, however the number of samples is far too low to make any inferences as to whether this result is statistically significant, or simply due to experimental error. It is also difficult to know how the other cell populations are organised without seeing where the RGCs are positioned. This is discussed further in the discussion section.

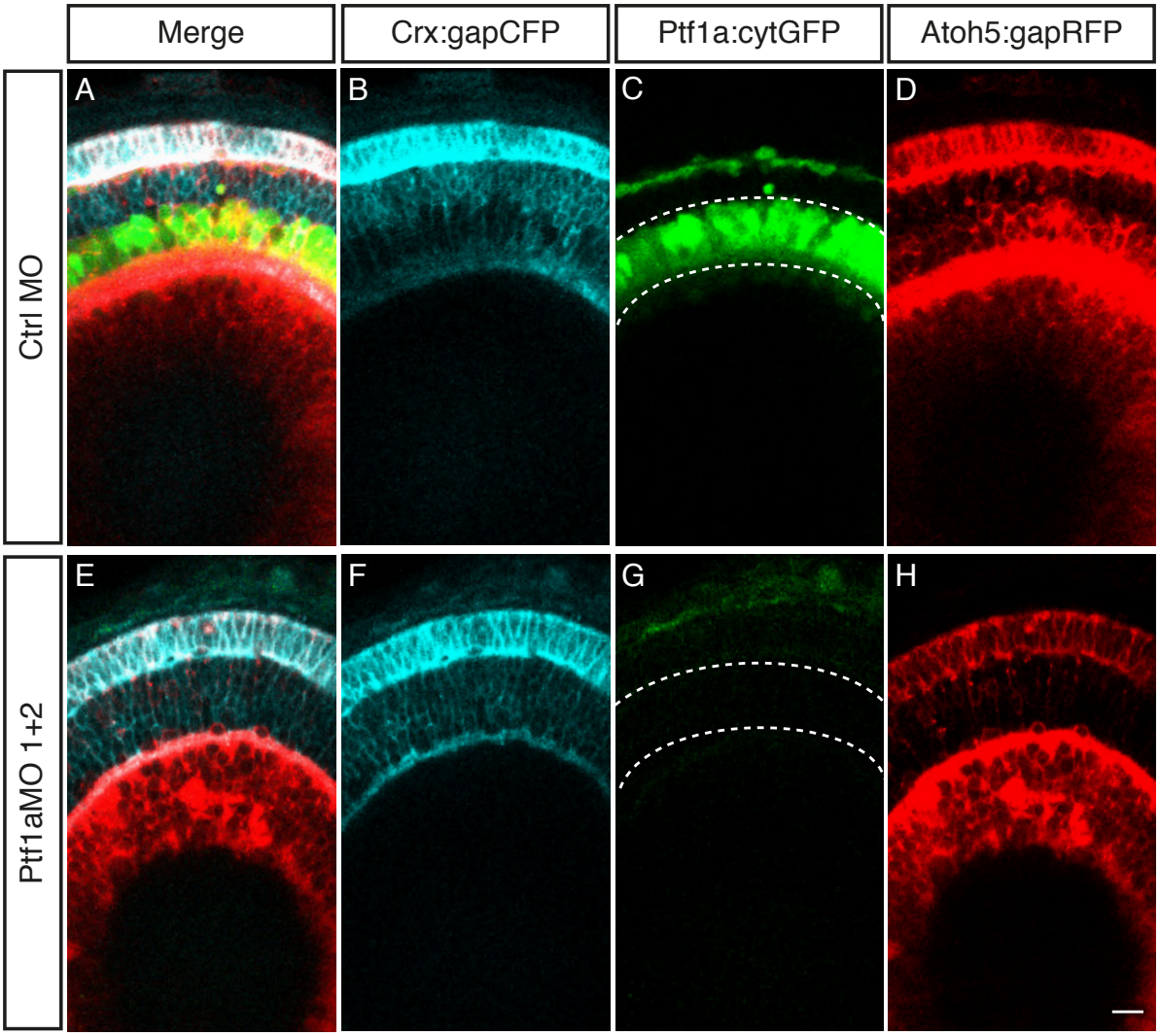

Figure 4-10: Amacrine and Horizontal cells are absent in embryos co-injected with 8ng Ptf1aMO1 and 8ng Ptf1aMO2

(A-H) Central sagittal section of the retina of a SoFa1 embryo injected with a control morpholino (A-D) where all retinal cell layers are present or 8ng Ptf1aMO1 and 8ng Ptf1aMO2 (E-H) where the AC and HC cell layers are absent (indicated with white dotted line lines). (n = 9 for each condition) Scale bar = 10 μm.

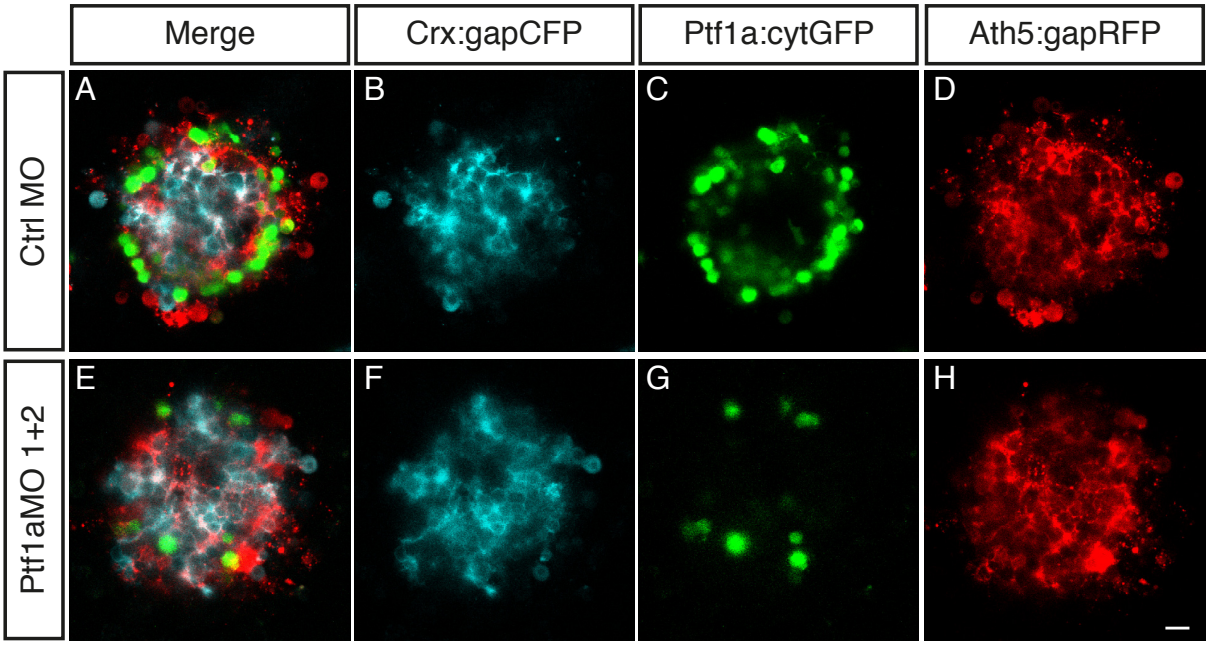

Figure 4-11: Aggregates lacking ACs and HCs

(A-D) Central sagittal section of a SoFa1 aggregate from embryos injected with a control morpholino. (A) Merge of channels represented in B-D. (B) Crx: gapCFP-expressing cells are found in the centre of the aggregate. (C) Ptf1a:cytGFPexpressing cells are found in a ring around the edge of the Crx:gapCFP population. (D) Atoh7:gapRFP-expressing cells are found throughout the aggregate. (E-H) Central sagittal section of a SoFa1 aggregate from embryos injected with a mix of Ptf1aMO1 and Ptf1aMO2 morpholino. (E) Merge of channels represented in F-H. (F) Crx: gapCFP-expressing cells are found throughout the aggregate. (G) Ptf1a:cytGFPexpressing cell numbers are greatly reduced, but still found in the outer ring of the aggregate. (H) Atoh7:gapRFP-expressing cells are found throughout the aggregate. (n = 3 for each condition) Scale bar = 10 μm.

4.6. Summary

After investigating the role of several cell types in my reaggregation system I have gained some surprising results, some of which agree with what is seen *in vivo* and some which don't, which will be discussed in the final chapter of this thesis. Firstly, MG seem to play an important role in self-organisation, although I cannot conclusively say whether this is due to the absence of MG or an effect of inhibiting Notch signalling. Secondly, it appears neither RPE, nor RGC cells are required for self-organisation in these aggregates, as aggregates organise just as well in their absence. Finally, AC and HCs may play a role in self-organisation, but unfortunately, I was unable to gain enough data to determine whether this observation is statistically significant or not.

CHAPTER 5

Discussion and Future Directions

5. Discussion and Future Directions

5.1. Building a novel model of retinal lamination *in vitro*

There are several ways to study cellular lamination of the retina. Looking at mutants for different cell types or molecules might tell us which are crucial for lamination, or one can study the migratory patterns of individual cells to understand which might interact with other to find their appropriate layers. But the cells of the retina are laminating within a complex environment, full of other influencing factors such as pre-existing polarity, surrounding tissues and scaffolds and guidance cues. To really understand the fundamental mechanisms of lamination it is necessary to look at the basic components of the system in a simplified environment. For this reason, I used the aggregation technique to build on previous investigations of retinal lamination. Previous aggregate studies began to reveal some of the cellular and molecular mechanisms of retinal lamination in chick, mouse and even gerbil, but the techniques used in these studies were time consuming and limited by the genetic tools available in those systems. In this thesis I decided to take advantage of the genetic tools available and ease of imaging of the zebrafish retina to allow me to easily image and manipulate cells and molecules of interest for my investigations. Zebrafish retinal cells had never before been cultured as a reaggregate culture, and so a large portion of the work in this thesis involves developing a novel protocol to culture zebrafish retinal cells in a 3D format and devising a way to image and quantitatively analyse their laminar organisation. In doing so I revealed several developmental mechanisms of zebrafish retinal lamination *in vitro* and used this system to expand on previous studies of retinal lamination, revealing the role of some cell types and molecules in this process. This thesis proves that zebrafish retinal reaggregates can be used as a simple, easy-to-manipulate model with which we can accelerate the studies of retinal lamination.

5.1.1. Development of a scaffold-free, 3D culture of zebrafish retinal cells

Zebrafish retinal cells are not commonly dissociated and cultured, and so I needed to establish a protocol to dissect, dissociate, and culture them in a 3D non-adhesive format.

The first step in developing this protocol was to adapt and optimise a pre-existing dissociation protocol (Almeida et al. 2014) to ensure retinas were dissociated into mostly single cells, while also producing a higher yield of cells than previously achieved and ensuring good viability before culture. This was achieved by altering length and temperature of enzyme incubation and adding extra washing steps after dissociation to inactivate the enzyme. This aimed to reduce the stress the cells encountered, thereby promoting viability, and normal cellular behaviour during culture. The next step was to optimise culture conditions. Zebrafish retinal cells have never before been cultured in a 3D format, so it was necessary to experiment with the culture medium and culture format. Cells could reaggregate in a minimal medium of just L-15 plus PSF, but it was clear that the addition of FBS and embryo extract promoted reaggregation and aggregate growth. It is unknown exactly why these promote reaggregation, but it could be because they are rich in proteins and cell growth factors. In agreement with previous reports (Zolessi et al. 2006), I also found that N2 supplement supports RGC growth and maturation in these cultures (data not shown), and it was later deemed necessary to include PTU to prevent pigment formation in the aggregates to aid in imaging. The 3D culture format was also crucial to these experiments. At first a simple hanging drop assay was used, which revealed that cells could reaggregate, but the level of aggregation and shape and size of the aggregates varied considerably from one sample to another, and particularly between experiments. The use of another culture format, the 3D Petri Dish solved these problems. These agarose microwells provided a confined, non-adhesive environment which minimises distance between cells. The cells within the wells aggregated quickly, and generated equally sized and shaped aggregates, useful for quantitative analysis.

The ability of zebrafish retinal progenitors to reaggregate without the need for a scaffold supports previous findings in chick (Moscona 1961; Sheffield & Moscona 1969), where dispersed chick retinal cells reaggregated in a simple gyratory culture, allowing initial observations of retinal cell organisation in reaggregated cultures. I was interested to see if this reaggregation was also dependant on R-Cognin, as it is in chick (Lilien & Moscona 1967), to get a sense of whether some of the mechanisms of reaggregation in zebrafish might be the same as those in chick. My data suggest R-Cognin is also crucial for zebrafish retinal cell reaggregation. Application of the small molecule inhibitor of R-

Cognin, PACMA31, prevented cell reaggregation after dissociation in a dose-dependent manner. I cannot say however, whether R-Cognin is involved in retinal lamination. It is expressed on the surface of all retinal cell types in chick (Dobi et al. 1986), therefore it could play a part in assisting the retinal cell types to establish and/or maintain their appropriate layering. However, as it is also crucial in reaggregation in my cultures I cannot explore this in my setup. It could be explored *in vivo*, where cells may be additionally supported by surrounding tissues, allowing them to attempt to establish their normal architecture. R-Cognin may also play a part in the age-dependant ability of retinal cells to reaggregate and laminate. R-Cognin is expressed more abundantly and promotes reaggregation better in cells from younger stage retinas in chick (Ben-Shaul et al. 1980). These studies suggested there was an age-dependent capacity of retinal cells to regenerate R-cognin and therefore reaggregate. It would be interesting to investigate the expression of R-Cognin at different stages of zebrafish retinal cell reaggregation to determine if it also plays an age-dependant role in my aggregates.

Finally, I validated the model to ensure it was representative of the developmental events occurring *in vivo*. I found the numbers of ACs, and HCs to be very similar to those in previously published *in vivo* studies (Boije et al. 2015; He et al. 2012) whereas the numbers of BCs and PRs were somewhat increased. The reason for this is unknown, but the overall change in proportions is fairly modest.

This model represents the early stages of retinal differentiation and lamination in the zebrafish retina, however it is unknown how mature these cells are and therefore whether it also represents later stages of differentiation. It must also be noted that these aggregates are very small in comparison to the retinas *in vivo*. It was observed that cells in larger aggregates, generated using the hanging drop method, were less organised than smaller aggregates generated using the agarose microwell dishes. Although we did not investigate the reasons for this, we should keep in mind that perhaps the environment in these aggregates is simpler than *in vivo* since cells do not have to migrate as far.

5.1.2. The process of lamination can be observed in real time using the Spectrum of Fates line

Many studies of tissue organisation use techniques such as immunohistochemistry or in situ hybridization to identify the different cell populations which can be quite time consuming. The use of the SoFa1 line for the starting material of my experiments allowed immediate and even live microscopic access to the process of lamination. I showed that the cell fate-tagged fluorophores (FPs) were expressed in the aggregates at roughly similar times to *in vivo*, although there was a modest delay. This could be due to the time the embryos spent outside of the incubator during preparation, dissection and dissociation. However, ultimately, all FPs were expressed in the 48hic aggregate, and the numbers of cells fates were in roughly the same proportions as a 72hpf retina. Therefore, perhaps it is not unreasonable to assume the developmental timing in my aggregates roughly resembles the situation *in vivo*.

Although all main cell types can be identified in the SoFa1 line *in situ*, I found it was difficult to distinguish some cell types from others in my aggregates, particularly when it came to quantify the patterning of large groups of cells. Although it would be interesting to gain a higher level of detail by identifying the patterning of each individual cell type, cells seemed to be grouped together in a way that meant I was still able to analyse the positioning of distinct populations of cells and gain insight into the basic mechanisms of lamination. I did however think it was important to understand where RGCs were positioned, given they are amongst the first cells to differentiate in the developing retina and form the most basal layer. To investigate their role in the layering of all other cells types, I thought it was necessary to understand their positioning within the aggregates under control conditions. I therefore looked at the expression of Zn5 and found RGCs to be positioned in the outer layer of the aggregates. This confirmed that the cells in the aggregates were layered in roughly the same order as they are *in vivo*, which is discussed later in this chapter.

In my experiments, I decided to fix and mount the aggregates prior to imaging to improve quality, however, an additional yet significant benefit to using the SoFa1 line is that cells could be imaged live. To do this would require imaging cells from above the micro-well plates using a water dipping lens but would be limited by the working distance of the objective and whether it can get close enough to the cells, due to the

limited space inside the seeding chamber. The benefits of this are discussed in the future directions section of this chapter.

5.1.3. Quantifying lamination

In this thesis, I describe a novel method for quantifying the lamination of cells in my aggregates, using the SoFa1 line. Due to the concentric patterning of these cells I decided the best method for analysis should be based on this geometry. I therefore devised a new method, together with Leila Muresan whereby fluorescence signal is measured along isocontours at 2-pixel thickness from the periphery to the centre of the aggregate. This accounts for differences in aggregate shape and for the unique patterning found in these aggregates. Using this method, we can see that the Crx:gapCFP-expressing population of cells are clearly clustered inside of the Ptf1a:cytGFP-expressing cells, and there isn't much intermingling between the two cell types. This allowed me to compare one condition to another, where perhaps one is organised, i.e. cell populations are spatially distinct, and one is disorganised, i.e. cells are found at any position in the aggregate. The script is easy to use and allows for quick and robust analysis of many samples, allowing better statistical certainty. By measuring the areas between these curves, I could derive a measure of laminar organization in my aggregates and can easily compare one experimental condition to another.

This method is fairly robust for this type of organisation, but it may only give limited information if the cells were to organise in a different pattern, for example several separate clusters. If alternate patterning were found, the user would need to adapt this method of analysis for the specific geometry found in their data.

5.1.4. Summary

This protocol allows for easy investigation of the mechanisms of neural lamination. Due to the rapid process of lamination in these aggregates, the transgenically labelled cells of the SoFa1 line, and a quick and robust method for quantifying lamination we can manipulate cells and molecules in this system and assess their importance in lamination.

5.2. Zebrafish retinal cells can self-organise

In developing this model I have shown for the first time that Zebrafish retinal cells are capable of self-organising, through some process of sorting, in a non-adhesive 3D culture format which agrees with previous studies in chick retinal reaggregates (Moscona 1961; Layer & Willbold 1993; Layer & Willbold 1994). I have also characterised this ability to self-organise both in terms of dependence on developmental time, and the ordering of layers.

5.2.1. Lamination is stage-dependant

During the optimisation of all these processes I investigated which stage would be most appropriate for the starting point of culture. I cultured cells from different stages, ranging from 24hpf, when cells are beginning to differentiate, to 72hpf, when cells are fully differentiated and laminated *in vivo*. The discovery that the cells from 24hpf retinas were better able to organise compared to cells from older stages is not unsurprising given that it is around this time that cells are laminating in the retina *in vivo*. It is also reported in previous studies of chick retinal reaggregation assays (Rothermel et al. 1997) that cells from younger stages were more capable of self-organising than those from older stages, suggesting the mechanisms responsible for retinal layering are more active during the earlier developmental stages and down-regulated in later stages.

5.2.2. Aggregates organise in the same order as *in vivo*

Using the SoFa1 transgenic line I could identify cell populations and analyse their organisation within the aggregates. The cell layers within the aggregates are organising in the same relative order as they do *in vivo*, with RPE next to photoreceptors and bipolar cells, next to horizontal and Amacrine cells, and finally, RGCs. At first glance, this normal progression of layers is apparently inverted with respect to the retina *in situ*, where the RPE is normally the outer cell layer and the RGCs comprise the inner. While situated near the basement membrane on the inner surface of the intact retina, RGCs in my aggregates are found near the outer surface, and photoreceptors and bipolar cells,

which populate the outer layers of the intact retina, are found near the centres. Such observations of inside-out organisation were also seen with rosettes of cells within the retinospheroids described by Layer and colleagues (Layer et al. 2001; Layer et al. 2002), and such photoreceptor-centred rosettes, surrounded by inner layer cells have frequently also been seen *in vivo* in pathological conditions (Wei et al. 2006; Johnson et al. 2007).

However, perhaps it is not fair to directly compare the layering *in vivo* and *in vitro* as it is not accurate to liken the spheroid shape of the aggregates with the curvature of the retina *in vivo*. The aggregates comprise a continuous sphere of cells, with an apical centre and a basal outer layer, much like in other neuroepithelium such as the neural tube. However, the retina *in vivo* is not spherical, in fact it is a layered sheet of cells which is curved around a lens. During retinal epithelium morphogenesis, these layers start off in the typical outside-in polarity but are seemingly inverted during optic cup morphogenesis. It is therefore not accurate to describe the apical surface as on the "outside" and the basal on the "inside" and we cannot liken this overall structure to a sphere. Taken out of the context of the embryo, perhaps my aggregates display the natural tendency for retinal cells to organise themselves in layers with RPE in the centre and RGCs on the outside, which does not rely on the polarity of the tissue generated by optic morphogenetic movements.

A more accurate description of the layering of these cells would be to compare their positioning relative to the apicobasal axis. We could look for polarity markers such as Pard3, an apically localised PDZ scaffold protein expressed in the OLM (Wei et al. 2004), or other adherens junction proteins such as ZO-1 or aPKC, also expressed near the OLM (Wu et al. 2014). It would also be interesting to look at cell migratory patterns. If cells are born at the centre of the aggregates, the "apical" surface, and migrate outwards to the "basal" surface, as they do *in vivo*, this would further indicate whether the polarity, and therefore layering is the same. By imaging cells continuously from the point of seeding onwards we would be able to follow their movements during lamination in culture. This is discussed further, near the end of the discussion chapter.

5.2.3. The Differential Adhesion Hypothesis

Zebrafish retinal cells are clearly capable of self-organising after dissociation but the mechanisms by which these cells are sorting into their correct layers without a scaffold or extrinsic cues is still not fully understood. The differential adhesion hypothesis (DAH) model of cellular organisation suggests that cells in an aggregate will laminate through cells minimising their interfacial free energies (Steinberg 1970; Foty & Steinberg 2005; Steinberg 2007). Cells with the strongest adhesions to each other in such aggregates move to the centre while cells with weaker adhesions sit further out in the cultures. Indeed it has recently been shown in other epithelial tissues, such as the kidney, that cells are organising by differential cadherin-based cell-cell adhesion (Lefevre et al. 2017). Recently, it has been shown that cell-cell surface tensions, rather than simple adhesion, may also drive lamination in tissues (Maître et al. 2012; Maître et al. 2015). The mechanism by which cells sort is still not clear, but it could be through either differential adhesion or tension, or a combination of both.

It would be very interesting to investigate in our aggregates how much of a role these physical factors play in retinal lamination. For instance, the DAH would suggest the strongest adhesions in my cultures are between RPE cells and the next strongest between photoreceptors and/or bipolar cells, which occupy the centre of the aggregates when the RPE is removed. These possibilities can be tested using new advances in micro-physical measurements of tension and adhesion. Measurements of adhesion taken by atomic force spectroscopy during a cell-binding assay can tell us which cell populations adhere more tightly to each other (Puech et al. 2006). Measurements of tension taken during dual pipette aspiration assays can tell us how much tension cells are under according to the angle of deformation between cells while being pulled apart (Maître et al. 2012). Using these methods one can gain a sense of the forces involved in the adhesion and tension of different groups of cells.

5.3. Cellular mechanisms of retinal lamination

Previous studies have begun to reveal the role of certain cell types and molecules in retinal lamination. Cell-type elimination experiments *in vivo* have shown that none of the neural cell types or the MG are essential for layering of the remaining cell types. However, *in vitro* studies have revealed a role of some cell types, including RPE and MG in lamination in aggregates. This suggests that possibly there are mechanisms *in vivo* that compensate for their loss but not *in vitro*. In this thesis, I have sought to continue and accelerate these investigations in my newly developed *in vitro* model of lamination, taking advantage of the ease of imaging and genetic manipulations in zebrafish. In this section I will discuss the results I achieved from removal of various cell types.

5.3.1. Retinal Pigment Epithelium

My data indicate that RPE cells are not crucial to the initial layering of all other retinal cell types. This is surprising since previous aggregate studies indicate that RPE has an appreciable influence on how retinal cells laminate. They show that in the absence of RPE, retinal cells generated rosetted aggregates, with inverted polarity, whereas those cultured in the presence of RPE generated fully stratified, and correctly polarised aggregates (Rothermel et al. 1997). My data indicate that RPE cells are not necessary to achieve basic laminar organisation in zebrafish retinal aggregates, but it remains to be seen whether they have a role in polarising the order of cell layers as the experimental setup in these experiments is quite different. Here, the RPE cells organise in the centre of the aggregates, whereas in previous studies, the RPE cells were cultured as a monolayer beneath the retinal cultures. Any influence of RPE on other cells would be coming from the outside of the aggregates, rather than from inside. Despite this, the order of layers of the other cell types is still the same, in respect to the RPE, as *in vivo*, however, it seems RPE are not necessary for their organisation in this way.

Although RPE cells are not necessary for lamination in my aggregates, some mutants of RPE genesis show a disorganisation of the retinal layers *in vivo*. The cause of this is unknown, but perhaps this effect is due to lack of a polarity signal. It would be interesting to culture zebrafish retinal cells in the presence of a monolayer of RPE cells

and see whether an external diffusible cue has any influence on the polarity of these aggregates, as they do in chick (Rothermel et al. 1997).

We should also consider how developmental time may be different in my experiments considering RPE cells were deemed necessary to achieve stage-dependent higher order of lamination in chick aggregates (Layer & Willbold 1989). Although it was only possible to eliminate RPE cells at 32 hpf and there is the possibility that RPE cells may have an organizing influence between 24 and 32 hpf I don't consider this to influence the outcomes of the experiments, as fully disaggregated cells from 24hpf and 32 hpf retinas organised achieved roughly the same level of patterning of cells. It would however be interesting to see if RPE plays a role in the higher order of lamination, such as IPL formation in these aggregates, which cannot currently be seen with the imaging techniques used.

Despite their apparent lack of importance in lamination in my setup, it is nevertheless interesting that RPE cells find themselves in the centre of these aggregates, considering that these cells are normally found around the outside of the retina i*n vivo*. One suggestion is that they organise in the centre simply due to high levels of adhesion or tension between cells. It was observed during dissection that the cells were very elastic and recoiled into themselves. This high tension could cause them to organise in the centre of the aggregates, although we cannot show this at this time.

5.3.2. Müller Glia

MG are specified in my aggregates at roughly similar times as they are *in vivo* and by using a time-sensitive treatment of DAPT I was able to eliminate MG and assess their role in lamination. My results show that MG are essential for lamination in zebrafish retinal aggregates which correlates with findings in chick reaggregates. It would be interesting to see what kind of a role they play in lamination, whether they act as a scaffold and help to stabilize cell columns as they do in chick (Willbold et al. 1995), or whether they act through a diffusible mechanism (Willbold et al. 2000) to aid in whole tissue organisation. Further investigation would be required to determine this.

In my experiments, a Notch inhibitor was used to eliminate MG, and so I cannot completely rule out the possibility that the phenotype I saw was due to other effects of Notch inhibition on retinal lamination such as during cell differentiation. Ideally, I would remove MG using another method such as targeting a gene essential for their differentiation, but currently we don't have a method for doing this. Together with a colleague in the lab who works on MG differentiation we explored alternative genetic targets, Lhx2b and Her2, but neither of these appeared to be specific to MG development in zebrafish and affected other aspects of embryo development, leading to lethality. This could be due to compensation by orthologues, however investigating this would require identifying novel genes or orthologues that are expressed in zebrafish MG and testing if they are required for MG specification/survival.

An alternative method would have been to remove MG through application of a selective gliotoxin, DL-α-aminoadipic acid, as it has been done in chick aggregates (Willbold et al. 1995). This could allow for a Notch-independent elimination of MG; however, this method would first need to be optimised for zebrafish and due to the lack of time this approach wasn't pursued.

Despite not being able to eliminate MG using a Notch-independent method, I carried out further control experiments to strengthen the correlation between the effects on lamination and MG differentiation. I applied DAPT at a later stage to allow some MG to differentiate and the aggregates could organise once again. This provided further evidence that it is the MG themselves that are critical for lamination in my aggregates.

It is interesting that MG seem to play an essential role in my aggregates, but are not essential for lamination *in vivo* (Randlett et al. 2013; MacDonald et al. 2015). There may be mechanisms operating *in vivo,* but not *in vitro* that compensate for the loss of MG. One possibility has to do with the fact that MG provide tensile strength to the retina (MacDonald et al. 2015), which is lost when these cells are dissociated but re-established as MG differentiate. Perhaps in my aggregates cells require this tensile strength provided by MG to be able to organise, since all other tension has been lost, whereas in the retina, surrounding tissues still provide enough tension for cells to organise in the absence of MG. One way to test this would be to assess the tension in

aggregates using AFM, by pushing down on MG-deficient aggregates and seeing whether they deform differently to WT aggregates.

Another possibility is that MG provide some sort of physical cue to the other retinal cells. In my aggregates, the apicobasal polarity of the native neuroepithelium has been badly degraded, if not completely destroyed, in the disaggregation-reaggregation process. Perhaps here MG play a role in re-establishing some sort of polarity for cells in my aggregates, whereas *in vivo* the cells may be able to sense other polarity gradients, i.e. from neighbouring tissues to organise themselves along. Furthermore, MG have intricate morphologies *in vivo,* extending processes into every cell layer (MacDonald et al. 2017). CRISPR knockout studies carried out in the lab (MacDonald and Charlton-Perkins, unpublished) show that Pax2a is involved in the maturation and correct lamination of MG. In the Pax2a mutant defects in MG range from: incorrect positioning of the cell body, to lack of mature processes extending into other cell layers, or even failure of the cell to span the width of the retina or adopt the correct polarity. Culturing cells from this mutant line, could tell us if this mature architecture is required for correct lamination of the retinal neurons, or simply the presence of MG is sufficient. Interestingly however, it was observed during my experiments that MG don't appear to span all cell layers in these aggregates as they do *in vivo* and in chick reaggregates which indicates that they may not be aiding lamination through stabilisation of cell columns as they do in chick (Willbold et al. 1995).

We haven't yet determined whether MG are acting through a physical or molecular mechanism. In chick reaggregates it appears that MG are acting through an unknown diffusible factor (Willbold et al. 2000). To test if this is also the case for zebrafish, I could culture my MG-deficient retinal aggregates above a monolayer of MG, or even simply in media conditioned with supernatant from previously cultured MG, to see if any diffusible factors will influence their ability to organise.

The timing of MG development could also influence their role in lamination. Mouse retinas treated with an antagonist of BMP to block MG differentiation have disrupted lamination and formation of rosettes in the postnatal retina (Ueki et al. 2015). MG in the mouse retina develop after all other cell types are born, and even after some have begun

to laminate. It may be that MG play a role in maintaining lamination, rather than establishing it, and that we have been looking at their role in zebrafish too early in the process of lamination. Indeed, layering of the retina after the loss of MG has only been observed up to 5dpf in zebrafish retina, and so they may be instead required later, in the more mature retina, to maintain lamination. It may be that in my aggregates, cells initially laminate, but cannot maintain their layers in the absence of other supporting tissues or MG. To determine this, we would need to look at how well the retinal cells are laminated before MG are born.

5.3.3. Retinal Ganglion Cells

Using the novel system developed during this thesis, I have begun to investigate the role of RGCs in retinal lamination for the first time *in vitro,* in a simplified system. In my cultures, I see that RGCs are layered in the outer layer, among the Amacrine Cells. It is perhaps therefore unsurprising that they don't seem to have an appreciable influence on the organisation of other cell types. Perhaps they organise in this layer in a passive way, and do not play an active role in lamination in aggregates. In fact, I show that when RGCs are removed from the culture, the resulting aggregates actually organise slightly better, which is surprising. Although I cannot explain why this is at this stage, there are several experimental flaws to consider. First, aggregates in the control morpholino (CtrlMO) condition were less organised than in previous control experiments, indicating the presence of a morpholino may be influencing the ability of the cells to organise. Second, it was observed that aggregates in the Ath5 morpholino (Ath5MO) condition contained slightly more ACs which correlates with what is seen in Ath5 morphant retinas *in vivo* (Kay et al. 2004; Almeida et al. 2014). Perhaps this result is not due to the lack of RGCs, but due to the increase in ACs, although we cannot know this without knowing the role of ACs in lamination.

Although RGCs appear not to be required for lamination in my aggregates, they may still have some organising qualities in the retina *in vivo* by providing instructive signals. Mis-localised RGCs *in vivo* are seen to influence the organisation of other cells and BPs are found organised around them in their ectopic position (Icha et al. 2016). It is unknown why they seem to have an influence on other cells but are not necessary for their

organisation. To learn more about what kind of role RGCs play in lamination it may be necessary to observe how they are organising in my aggregates in live imaging studies to decipher whether they play an active or passive role in lamination in the absence of other cues.

5.3.4. Amacrine and Horizontal Cells

It would be interesting to understand if ACs and HCs play a role in lamination, given their dynamic nature during lamination *in vivo* (Chow et al. 2015) and their distinctive ring-like patterning in my aggregates. However, despite several attempts, I was only able to successfully culture aggregates from embryos injected with Ptf1aMO1+2 once and yield just 3 aggregates from each of the experimental conditions. Although it appears the Crx:gapCFP cells are less organised in the Ptf1aMO 1+2 condition, the number of repeats is far too low to make any inferences about the strength of this data. I would need to repeat the experiment several more times, and analyse the organisation using the Isocontour profiling script to gain a quantitative measure of organisation. I would also need to see the relative position of the remaining cell populations, in particular the RGCs and the PRs/BPs.

To increase numbers of repeats I would need to make some changes to the experimental conditions. First, I would make fresh solutions and use new morpholinos to check whether there might have been a batch effect, or if anything was contaminated. If the solutions and morpholinos were deemed not to be the cause then perhaps retinas in the Ptf1aMO 1+2 condition are more susceptible to dissociating, and the lack of calcium in the dissociation medium exaggerates this. Collecting in culture medium instead of dissociation medium could allow the eyes to remain intact until I am ready to dissociate them. If retinas from the Ptf1aMO 1+2 condition do indeed dissociate more easily than retinas from other conditions, this may tell us something about the role of ACs and HCs in retinal integrity. Perhaps these cells are important for holding other retinal cell layers together and this could have implications in retinal lamination as well.

Finally, to analyse the layering in these aggregates I would also need to adapt some of the parameters of the Matlab script. The script predominantly analyses the

organisations of the Crx:gapCFP and Ptf1a:cytGFP cell populations, but the Ptf1a:cytGFP population would be eliminated in this experiment. I would therefore stain the aggregates with Zn5 to label RGC cells and use this as the second population of cells to analyse the organisation. Alternatively, I could culture cells from a transgenic cross of Isl3:GFP, which labels RGCs, with Crx:gapCFP to negate any need for staining. RGCs normally reside in the outer layer of the aggregates, with the Crx:gapCFP cells clustered within them. Perhaps if ACs / HCs play an important role in lamination we would see less spatial distinction between these two populations of cells.

5.4. General discussion and future directions

In this thesis, I have developed a novel method for investigating neural lamination *in vitro* and found that zebrafish retinal cells reaggregate quickly and are capable of self-organising in a simple, non-adhesive 3D format. As with previous findings in other systems I found that zebrafish retinal cells were most capable of organising at younger stages, and that they are dependent on R-Cognin to reaggregate. I have also developed a novel method of analysing the layering of these aggregates that gives a robust, quantitative metric of organisation.

5.4.1. Early vs later lamination events

While this is a simple and easy to manipulate system, it must also be noted that it is likely this system represents a model or primary reaggregation, based mostly on mechanisms of cell adhesion and sorting-out. It is unknown to what extent this model represents a mature, stratified retina and whether the cells in this system are capable of forming functional connections as they do *in vivo*. For instance, in some aggregates it was observed that RGCs were extending axons around the outer edge of the aggregates, and that some ACs also extended axons within close proximity to RGCs indicating that some cells in these aggregates may be adopting their mature morphologies and beginning to form synapses or an immature IPL. It would be interesting to see to what extent these cells are maturing in culture, whether they are capable of making synaptic connections and how mature the aggregates are in terms of developing synaptic layers. This would help us to draw more links with studies in other organisms such as the chick, mouse and gerbil where they have been able to describe some of the later lamination events.

5.4.2. Cellular mechanisms

Nevertheless, using this novel model of retinal reaggregation, I have built upon previous investigations of some of the mechanisms of lamination finding some results that agree with previous findings and some that have highlighted new mechanisms. Like in *in vivo* studies, it seems RGCs are not required for lamination in my aggregates, however I

cannot say whether they may still provide some organising influence. It seems that ACs/HCs may play a role in lamination, due to their robust ring-like organisation, but there was insufficient data to make any inferences about this at this stage. When looking at the supporting cells of the retina, I have however built upon previous findings and provided some new insights. For instance, unlike in chick aggregates, RPE cells seem not to be necessary for full retinal lamination in zebrafish retinal aggregates, although we cannot discount the possibility that they may play a role in higher order lamination such as IPL formation or provide a polarity cue, as they do in chick. Also, the finding that MG are necessary for lamination *in vitro* contradicts findings in the zebrafish retina *in vivo* but agrees with findings in chick aggregates. This suggests there are mechanisms occurring *in vivo* to compensate for the loss of MG that are not present *in vitro*, at least in zebrafish. This could be due to the dissociation and reaggregation process, or due to the lack of surrounding tissues providing support to the retina, revealing the importance of MG, possibly to provide tensile strength to the aggregate of cells. I cannot determine this in my current experiments, but it is an interesting result to consider when investigating mechanisms of neural lamination.

5.4.3. Molecular mechanisms

We cannot simply look at the roles of each cell type to truly understand this picture of lamination, we must also look at the molecules. Some molecules may be providing positional cues for cells to orient themselves or migrate along, and some may be involved in direct cell-cell communication. Unfortunately, due to time constraints, I did not have time to investigate these, but there are several candidate molecules that are likely to be involved in lamination.

For example, the family of laminins are well known for their role in cell-cell and cell-ECM communications involved in tissue morphogenesis. Laminin 1 is expressed at the basal lamina of the zebrafish retina (Lee & Gross 2007). The loss of its Lamα1 subunit leads to loss of cell-cell adhesion and epithelial polarity, resulting in a disorganised retina (Bryan et al. 2016). To investigate the role of Laminin 1 in lamination of my aggregates, first I would need to determine if it is indeed expressed in my cultures, and if so, where? Could it be providing a polarity cue to the cells? I could then investigate its

role by culturing cells from the lamα1UW1 mutant (Bryan et al. 2016), or embryos injected with the Lamα1 morpholino at the 1-2 cell stage (Pollard et al. 2006) and assessing the ability of the laminin-deficient cells to laminate. It should however be considered that there may be laminin in the embryo extract in the culture medium, which could prevent us from gaining clear data on the role of laminin in these cultures. Since it may be difficult to completely remove laminin from my cultures. It therefore may be a better approach to replace laminin into the system to investigate its role, rather than trying to remove it.

Since Laminin 1 has been shown to provide a polarity cue to the developing retina (Randlett et al. 2011), it would be interesting to see if this is the case in my aggregates. To do this we must restrict where the laminin is expressed within the cultures. *In vivo* studies have investigated the role of laminin using laminin-coated beads injected into the developing retina (Randlett et al. 2011). In these studies, they see that RGC axons grow toward the beads, highlighting the positive cue that laminin provides in this circumstance. I could take advantage of this setup and introduce laminin-coated beads into our cultures to see if the cells react to this localised cue. It is hypothesised that, since Laminin 1 is normally expressed in the basal membrane of the retina, if it does provide a polarity cue to the retinal cells in terms of ordering of layering then perhaps it would promote the reverse layering of the retinal cells: RGCs next to the source of laminin, followed by ACs, BPs, HCs then PRs, reminiscent of how the cells layer in respect to the lens. I tested the practicality of this experiment and found that agarose beads could be easily coated with laminin 1 and individually placed inside single wells within the agarose microwell dishes. This would allow the introduction of laminin, or indeed any molecule that could be coated onto the beads, into the culture at any time.

There are a whole range of molecules that could be involved in retinal lamination, including adhesion molecules such as cadherins, components of the extracellular matrix and even guidance cues, as discussed in the introduction of this thesis. The experimental setup described in this thesis provides a platform whereby we can easily remove or introduce molecules of interest to the culture to assess their role in neural lamination. However, in doing this we must consider the potential impact of molecules in the surrounding culture medium, since a component of this is zebrafish extract.

Molecules in this extract may be playing a role in lamination by providing a polarity cue to the outside of the aggregates. Any investigations of the molecular mechanisms of lamination must therefore use extra controls in experiments, possibly by using zebrafish extract from embryos also void of the molecule being investigated.

5.4.4. Physical mechanisms

Finally, one must consider the physical mechanisms at play during lamination. Firstly, it cannot be determined if the cells are self-organising by interacting with each other and actively migrating through the aggregates, or if they are organising through a more passive process of cell sorting. To determine this, we would likely need to observe the cells organising in real time to see if they are undergoing active cell migration to reach their final destination.

Perhaps the cells in my aggregates simply order according to differential adhesion or tension. We could examine this by first just culturing various combinations of cell populations and assessing if the relative ordering of cells is the same, despite lacking the other populations of cells. We could also look at the adhesion and tension between different populations of cells using micro-physical measurements of adhesion and tension (Puech et al. 2006; Maître et al. 2012).

5.4.5. Multiple mechanisms

While I have aimed to tease apart the mechanisms of lamination in this thesis, it is unlikely to be governed by any of these mechanisms in isolation and we must consider how they might interact with each other. An example being that MG appear to be important in lamination *in vitro* but not *in vivo* and that this might be due to a diffusible factor produced by the cells, as shown in chick reaggregates (Willbold et al. 2000), or it could be due to the tensile strength provided by the cells (MacDonald et al. 2015), or both. The picture of lamination appears complex and there is much to be done to truly understand the picture of which mechanisms are involved and how they might interact, and these aggregates are a simplified format with which to continue these investigations. Not only can we remove cells or molecules of interest, but we can also

reintroduce components of the system one at a time, or in combination to assess their role in lamination.

5.4.6. Lamination is a dynamic process

Lamination does not occur as a series of static events. It is a dynamic process involving cells differentiation, migration and interaction with other cells to find their correct layers. The zebrafish retinal reaggregates developed in this thesis using the Spectrum of Fates transgenic line provide the opportunity to study the dynamics of lamination in the absence of pre-existing scaffolds or polarity. By imaging from above the microwell dish, using a water dipping lens, we can look at the cells live as they aggregate and laminate. Using this imaging technique, we could establish whether zebrafish retinal cells first produce rosettes or columns of cells in the early stages of lamination, before the whole aggregate becomes fully laminated, as they do in chick aggregates. Cells could be identified in real time with the SoFa1 line, however, we must consider that in the early stages of aggregation and lamination in these aggregates cells have not yet specified, therefore cannot be identified with the corresponding genetic markers. A method currently being developed in the lab to look at cell-cell interactions during differentiation and layering *in vivo* (Afnan Azizi, personal communication) uses tracking of cells labelled with a ubiquitous nuclear marker, H2B, followed by identification using the SoFa1 markers at the end imaging. Cell movements are then back-tracked to cell movements with fate. This method could eventually be adopted in my cultures to examine cell movements during reaggregation, differentiation, and lamination.

5.5. Concluding remarks

In this thesis, I have presented a novel model for analysing the cellular and molecular mechanisms that drive cellular lamination in the retina. I show that dissociated zebrafish retinal progenitors reaggregate quickly, and within just 48 hours in vitro differentiate into all retinal cell types and organise into layers. I show that this is dependent on developmental time, and that they require R-Cognin to reaggregate. With the aid of the SoFa1 line, I developed a simple analysis of this layering that can be easily and reliably quantified to give us a measure of organisation. Using this model, I have revealed that Müller Glial cells are important for zebrafish retinal lamination *in vitro*, but not *in vivo*, whereas RPE cells and RGCs do not appear to be required. I also reveal a potential role for ACs and HCs in lamination due to their distinct patterning in these aggregates. These results indicate that some mechanisms may be operating *in vitro* but not *in vivo* or that perhaps there are multiple mechanisms governing lamination that compensate for each other when one is lost. The picture of retinal lamination is still far from clear, but this model provides a simplified platform upon which to accelerate investigations of the basic cellular, molecular and physical mechanisms of neural lamination and how they might integrate.

6. References

Agathocleous, M. & Harris, W.A., 2009. From progenitors to differentiated cells in the vertebrate retina. *Annual review of cell and developmental biology*, 25, pp.45–69.

Almeida, A.D. et al., 2014. Spectrum of Fates: a new approach to the study of the developing zebrafish retina. *Development (Cambridge, England)*, 141(9), pp.1971–80.

Amann, A. et al., 2014. Development of an innovative 3D cell culture system to study tumour--stroma interactions in non-small cell lung cancer cells. *PloS one*, 9(3), p.e92511.

Angevine, J.B. & Sidman, R.L., 1961. Autoradiographic study of cell migration during histogenesis of cerebral cortex in the mouse. *Nature*, 192, pp.766–8.

Babb, S.G. et al., 2005. Zebrafish R-cadherin (Cdh4) controls visual system development and differentiation. *Developmental dynamics : an official publication of the American Association of Anatomists*, 233(3), pp.930–45.

Baye, L.M. & Link, B.A., 2008. Nuclear migration during retinal development. *Brain research*, 1192, pp.29–36.

Ben-Shaul, Y., Hausman, R.E. & Moscona, A.A., 1980. Age-dependent differences in cognin regeneration on embryonic retina cells: immunolabeling and SEM studies. *Developmental neuroscience*, 3(2), pp.66–74.

Bernardos, R.L. & Raymond, P.A., 2006. GFAP transgenic zebrafish. *Gene Expression Patterns*, 6(8), pp.1007–1013.

Boije, H. et al., 2015. The Independent Probabilistic Firing of Transcription Factors: A Paradigm for Clonal Variability in the Zebrafish Retina. *Developmental Cell*, 34(5), pp.532–543.

Bradford, C.S. et al., 1994. Cell cultures from zebrafish embryos and adult tissues. *Journal of Tissue Culture Methods*, 16, pp.99–107.

Broutier, L. et al., 2016. Culture and establishment of self-renewing human and mouse adult liver and pancreas 3D organoids and their genetic manipulation. *Nature Protocols*, 11(9), pp.1724–1743.

Bryan, C.D., Chien, C.-B. & Kwan, K.M., 2016. Loss of laminin alpha 1 results in multiple structural defects and divergent effects on adhesion during vertebrate optic cup

morphogenesis. *Developmental biology*, 416(2), pp.324–37.

Caviness, V.S. & Sidman, R.L., 1973. Time of origin of corresponding cell classes in the cerebral cortex of normal and reeler mutant mice: An autoradiographic analysis. *The Journal of Comparative Neurology*, 148(2), pp.141–151.

Cepko, C.L. et al., 1996. Cell fate determination in the vertebrate retina. *Proceedings of the National Academy of Sciences of the United States of America*, 93(2), pp.589–95.

Chen, Z. et al., 2013. Primary neuron culture for nerve growth and axon guidance studies in zebrafish (Danio rerio). *PloS one*, 8(3), p.e57539.

Cheng, Y.-C. et al., 2015. The transcription factor hairy/E(spl)-related 2 induces proliferation of neural progenitors and regulates neurogenesis and gliogenesis. *Developmental Biology*, 397(1), pp.116–128.

Chow, R.W.-Y. et al., 2015. Inhibitory neuron migration and IPL formation in the developing zebrafish retina. *Development (Cambridge, England)*.

D'Arcangelo, G. & Curran, T., 1998. Reeler: new tales on an old mutant mouse. *BioEssays : news and reviews in molecular, cellular and developmental biology*, 20(3), pp.235–44.

Dahl-Jensen, S. & Grapin-Botton, A., 2017. The physics of organoids: a biophysical approach to understanding organogenesis. *Development*, 144(6).

Das, T. et al., 2003. In vivo time-lapse imaging of cell divisions during neurogenesis in the developing zebrafish retina. *Neuron*, 37(4), pp.597–609.

Dobi, E.T., Troccoli, N.M. & Hausman, R.E., 1986. Distribution of R-cognin in late embryonic and post-hatching chicken retina. *Investigative ophthalmology & visual science*, 27(3), pp.323–9.

Eiraku, M. et al., 2011. Self-organizing optic-cup morphogenesis in three-dimensional culture. *Nature*, 472(7341), pp.51–6.

Eiraku, M. & Sasai, Y., 2012. Mouse embryonic stem cell culture for generation of three-dimensional retinal and cortical tissues. *Nature protocols*, 7(1), pp.69–79.

Foty, R., 2011. A simple hanging drop cell culture protocol for generation of 3D spheroids. *Journal of visualized experiments : JoVE*, 20(51), pp.4–7.

Foty, R.A. & Steinberg, M.S., 2005. The differential adhesion hypothesis: A direct evaluation. *Developmental Biology*, 278(1), pp.255–263.

Franze, K. et al., 2007. Muller cells are living optical fibers in the vertebrate retina. *Proceedings of the National Academy of Sciences of the United States of America*,

104(20), pp.8287–92.

Fuhrmann, S., 2010. Eye Morphogenesis and Patterning of the Optic Vesicle. In *Current topics in developmental biology*. pp. 61–84.

Fuhrmann, S., Zou, C. & Levine, E.M., 2014. Retinal pigment epithelium development, plasticity, and tissue homeostasis. *Experimental Eye Research*, 123, pp.141–150.

Godinho, L. et al., 2005. Targeting of amacrine cell neurites to appropriate synaptic laminae in the developing zebrafish retina. *Development (Cambridge, England)*, 132(22), pp.5069–79.

Goodman, K.M. et al., 2016. Molecular basis of sidekick-mediated cell-cell adhesion and specificity. *eLife*, 5.

Green, E.S., Stubbs, J.L. & Levine, E.M., 2003. Genetic rescue of cell number in a mouse model of microphthalmia: interactions between Chx10 and G1-phase cell cycle regulators. *Development (Cambridge, England)*, 130(3), pp.539–52.

Greggio, C. et al., 2013. Artificial three-dimensional niches deconstruct pancreas development in vitro. *Development*, 140(21), pp.4452–4462.

Ha, T. et al., 2017. The Retinal Pigment Epithelium Is a Notch Signaling Niche in the Mouse Retina. *Cell Reports*, 19(2), pp.351–363.

Harris, W.A., 1997. Cellular diversification in the vertebrate retina. *Current Opinion in Genetics & Development*, 7(5), pp.651–658.

Harris, W.A. & Messersmith, S.L., 1992. Two cellular inductions involved in photoreceptor determination in the Xenopus retina. *Neuron*, 9(2), pp.357–72.

Harrison, S.E. et al., 2017. Assembly of embryonic and extraembryonic stem cells to mimic embryogenesis in vitro. *Science*, 356(6334), p.eaal1810.

Hausman, R.E. & Moscona, A.A., 1979. Immunologic detection of retina cognin on the surface of embryonic cells. *Experimental cell research*, 119(2), pp.191–204.

Hausman, R.E. & Moscona, A.A., 1976. Isolation of retina-specific cell-aggregating factor from membranes of embryonic neural retina tissue. *Proceedings of the National Academy of Sciences of the United States of America*, 73(10), pp.3594–8.

He, J. et al., 2012. How variable clones build an invariant retina. *Neuron*, 75(5), pp.786–98.

Heermann, S. et al., 2015. Eye morphogenesis driven by epithelial flow into the optic cup facilitated by modulation of bone morphogenetic protein. *eLife*, 4.

Heisenberg, C.-P. & Bellaïche, Y., 2013. Forces in Tissue Morphogenesis and Patterning.

Cell, 153(5), pp.948–962.

Herbst, C., 1900. über das Auseinandergehen von Furchungs- und Gewebezellen in kalkfreiem Medium. *Archiv für Entwicklungsmechanik der Organismen*, 9(3), pp.424–463.

Hinds, J.W. & Hinds, P.L., 1983. Development of retinal amacrine cells in the mouse embryo: Evidence for two modes of formation. *The Journal of Comparative Neurology*, 213(1), pp.1–23.

Hinds, J.W. & Hinds, P.L., 1979. Differentiation of photoreceptors and horizontal cells in the embryonic mouse retina: An electron microscopic, serial section analysis. *The Journal of Comparative Neurology*, 187(3), pp.495–511.

Hinds, J.W. & Hinds, P.L., 1978. Early development of amacrine cells in the mouse retina: An electron microscopic, serial section analysis. *The Journal of Comparative Neurology*, 179(2), pp.277–300.

Hinds, J.W. & Hinds, P.L., 1974. Early ganglion cell differentiation in the mouse retina: an electron microscopic analysis utilizing serial sections. *Developmental biology*, 37(2), pp.381–416.

Hoff, A., Hämmerle, H. & Schlosshauer, B., 1999. Organotypic culture system of chicken retina. *Brain research. Brain research protocols*, 4(3), pp.237–48.

Holt, C.E. et al., 1988. Cellular determination in the xenopus retina is independent of lineage and birth date. *Neuron*, 1(1), pp.15–26.

Hu, M. & Easter, S.S., 1999. Retinal Neurogenesis: The Formation of the Initial Central Patch of Postmitotic Cells. *Developmental Biology*, 207(2), pp.309–321.

Huang, Z., 2009. Molecular regulation of neuronal migration during neocortical development. *Molecular and Cellular Neuroscience*, 42(1), pp.11–22.

Icha, J. et al., 2016. Independent modes of ganglion cell translocation ensure correct lamination of the zebrafish retina. *The Journal of cell biology*, 215(2), pp.259–275.

Inuzuka, H., Miyatani, S. & Takeichi, M., 1991. R-cadherin: a novel Ca(2+)-dependent cell-cell adhesion molecule expressed in the retina. *Neuron*, 7(1), pp.69–79.

Inuzuka, H., Redies, C. & Takeichi, M., 1991. Differential expression of R- and N-cadherin in neural and mesodermal tissues during early chicken development. *Development*, 113(3).

Jadhav, A.P., Roesch, K. & Cepko, C.L., 2009. Development and neurogenic potential of Müller glial cells in the vertebrate retina. *Progress in retinal and eye research*, 28(4),

pp.249–62.

Jensen, A.M., Walker, C. & Westerfield, M., 2001. mosaic eyes: a zebrafish gene required in pigmented epithelium for apical localization of retinal cell division and lamination. *Development (Cambridge, England)*, 128(1), pp.95–105.

Johnson, D.A. et al., 2007. Neuronal differentiation and synaptogenesis in retinoblastoma. *Cancer research*, 67(6), pp.2701–11.

Johnson, E. et al., 2004. R-cadherin influences cell motility via Rho family GTPases. *The Journal of biological chemistry*, 279(30), pp.31041–9.

Jusuf, P.R. & Harris, W.A., 2009. Ptf1a is expressed transiently in all types of amacrine cells in the embryonic zebrafish retina. *Neural development*, 4, p.34.

Kay, J.N. et al., 2001. Retinal ganglion cell genesis requires lakritz, a Zebrafish atonal Homolog. *Neuron*, 30(3), pp.725–36.

Kay, J.N. et al., 2004. Transient requirement for ganglion cells during assembly of retinal synaptic layers. *Development (Cambridge, England)*, 131(6), pp.1331–42.

Kim, J. Bin, 2005. Three-dimensional tissue culture models in cancer biology. *Seminars in Cancer Biology*, 15(5), pp.365–377.

Kimmel, C.B. et al., 1995. Stages of embryonic development of the zebrafish. *Developmental dynamics : an official publication of the American Association of Anatomists*, 203(3), pp.253–310.

Klopper, A. V et al., 2010. Finite-size corrections to scaling behavior in sorted cell aggregates. *The European physical journal. E, Soft matter*, 33(2), pp.99–103.

Lancaster, M.A. et al., 2013. Cerebral organoids model human brain development and microcephaly. *Nature*, 501(7467), pp.373–9.

Lancaster, M.A. & Knoblich, J.A., 2014. Generation of cerebral organoids from human pluripotent stem cells. *Nature protocols*, 9(10), pp.2329–2340.

Layer, P.G. et al., 2002. Of layers and spheres: the reaggregate approach in tissue engineering. *Trends in neurosciences*, 25(3), pp.131–4.

Layer, P.G., Rothermel, A. & Willbold, E., 2001. From stem cells towards neural layers: a lesson from re-aggregated embryonic retinal cells. *Neuroreport*, 12(7), pp.A39-46.

Layer, P.G. & Willbold, E., 1989. Embryonic chicken retinal cells can regenerate all cell layers in vitro, but ciliary pigmented cells induce their correct polarity. *Cell and tissue research*.

Layer, P.G. & Willbold, E., 1993. Histogenesis of the avian retina in reaggregation

culture: from dissociated cells to laminar neuronal networks. *International review of cytology*, 146, pp.1–47.

Layer, P.G. & Willbold, E., 1994. Regeneration of the avian retina by retinospheroid technology. *Progress in Retinal and Eye Research*, 13(1), pp.197–230.

Lee, J. & Gross, J.M., 2007. Laminin β1 and γ1 Containing Laminins Are Essential for Basement Membrane Integrity in the Zebrafish Eye. *Investigative Opthalmology & Visual Science*, 48(6), p.2483.

Lefevre, J.G. et al., 2017. Self-organisation after embryonic kidney dissociation is driven via selective adhesion of ureteric epithelial cells. *Development*, 144(6), pp.1087–1096.

Leung, L. et al., 2011. Apical migration of nuclei during G2 is a prerequisite for all nuclear motion in zebrafish neuroepithelia. *Development*, 138(22), pp.5003–5013.

Li, M. & Sakaguchi, D.S., 2004. Inhibition of integrin-mediated adhesion and signaling disrupts retinal development. *Developmental Biology*, 275(1), pp.202–214.

Lilien, J.E. & Moscona, A.A., 1967. Cell Aggregation: Its Enhancement by a Supernatant from Cultures of Homologous Cells. *Science*, 157(3784), pp.70–72.

Link, B.A. & Godinho, L., 2006. Cell Migration. In E. Sernagor et al., eds. *Retinal Development*. pp. 59–74.

Livesey, F.J. & Cepko, C.L., 2001. Vertebrate neural cell-fate determination: lessons from the retina. *Nature reviews. Neuroscience*, 2(2), pp.109–18.

MacDonald, R.B. et al., 2015. Müller glia provide essential tensile strength to the developing retina. *The Journal of Cell Biology*, 210(7), pp.1075–1083.

MacDonald, R.B., Charlton-Perkins, M. & Harris, W.A., 2017. Mechanisms of Müller Glial cell morphogenesis (in press).

Maître, J.-L. et al., 2012. Adhesion functions in cell sorting by mechanically coupling the cortices of adhering cells. *Science (New York, N.Y.)*, 338(6104), pp.253–6.

Maître, J.-L. et al., 2015. Pulsatile cell-autonomous contractility drives compaction in the mouse embryo. *Nature Cell Biology*, 17(7), pp.849–855.

Malicki, J., Jo, H. & Pujic, Z., 2003. Zebrafish N-cadherin, encoded by the glass onion locus, plays an essential role in retinal patterning. *Developmental Biology*, 259(1), pp.95–108.

Marcus, R.C., Delaney, C.L. & Easter, S.S., 1999. Neurogenesis in the visual system of embryonic and adult zebrafish (Danio rerio). *Visual neuroscience*, 16(3), pp.417–24.

Masai, I. et al., 2003. N-cadherin mediates retinal lamination, maintenance of forebrain compartments and patterning of retinal neurites. *Development (Cambridge, England)*, 130(11), pp.2479–94.

Matsunaga, M., Hatta, K. & Takeichi, M., 1988. Role of N-cadherin cell adhesion molecules in the histogenesis of neural retina. *Neuron*, 1(4), pp.289–295.

Matsuoka, R.L., Chivatakarn, O., et al., 2011. Class 5 transmembrane semaphorins control selective Mammalian retinal lamination and function. *Neuron*, 71(3), pp.460–73.

Matsuoka, R.L., Nguyen-Ba-Charvet, K.T., et al., 2011. Transmembrane semaphorin signalling controls laminar stratification in the mammalian retina. *Nature*, 470(7333), pp.259–63.

McConnell, S.K., 1995. Constructing the cerebral cortex: Neurogenesis and fate determination. *Neuron*, 15(4), pp.761–768.

Meller, K. & Tetzlaff, W., 1976. Cell and Tissue Scanning Electron Microscopic Studies on the Development of the Chick Retina. *Cell and tissue research*, 159(2), pp.145–159.

de Melo, J. et al., 2016. Lhx2 Is an Essential Factor for Retinal Gliogenesis and Notch Signaling. *The Journal of neuroscience : the official journal of the Society for Neuroscience*, 36(8), pp.2391–405.

Meyer, E.J., Ikmi, A. & Gibson, M.C., 2011. Interkinetic Nuclear Migration Is a Broadly Conserved Feature of Cell Division in Pseudostratified Epithelia. *Current Biology*, 21(6), pp.485–491.

Miesfeld, J.B. et al., 2015. Yap and Taz regulate retinal pigment epithelial cell fate. *Development (Cambridge, England)*, 142(17), pp.3021–32.

Mitteregger, R. et al., 1999. Rotary cell culture system (RCCS): a new method for cultivating hepatocytes on microcarriers. *The International journal of artificial organs*, 22(12), pp.816–22.

Moscona, A., 1961. Rotation-mediated histogenetic aggregation of dissociated cells. *Experimental Cell Research*, 22, pp.455–475.

Moscona, A. & Moscona, H., 1952. The dissociation and aggregation of cells from organ rudiments of the early chick embryo. *Journal of anatomy*, 86(3), pp.287–301.

Nadarajah, B. et al., 2003. Neuronal migration in the developing cerebral cortex: observations based on real-time imaging. *Cerebral cortex (New York, N.Y. : 1991)*, 13(6), pp.607–11.

Nadarajah, B. et al., 2001. Two modes of radial migration in early development of the cerebral cortex. *Nature Neuroscience*, 4(2), pp.143–150.

Nadarajah, B. & Parnavelas, J.G., 2002. Modes of neuronal migration in the developing cerebral cortex. *Nature Reviews Neuroscience*, 3(6), pp.423–432.

Nagendran, M. et al., 2015. Canonical Wnt signalling regulates epithelial patterning by modulating levels of laminins in zebrafish appendages. *Development (Cambridge, England)*, 142(2), pp.320–30.

Nakagawa, S. et al., 2003. Identification of the laminar-inducing factor: Wnt-signal from the anterior rim induces correct laminar formation of the neural retina in vitro. *Developmental Biology*, 260(2), pp.414–425.

Napolitano, A.P. et al., 2007. Scaffold-free three-dimensional cell culture utilizing micromolded nonadhesive hydrogels. *BioTechniques*, 43(4), pp.494, 496–500.

Nawrocki, L.W., 1985. *Development of the neural retina in the zebrafish, Brachydanio rerio (neurogenesis)*. University of Oregon.

Noguchi, T.K. et al., 2015. Generation of stomach tissue from mouse embryonic stem cells. *Nature Cell Biology*, 17(8), pp.984–993.

Pariser, H.P., Zhang, J. & Hausman, R.E., 2000. The cell adhesion molecule retina cognin is a cell surface protein disulfide isomerase that uses disulfide exchange activity to modulate cell adhesion. *Experimental cell research*, 258(1), pp.42–52.

Peukert, D. et al., 2011. Lhx2 and Lhx9 Determine Neuronal Differentiation and Compartition in the Caudal Forebrain by Regulating Wnt Signaling W. A. Harris, ed. *PLoS Biology*, 9(12), p.e1001218.

Poggi, L. et al., 2005. Influences on neural lineage and mode of division in the zebrafish retina in vivo. *The Journal of Cell Biology*, 171(6), pp.991–999.

Pollard, S.M. et al., 2006. Essential and overlapping roles for laminin α chains in notochord and blood vessel formation. *Developmental Biology*, 289(1), pp.64–76.

Prada, C., Puelles, L. & Génis-Gálvez, J.M., 1981. A golgi study on the early sequence of differentiation of ganglion cells in the chick embryo retina. *Anatomy and embryology*, 161(3), pp.305–17.

Puech, P.-H. et al., 2006. A new technical approach to quantify cell–cell adhesion forces by AFM. *Ultramicroscopy*, 106(8), pp.637–644.

Rakic, P., 1970. Golgi and electronmicroscopic cytology of migrating granule cells during late stages of histogenesis of macaque cerebellar cortex. (Abstract). *The Anatomical*

Record, 166, p.364.

Ramón y Cajal, S., 1892. La rétine des vertébrés. *La Cellule*, (9), pp.119–257.

Randlett, O. et al., 2013. Cellular requirements for building a retinal neuropil. *Cell reports*, 3(2), pp.282–90.

Randlett, O. et al., 2011. The oriented emergence of axons from retinal ganglion cells is directed by laminin contact in vivo. *Neuron*, 70(2), pp.266–80.

Reichenbach, A. & Bringmann, A., 2013. New functions of Müller cells. *Glia*, 61(5), pp.651–678.

Roesch, K. et al., 2008. The transcriptome of retinal Müller glial cells. *The Journal of Comparative Neurology*, 509(2), pp.225–238.

Rothermel, A. et al., 1997. Pigmented epithelium induces complete retinal reconstitution from dispersed embryonic chick retinae in reaggregation culture. *Proceedings. Biological sciences / The Royal Society*, 264(1386), pp.1293–302.

Rzeczinski, S. et al., 2006. Roller Culture of Free-Floating Retinal Slices: A New System of Organotypic Cultures of Adult Rat Retina. *Ophthalmic Research*, 38(5), pp.263–269.

Sato, T. et al., 2009. Single Lgr5 stem cells build crypt–villus structures in vitro without a mesenchymal niche. *Nature*, 459(7244), pp.262–265.

Schmitt, E.A. & Dowling, J.E., 1999. Early retinal development in the zebrafish, Danio rerio: light and electron microscopic analyses. *The Journal of comparative neurology*, 404(4), pp.515–36.

Sheffield, J. & Moscona, A., 1969. Early stages in the reaggregation of embryonic chick neural retina cells. *Experimental Cell Research*, 57(2–3), pp.462–466.

Sheffield, J.B. & Moscona, A.A., 1970. Electron microscopic analysis of aggregation of embryonic cells: the structure and differentiation of aggregates of neural retina cells. *Developmental biology*, 23(1), pp.36–61.

Sidman, R.L., 1961. *Histogenesis of mouse retina studied with thymidine-H3*, Academic Press, New York (NY).

Sinn, R. & Wittbrodt, J., 2013. An eye on eye development. *Mechanisms of Development*, 130(6–8), pp.347–358.

Snow, R.L. & Robson, J.A., 1994. Ganglion cell neurogenesis, migration and early differentiation in the chick retina. *Neuroscience*, 58(2), pp.399–409.

Spence, J.R. et al., 2011. Directed differentiation of human pluripotent stem cells into intestinal tissue in vitro. *Nature*, 470(7332), pp.105–9.

Steinberg, M.S., 2007. Differential adhesion in morphogenesis: a modern view. *Current Opinion in Genetics & Development*, 17(4), pp.281–286.

Steinberg, M.S., 1970. Does differential adhesion govern self-assembly processes in histogenesis? Equilibrium configurations and the emergence of a hierarchy among populations of embryonic cells. *Journal of Experimental Zoology*, 173(4), pp.395–433.

Stemple, D.L. & Anderson, D.J., 1992. Isolation of a stem cell for neurons and glia from the mammalian neural crest. *Cell*, 71(6), pp.973–85.

Sutherland, R.M. et al., 1970. A multi-component radiation survival curve using an in vitro tumour model. *International journal of radiation biology and related studies in physics, chemistry, and medicine*, 18(5), pp.491–5.

Takasato, M. et al., 2015. Kidney organoids from human iPS cells contain multiple lineages and model human nephrogenesis. *Nature*, 526(7574), pp.564–568.

Ueki, Y. et al., 2015. A transient wave of BMP signaling in the retina is necessary for Müller glial differentiation. *Development (Cambridge, England)*, 142(3), pp.533–43.

Vitorino, M. et al., 2009. Vsx2 in the zebrafish retina: restricted lineages through derepression. *Neural Development*, 4(1), p.14.

Vollmer, G. & Layer, P.G., 1986. Reaggregation of chick retinal and mixtures of retinal and pigment epithelial cells: the degree of laminar organization is dependent on age. *Neuroscience letters*.

Vollmer, G., Layer, P.G. & Gierer, A., 1984. Reaggregation of embryonic chick retina cells: pigment epithelial cells induce a high order of stratification. *Neuroscience letters*.

Wan, Y. et al., 2016. The ciliary marginal zone of the zebrafish retina: clonal and time-lapse analysis of a continuously growing tissue. *Development*, 143(7).

Wässle, H., 2004. Parallel processing in the mammalian retina. *Nature Reviews Neuroscience*, 5(10), pp.747–757.

Wei, X. et al., 2006. Nok plays an essential role in maintaining the integrity of the outer nuclear layer in the zebrafish retina. *Experimental Eye Research*, 83(1), pp.31–44.

Wei, X. et al., 2004. The zebrafish Pard3 ortholog is required for separation of the eye fields and retinal lamination. *Developmental Biology*, 269(1), pp.286–301.

Westerfield, M., 2007. *The Zebrafish Book. A Guide for the Laboratory Use of Zebrafish (Danio rerio), 5th Edition*,

Willbold, E. et al., 2000. Müller glia cells reorganize reaggregating chicken retinal cells

into correctly laminated in vitro retinae. *Glia*, 29(1), pp.45–57.

Willbold, E. et al., 1995. Müller Glia Stabilizes Cell Columns During Retinal Development: Lateral Cell Migration but not Neuropil Growth is Inhibited in Mixed Chick-Quail Retinospheroids. *European Journal of Neuroscience*, 7(11), pp.2277–2284.

Williams, P.R. et al., 2010. In Vivo Development of Outer Retinal Synapses in the Absence of Glial Contact. *Journal of Neuroscience*, 30(36), pp.11951–11961.

Wilson, H. V., 1907. On some phenomena of coalescence and regeneration in sponges. *Journal of Experimental Zoology*, 5(2), pp.245–258.

Wu, Y.-C. et al., 2014. Knockdown of zebrafish blood vessel epicardial substance results in incomplete retinal lamination. *TheScientificWorldJournal*, 2014, p.803718.

Xu, S. et al., 2012. Discovery of an orally active small-molecule irreversible inhibitor of protein disulfide isomerase for ovarian cancer treatment. *Proceedings of the National Academy of Sciences of the United States of America*, 109(40), pp.16348–53.

Yamagata, M. & Sanes, J.R., 2008. Dscam and Sidekick proteins direct lamina-specific synaptic connections in vertebrate retina. *Nature*, 451(7177), pp.465–9.

Yamagata, M. & Sanes, J.R., 2012. Expanding the Ig superfamily code for laminar specificity in retina: expression and role of contactins. *The Journal of neuroscience : the official journal of the Society for Neuroscience*, 32(41), pp.14402–14.

Zolessi, F.R. et al., 2006. Polarization and orientation of retinal ganglion cells in vivo. *Neural development*, 1(1), p.2.

Zou, J. et al., 2008. Intact retinal pigment epithelium maintained by Nok is essential for retinal epithelial polarity and cellular patterning in zebrafish. *The Journal of neuroscience : the official journal of the Society for Neuroscience*, 28(50), pp.13684–95.